STIC-ILL

QR180.I52

From: Murphy, Joseph
Sent: Tuesday, August 22, 2000 1:37 PM
To: STIC-ILL
Subject: 09256156

Please send me the following references:

Hoogenboom HR, Volckaert G, Raus JC.
Construction and expression of antibody-tumor necrosis factor fusion proteins.
Mol Immunol. 1991 Sep;28(9):1027-37.

Xiang J, Moyana T, Qi Y.
Genetic engineering of a recombinant fusion possessing anti-tumor F(ab')2 and tumor necrosis factor.
J Biotechnol. 1997 Feb 28;53(1):3-12.

Rybak SM, Hoogenboom HR, Meade HM, Raus JC, Schwartz D, Youle RJ.
Humanization of immunotoxins.
Proc Natl Acad Sci U S A. 1992 Apr 15;89(8):3165-9.

Knight DM, Trinh H, Le J, Siegel S, Shealy D, McDonough M, Scallon B, Moore MA, Vilcek J, Daddona P, et al.
Construction and initial characterization of a mouse-human chimeric anti-TNF antibody.
Mol Immunol. 1993 Nov;30(16):1443-53.

Varki et al.
Antigens associated with a human lung adenocarcinoma defined by monoclonal antibodies.
Cancer research. 44:681-687, 1984

Thanks a lot...

Joseph F. Murphy, Ph.D.
Patent Examiner, Art Unit 1646
CM1 9D11
(703) 305-7245

1: Immunotechnology 1995 Aug;1(2):95-105 Related Articles, Links

Entrez PubMed

PubMed Services

Related Resources

An IgG3-IL2 fusion protein activates complement, binds Fc gamma RI, generates LAK activity and shows enhanced binding to the high affinity IL-2R.

Harvill ET, Morrison SL.

Department of Microbiology and Molecular Genetics, University of California, Los Angeles 90024-1489, USA.

The therapeutic value of Interleukin 2 (IL-2) is limited by its short half life and systemic toxicity. One approach to overcoming these problems is to fuse this protein to an antibody, a protein with a long half life and the ability to target a unique antigen within the body. To examine the biochemical properties of such a molecule a fusion protein was constructed linking the N-terminus of human IL-2 to the C-terminus of IgG3. A similar fusion between IgG1 and IL-2 has previously been shown to bind antigen, generate antibody-dependent cellular cytotoxicity (ADCC) and stimulate T cell proliferation and cytotoxicity. We now extend these studies and show that the fusion protein, termed IgG3-IL2, is appropriately N-glycosylated within the IgG3 CH2 domain, binds the human high affinity Fc receptor (Fc gamma RI) with an affinity slightly lower than that of IgG3, and is able to activate complement via the classical pathway to lyse antigen coated sheep red blood cells (SRBC). When used to stimulate the proliferation of the IL-2 dependent cell line CTLL-2, IgG3-IL2 has a specific activity slightly lower than that of human recombinant IL-2 (hrIL-2). In marked contrast, when comparable unit concentrations, as defined by the standard CTLL-2 proliferation assay, are used to stimulate human peripheral blood lymphocytes (PBL), IgG3-IL2 generates significantly greater lymphokine activated killer (LAK) cell cytotoxicity than does hrIL-2. Competition studies show that IgG3-IL2 binds the intermediate affinity form of the IL-2 receptor (IL-2R), consisting of the beta and gamma subunits, with an affinity slightly less than that of hrIL-2. In contrast, IgG3-IL2 shows a greater affinity than hrIL-2 for the high affinity IL-2R, consisting of alpha, beta and gamma subunits. Our studies show that the IgG3-IL2 fusion protein possesses a combination of the biological properties of IgG3 and IL-2 including antigen binding, complement activation, Fc gamma RI binding, IL-2R binding and stimulation of both proliferation and LAK activity. This

combination of activities may allow IgG3-IL2 to target humoral and cell-mediated immune activation to the site of an antigen of interest or target an antigen to IL-2R bearing cells or organs.

PMID: 9373338 [PubMed - indexed for MEDLINE]

Biochimica et Biophysica Acta, 1096 (1991) 345–354

ADONIS 092544399100087U

BBADIS 61040

Targeting of tumor necrosis factor to tumor cells: secretion by myeloma cells of a genetically engineered antibody-tumor necrosis factor hybrid molecule

Hennie R. Hoogenboom [1,*], Jef C.M. Raus [1] and Guido Volckaert [2]

[1] *Dr. L. Willems-Instituut en Departement WNIF, Limburgs Universitair Centrum, Universitaire Campus, Diepenbeek (Belgium) and* [2] *Laboratorium voor Gentechnologie, Katholieke Universiteit Leuven, Leuven (Belgium)*

(Received 20 November 1990)

Key words: Tumor necrosis factor; Antibody; Hybrid protein; (Mouse myeloma cell)

The construction, synthesis and secretion of a genetically engineered antibody-cytokine fusion molecule is described. To target tumor necrosis factor (TNF) to tumor cells, recombinant antibody techniques were used to produce a Fab-like antibody-TNF conjugate. At the gene level, the heavy chain gene of an antitransferrin receptor antibody was linked to a synthetic TNF gene encoding human TNF. Transfection of the heavy chain-TNF gene into a myeloma derived cell line which was producing the light chain of the same antibody, allowed the isolation of a cell line secreting a fusion protein f th expected molecular weight and composition. The culture supernatant of the cell line contained TNF cytotoxic activity towards murine L929 cells and human MCF-7 cells. Cytotoxicity towards the human cancer cells was inhibited by an excess of the original antitransferrin receptor antibody, indicating that the antibody-TNF molecules are targeted to the transferrin receptor rich tumor cells. Since the antibody genes used are chimeric (i.e. composed of mouse variable and human constant regions) and since DNA encoding human TNF was used, the hybrid protein is an example of a humanized immunotoxin-like molecule. These results illustrate the possibilities of antibody engineering technology to create and produce improved agents for cancer therapy. Furthermore, they demonstrate for the first time the ability of myel ma cells to secrete an antibody-cytokine chimeric molecule.

Introduction

Tumor necrosis factor (TNF) was originally identified as a tumoricidal protein causing an hemorrhagic necrosis of transplanted solid tumors in mice [1]. Since TNF also exhibited a striking cytotoxicity against various tumor target cell lines in vitro whilst causing minimal harm to normal cells, it attracted attention as a potential anticancer drug. However, TNF has a broad range of effects and appears to be involved in diverse biological processes including inflammation and immunoregulation, antiviral defense, endotoxic shock, cachexia, angiogenesis and mitogenesis [2–4]. The mechanisms through which TNF mediates these multiple activities as a multipotent immunological regulatory molecule, a cytokine, remain poorly understood. TNF has a cellular surface receptor, but there is no clear correlation between TNF sensitivity and density or affinity of the receptor. The DNA coding for human TNF has been cloned, sequenced and expressed at high efficiency in *E. coli*, yielding large amounts of purified recombinant material which has been used for human cancer therapy (for review see Ref. 4). Results of Phase 1 clinical trials show that in vivo administration of TNF results in severe side-effects, ranging from nausea and vomiting, fever, headache, diarrhea and hypotension to death [5]. Hence, the dose of TNF used in clinical trials for the treatment of cancers is limited.

In an attempt to modify the characteristics of TNF, we describe here the design and production of a genetically engineered antibody-TNF hybrid molecule. Recent developments in the field of antibody engineering made it possible to create recombinant antibodies, the products of immunoglobulin genes constructed in vitro and expressed in transfected cells [6–8]. Also, gencti-

* Present address: M.R.C. Laboratory of Molecular Biology, Hills Road, Cambridge CB2 2QH, U.K.

Abbreviations: *gpt*, xanthine-guanine phosphoribosyl transferase; SP2/0, SP2/0-Ag14; TNF, Tumor necrosis factor.

Correspondence: J.C.M. Raus, Dr. L. Willems-Instituut, Universitaire Campus, B-3610 Diepenbeek, Belgium.

cally engineered antibody-enzyme molecules have been produced [9,10]. By linking TNF to an antitransferrin receptor antibody, we aim to target TNF to transferrin receptor-rich cancer cells. Since the transferrin receptor is a growth related cellular surface antigen found on most proliferating cells [11], all dividing cells have the capability of binding the antibody-cytokine hybrid molecule. However, the selective antitumor activity of TNF would provide the killing of tumor cells only. In this way TNF might be targeted to the surface of cancer cells and killing of cells might be achieved with smaller amounts of TNF. As a result, the dose necessary to kill tumor cells could be reduced and the side-effects would disappear or decrease in intensity.

The antibody used is directed against the human transferrin receptor, and does not compete with transferrin for binding to the receptor, which is important for in vivo use [12]. The heavy and light chain genes of this antibody have been cloned previously [13]. In order to minimize the immune response towards this mouse antibody, mouse-human chimeric genes were constructed and expressed in myeloma cells. The resulting chimeric antibody retained its antigen-binding capacity [13]. These antibody genes were used in the present study to create an Fab-like antibody-TNF hybrid protein. A Fab-like molecule lacks immunoglobulin effector functions, which might interfere with the projected anticancer activity. Furthermore, a Fab-like molecule will be monovalent for transferrin receptor binding, and thus can not induce capping upon cellular membranes. It also could be assembled more readily and, since it is smaller, should migrate faster into a solid tumor mass than a whole immunoglobulin-TNF conjugate.

Materials and Methods

Materials

Restriction endonucleases and mycophenolic acid were obtained from Bethesda Research Laboratories (Gaithersburg, MD, U.S.A.). DNA-modifying enzymes, [α-^{32}P]dCTP, [γ-^{32}P]ATP and [^{35}S]methionine were supplied by Amersham (Buckinghamshire, U.K). Xanthine and hypoxanthine were purchased from Sigma (St. Louis, MO, U.S.A.). Oligonucleotides were obtained from Eurogentec (Liège, Belgium).

Cloning procedures and DNAs

The antibody genes used in this study were previously cloned, sequenced and used to construct mouse/human chimeric genes [13]. The genomic human gamma-1 clone [14] and the expression vector pSVgpt-MOV$_H$NP (pSVgpt) containing regulatory sequences for Ig gene expression in lymphoid cells [15] were gifts from Dr. M.S. Neuberger (MRC Laborat ry of Molecular Biology, Cambridge, U.K.). pSVhyg (palys 17), the selectable shuttle vector with the hygromycine resistance gene, was a gift from Dr. J. Foote (MRC Laboratory of Molecular Biology, Cambridge, U.K) [16]. The TNF DNA was obtained from Dr. K. Ashman (E.M.B.L., Heidelberg, F.R.G.) [17]. The recombinant DNA work was performed by standard procedures [18]. Sequencing was done as described [19].

Cell lines and cell culture

SP2/0-Ag14 (SP2/0; ATCC CRL 1581) is a non-Ig producing murine hybridoma. L929 (ATCC CCL1) is a murine fibroblastic cell line; MCF-7 (ATCC HTB 22) is a breast adenocarcinoma; HL-60 (ATCC CCL240) is a promyeloid leukemia; MOLT-4 (ATCC CRL 1582) is an acute lymphoblastic T-cell leukemia. All cell lines and all transfectomas were grown in RPMI1640 supplemented with 2 mM L-glutamine, 1 mM sodium pyruvate, non-essential amino acids and 10% FCS, all purchased from Bethesda Research Laboratories.

Transfection of DNA into myeloma cells and selection of transfected cells

Cells were transfected by electroporation [20] with the Gene Pulser Apparatus of Biorad (Richmond, CA, U.S.A.), as described previously [13]. Briefly, 10^6 cells and 1–20 μg *Bam*HI or *Pvu*I-linearized plasmid in 0.8 ml of PBS at 0 °C in an electroporation cuvette (0.4 cm electrode gap) were subjected to a single voltage pulse at 200 V using a capacitance setting of 960 μF. Selection for transfected cells containing the *gpt* gene was carried out 48 h later, with 1 μg/ml mycophenolic acid, 250 μg/ml xanthine and 15 μg/ml hypoxanthine. Hygromycine selection was done with 400 μg/ml hygromycine. Clones were visible after 1–2 weeks. Individual clones were selected by limiting dilution in the absence of feeder cells.

Detection of antibody secreting cell lines

Screening for antibody production was done by an ELISA method, detecting human IgG or kappa chain, as described elsewhere [13]. The assay measures antibody concentrations ranging from 1 ng/ml to 100 ng/ml. Briefly, microtiter plates were coated with goat anti-human IgG (Tago Inc., Burlingame, CA, U.S.A.) overnight at 4 °C (100 μl/well of a 1/1000 diluti n in 0.1 M $NaHCO_3$ buffer, pH 9.6). After washing with PBS/0.05% Tween-20, the supernatant samples were added to the wells and the plates were incubated for 2 h at 37 °C. Bound antibody was detected with biotinylated goat anti-human IgG (Amersham) and subsequently with streptavidin-peroxidase conjugate (both 100 μl/well of a 1/1000 dilution in PBS; incubate 2 h at 37 °C). After the final wash, 100 μl f a 0.1% *o*-phenylenediamine/0.1% H_2O_2/17 mM citric acid/65 mM sodium phosphate (pH 6.3) was added to each well. The reaction was stopped after 10 min by adding 25 μl 2 M HCl. The *A* was measured at 492 nm in an

automatic Titertek microtiter plate reader (Flow, Irvine, U.K.). This ELISA only detects human IgG; human kappa light chain is not detected.

Detection f human kappa light chain was carried out as described for human IgG, while using rabbit anti-human kappa Ig (Nunc, Roskilde, Denmark) for coating and biotinylated goat anti-human kappa (Amersham) for detection. In this ELISA, an overcoating step of 1 h with 1% BSA in PBS appeared necessary to reduce background.

SDS-PAGE, immunoblotting, in vivo cell labeling and immunoprecipitation

Protein analysis by SDS-PAGE was performed with the discontinuous buffer system according to Laemmli [21], using 12.5% crosslinked gels under reducing conditions. Samples were prepared in 0.1 M Tris-HCl (pH 7.0) containing 2% SDS, 2% mercaptoethanol and 10% sucrose and heated at 95°C for 5 min prior to electrophoresis. For immunoblotting, samples after electrophoresis were transferred to polyvinylidene difluoride (PVDF) membrane (Millipore, Bedford, IL, U.S.A.) by electroblotting (Novablot, LKB-Pharmacia, Uppsala, Sweden) at 0.8 mA/cm^2 for 1 h. The filter was incubated overnight in 3% BSA at 4°C and washed afterwards in PBS + 0.05% Tween-20. For detection of the heavy chain, the filter was incubated for 2 h at room temperature with a 1/500 dilution in PBS of goat anti-human IgG antibody (Tagó Inc.). The filter was washed and incubated with a 1/250 dilution in PBS + 1% BSA of peroxidase labeled rabbit anti-goat Ig (Dakopatts, Copenhagen, Denmark). Staining was carried out with 0.05% diaminobenzidine/0.1% H_2O_2 in PBS. The reaction was stopped by rinsing the filter with water. Detection of TNF was done with rabbit anti-TNF antiserum (1/500 in PBS) (Genzyme, Boston, U.S.A.) and a 1/500 dilution in PBS of peroxidase labeled swine anti-rabbit Ig (Dakopatts). Light chain was detected using biotinylated goat anti-human kappa Ig (1/500 in PBS) (Amersham).

In vivo cell labeling and immunoprecipitations were carried out as described [13], using goat anti-human IgG-Sepharose beads. After electrophoresis, the gel was treated with Amplify (Amersham) and dried. Autoradiography was performed at −70°C using intensifier screens (Cronex Lighting Plus, Dupont, Boston, MA, U.S.A.).

TNF-assay

The cytotoxic activity of TNF was determined using mouse L929 fibroblast cells [22]. The cells were incubated with increasing amounts of the TNF containing sample, in the presence of actinomycin D (1 μg/ml). The assay was carried out in microtiter plates, with 2–5.10^4 cells/well, 200 μl/well. After an 18 h incubation period, the living cells were quantitated with MTT (3-(4,5-dimethyl-thiazol-2-yl)-2,5-di-phenyltetrazolium-bromid) [23]. MTT (20 μl/well of a 5 mg/ml stock) was added to each well. After 1–4 h incubation the produced formazan crystals were redissolved by adding 100 μl/well 10% SDS + 0.01 N HCl and incubating for 4–16 h. The A was measured at 540 nm in an automatic Titertek microtiter plate reader (Flow). TNF protein was purchased from Genzyme and had a specific activity of $2 \cdot 10^7$ U/mg protein. The activity of TNF (in units) was defined as the reciprocal of the dilution at which a 50% reduction in A was observed compared with control cultures containing no TNF. For MCF-7, MOLT4 and HL-60 cells no actinomycin D was used in the assay and the incubation period was prolonged to 48 h.

Results

Construction of a chimeric heavy chain-TNF gene

The IgG molecule consists of compact protein domains with the hinge region serving as a spacer separating the C_H1 from C_H2 domains. This domain structure is reflected at the gene level: in the human gamma-1

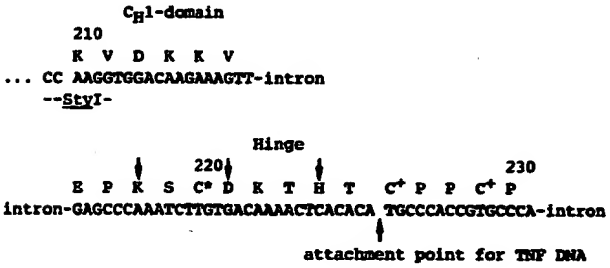

Fig. 1. Structure of the 3′ region of the C_H1-exon and the compleie hinge exon of the human gamma-1 gene. C*: cysteine necessary for disulphide link with the light chain ; C+: cysteines necessary for dimerization of the heavy chains. Amino acid residues in the hinge exon strongly interacting with residues in the C_H1-domain are indicated with an arrow. The hinge exon extends from residues 216–230 (EU numbering [40]).

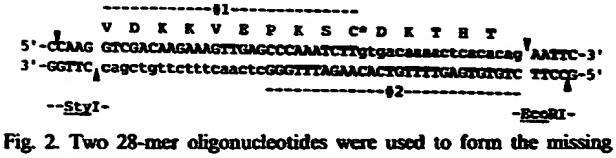

Fig. 2. Two 28-mer oligonucleotides were used to form the missing region between the *Sty*I site in the C_H1-domain and the *Eco*RI site in the TNF DNA. The two 28-mers were annealed, treated with Klenow polymerase and dNTPs to make a 46 bp blunt end fragment and this DNA was cloned into *Sty*I and *Eco*RI sites, which had been made blunt end with Klenow polymerase and dNTPs. After ligation, both sites were restored only if the fragment was inserted in the orientation shown. The sequence of the 46 bp fragment and its junctions was checked after subcloning into M13mp18. The oligonucleotides (No. 1 and No. 2) are depicted in capitals the enzymatically filled-in nucleotides are shown in lowercase letters. Also indicated are the encoding amino acid residues. The sequence is flanked by the *Sty*I and *Eco*RI cloning sites.

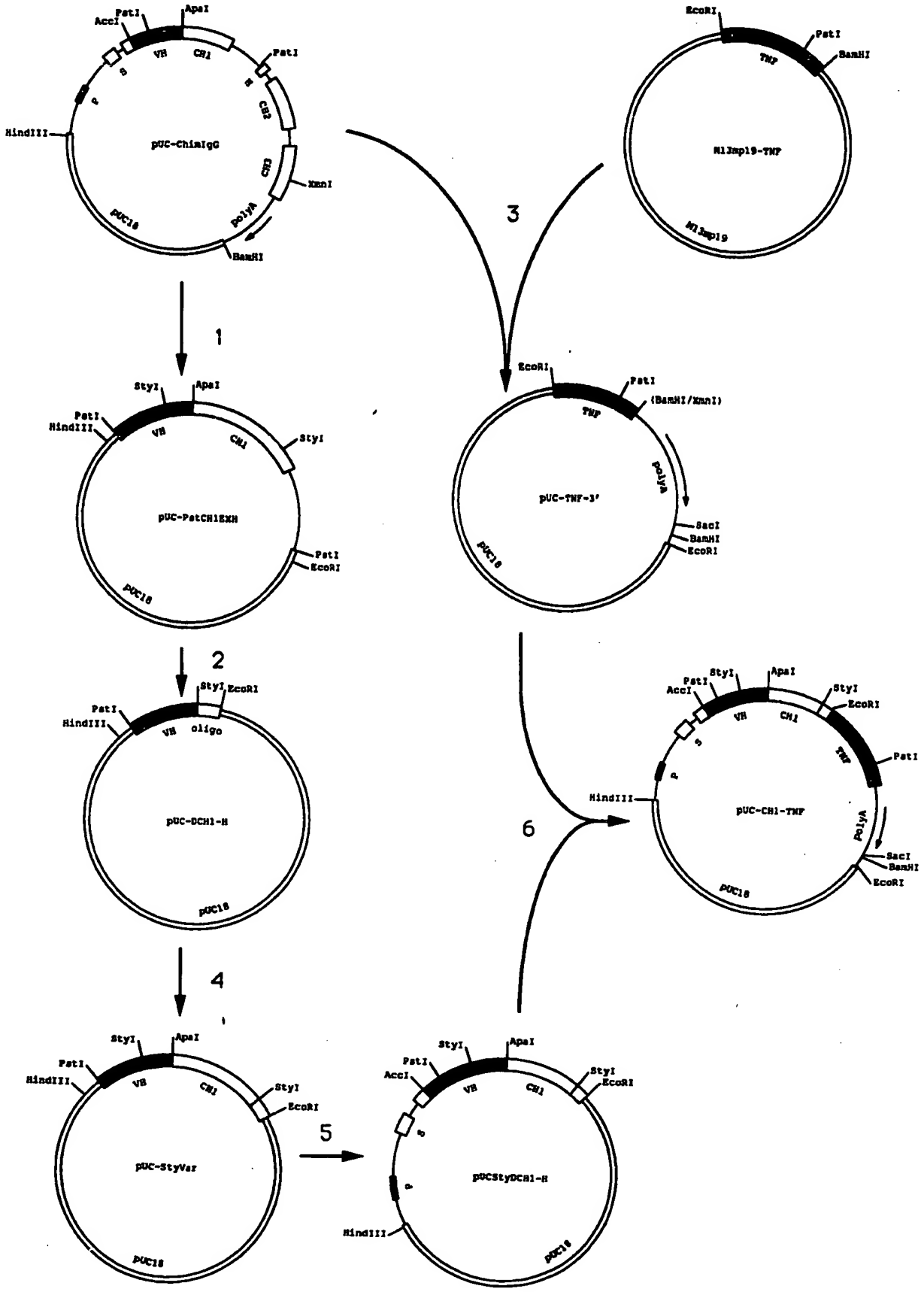
pUC-ChimIgG
PstI
AccI
ApaI
VH
CH1
PstI
CH2
CH3
XmnI
HindIII
pUC18
polyA
BamHI
M13mp19-TNF
EcoRI
PstI
TNF
BamHI
M13mp19
1
3
pUC-PstCH1EXH
StyI
ApaI
PstI
HindIII
VH
CH1
StyI
PstI
EcoRI
pUC18
pUC-TNF-3'
EcoRI
PstI
(BamHI/XmnI)
TNF
polyA
SacI
BamHI
EcoRI
pUC18
2
pUC-DCH1-H
StyI
EcoRI
PstI
HindIII
VH
oligo
pUC18
6
pUC-CH1-TNF
StyI
ApaI
PstI
AccI
VH
CH1
StyI
EcoRI
TNF
PstI
HindIII
polyA
SacI
BamHI
EcoRI
pUC18
4
pUC-StyVar
StyI
ApaI
PstI
HindIII
VH
CH1
StyI
EcoRI
pUC18
5
pUCStyDCH1-H
StyI
ApaI
PstI
AccI
VH
CH1
StyI
EcoRI
HindIII
pUC18

gene, each d main, also the hinge region, is encoded by a separate exon. Yet the hinge exon encodes part of the structural C_H1 domain, including the cysteine necessary for connecting the heavy to the light chain (Fig. 1) [24]. Furthermore, it has been sh wn that some amino acid residues in the upper part of the hinge interact with residues in the C_H1-domain (indicated in Fig. 1) [25]. The lower part of the hinge is a rigid region of prolines and cysteines necessary for dimerization of the heavy chain. Therefore, to retain the C_H1-domain structure as much as possible, we decided to remove only the lower part of the hinge when developing a Fab-like heavy chain-TNF construct.

The TNF DNA comprises a synthetic gene encoding the mature human TNF protein [17]. The TNF DNA does not encode the first two amino acid residues of native TNF (Val-Arg), but this deletion has no influence on the activity [26]. A translation initiation codon and an *Eco*RI restriction site were added to the 5′ end and two tandem stop codons and a *Bam*HI restriction site to the 3′ end. The *Eco*RI site was used for linking the gene to the C_H1-domain.

The chimeric heavy chain gene of the antitransferrin receptor antibody is composed of a murine variable region, linked to the human gamma-I constant region. While manipulating the original genomic human gamma-I constant region DNA, the intron between C_H1 domain and genetic hinge was removed. By using two synthetic oligonucleotides, a linkage was made between a *Sty*I site at the 3′ end of the C_H1 domain (indicated in Fig. 1) and an *Eco*RI site at the 5′ end of the TNF gene. The two synthetic primers encode the missing C_H1-hinge amino acid residues (Fig. 2). The intron was deleted for possible future expression of the chimeric gene in a prokaryotic system.

Since the synthetic TNF gene fragment does not include a polyadenylation signal, the human gamma-I polyadenylation signal was added to the 3′ site of the chimeric construct. Therefore, the signal containing *Xmn*I-*Sac*I restriction fragment of the human gamma-1 gene was ligated to the *Bam*HI site of the TNF gene, after filling in of the latter site with Klenow polymerase and dNTPs. Thus, both *Xmn*I and *Bam*HI sites were deleted, but the stop codons at the 3′ end of the TNF gene were left intact. In this way, the polyadenylation signal is preceded by 78 nucleotides of the C_H3 coding region of the gamma-I gene, creating an immunoglobulin-like gene and mRNA. This strategy was followed, because non-Ig derived untranslated 3′ regions of immunoglobulin gene constructs can decrease expression levels by destabilizing the mRNA [27]. Fig. 3 depicts the cloning scheme that was used to build the heavy chain-TNF gene. The junction between antibody heavy chain and TNF DNA is depicted in Fig. 4. Note that three amino acid residues in that junction are added, one of which is the methionine, the first residue translated during the expression of the genetically engineered TNF DNA in *E. coli* [17].

```
          (1)                    (2)          (3)
C*  D   K   T   H   T     E   F   M     S   S   S
TGT GAC AAA ACT CAC ACA   GAA TTC ATG   TCT TCT TCT
                          -EcoRI-
```

Fig. 4. Junction between antibody heavy chain and TNF DNAs. (1) part of the hinge region, including the cysteine for disulphide formation with light chain (C*); (2) amino acid residues introduced while cloning, including the methionine, used for expression of the TNF DNA in *E. coli*; (3) mature TNF sequence, of which the first two codons were deleted.

Establishment of a cell line secreting the Fab-like hybrid protein

The chimeric heavy chain-TNF gene was cloned as a *Hin*dIII-*Bam*HI fragment into the SV40-derived selectable shuttle vector, pSVgptMOV$_H$NP, which contains the *gpt* gene as a selection marker (see Materials and Methods). In the final construct, the expression of the fusion protein is regulated by an immunoglobulin transcription enhancer element and promoter, both situated upstream of the chimeric gene (Fig. 5A). The presence of an immunoglobulin gene derived signal peptide sequence should direct the secretion of the hybrid protein. The chimeric light chain gene was cloned into pSVhyg, a pSVneo derived plasmid containing the hygromycine resistance gene (Fig. 5B).

Fig. 3. Construction scheme of the heavy chain-TNF fusion gene. Vector sequences and promoters are shown as small boxes, introns and other non-coding regions as lines and exons as large boxes. The heavy chain variable region sequence is shown in black, Ig constant regions are white boxes and the TNF DNA box is stippled. Only restriction sites relevant to this construction scheme are shown; structural features of the vectors (antibiotic resistance genes, etc.) are not shown. (1) An 0.8-kb *Pst*I fragment of the chimeric heavy chain gene was recloned into the *Pst*I polylinker site of pUC18 and a clone of the right orientation (as depicted in figure) isolated. (2) This plasmid was cut with *Sty*I and *Eco*RI, treated with Klenow polymerase and dNTPs, and dephosphorylated. The 46 bp fragment, made with the two oligonucleotides No. 1 and No. 2, was subcloned into this vector, yielding pUC-DCH1-H. (3) The TNF gene was isolated as an 0.5-kb *Eco*RI-*Bam*HI fragment from M13mp19-TNF, by first digesting the plasmid with *Bam*HI, treating with Klenow polymerase and dNTPs and subsequently digesting with *Eco*RI. This fragment was subcloned into the *Eco*RI-*Sac*I polylinker sites of a pUC18 derived plasmid, together with a 0.7-kb *Xmn*I-*Sac*I fragment from the human gamma-1 gene, containing part of the C_H3-domain and the poly A signal sequence. After additional subcloning experiments (not shown), an *Eco*RI site at the 3′ region of the TNF DNA was created, yielding pUC-TNF-3′. The Ig gene was reconstituted by inserting into pUC-DC$_H$1-H (4) the 0.4-kb *Sty*I fragment derived from pUC-PstCH1EXH and (5) the 1.9-kb *Hin*dIII-PstI fragment derived from pUC-ChimIgG. (6) The chimeric heavy chain-TNF gene was completed by inserting the 1.3-kb *Eco*RI fragment of pUC-TNF-3′ into pUCStyDCH1-H, yielding pUC-CH1-TNF. All junctions were checked by sequencing.

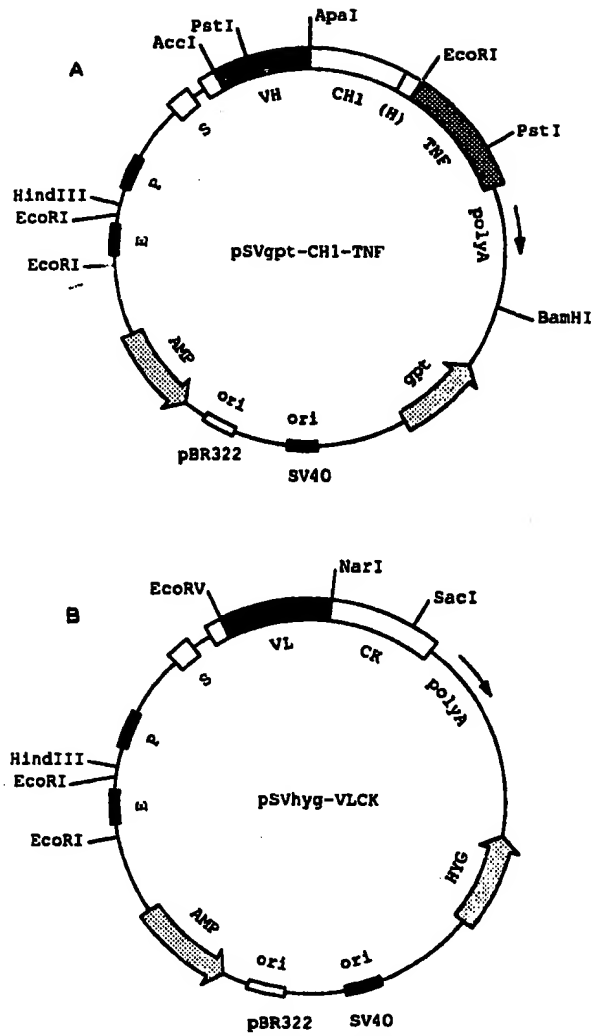

Fig. 5. Structures of the plasmids containing (A) the chimeric heavy chain-TNF gene or (B) the chimeric light chain. The chimeric heavy chain-TNF gene of pUC-CH1-TNF was subcloned into expression vector pSVgpt as a 4-kb *Hin*dIII-BamH fragment, yielding pSVgpt-CH1-TNF. P, promoter; S, signal peptide sequence; E, enhancer; AMP (HYG), ampicillin (hygromycin) resistance gene; ori, origin of replication.

The light chain gene containing expression vector was used to transfect mouse SP2/0 cells. After transfection, selection with hygromycin yielded several light chain secreting clones, detected by human kappa-detecting ELISA. One of the clones, clone 12B5, was selected for subcloning by limiting dilution and further use.

After transfection of cell line 12B5 with the heavy chain-TNF gene containing vector, and selection for the presence of the *gpt* gene, clones were isolated of which the culture supernatant was positive in the human IgG1-detecting ELISA. The polyspecific anti-IgG antibodies used for coating and detecting the human antibody, apparently recognize en ugh epitopes in the C_H1-domain to render the samples positive in the ELISA. One clone, 5B4, was identified as the best producer and used for further analysis. The amount f secreted fusion protein of this clone gave the same optical density in the human IgG-ELISA as a 15–25 ng/ml solution of pure human IgG protein. The actual concentration of fusion protein will be higher, because the ELISA was standardized with intact human IgG-protein and the fusion protein is much smaller.

Characterization of the Fab-like hybrid protein

Supernatant of clone 5B4 (15 ml) was used for immunoprecipitation with goat anti-human IgG-Sepharose beads. The precipitated proteins were eluted, fractionated on SDS-PAGE and transferred to PVDF membrane for immunoblotting analysis. Supernatant of transfectoma 13A5, a cell line secreting the mouse/human chimeric antibody directed to the human transferrin receptor [12] was treated in the same way as a control. Immunoblot analysis was carried out with human IgG or TNF detecting reagents (see Materials and Methods). As seen in Fig. 6B, cell line 13A5 secretes a n rmal heavy chain, which can be detected using the anti-human IgG antisera only. Transfectoma 5B4 on the contrary secretes a fusion protein which reacts with b th antihuman IgG (Fig. 6B) and anti-TNF (Fig. 6A) antisera. The molecular weight of the fusion protein is as expected : 45 kDa (28 kDa from the antibody portion, 17 kDa from the TNF portion). A TNF-detecting immunoblot analysis of another sample, treated in the same way, revealed an additional band of higher molecular weight (Fig. 6C). This additional band might have arisen from incomplete processing of the hybrid molecule. Differences in glycosylation are unlikely to be the cause, because there are no potential *N*-glycosylation sites, neither in this part of the antibody heavy chain, nor in the TNF region. The same doublet of bands has been seen for the gene products of the fusions of the murine IgG2b heavy chain and the *S. aureus* nuclease [9] and a similar fusion of aequorin [29].

In the immunoblot analysis, no degradation products can be detected. In addition, culturing the 5B4 cells in serum free medium for three days, which results in massive cell death and subsequently release of intracellular proteinases, did not harm the integrity of the fusion protein, as verified by immunoblot analysis (results not shown). These results indicate that the fusion protein is secreted as a stable and relatively proteinase-resistant protein. As expected, protein A-Sepharose failed to precipitate the fusion protein (the binding site of protein A is believed to be near the junction of the C_H2 and C_H3 domains, which was deleted in the construct).

The native structure of the protein is not yet kn wn. Immunoprecipitation with antihuman IgG-Sepharose of in vivo radiolabeled 5B4 supernatant showed that the light chain coprecipitated with the heavy chain-TNF

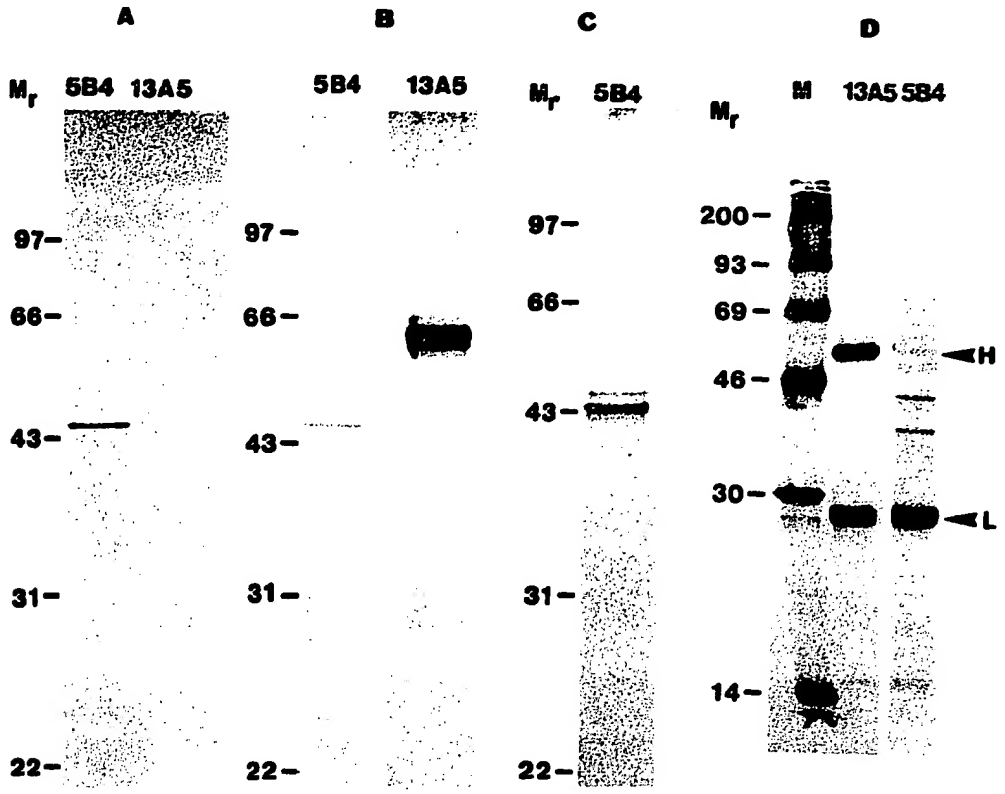

Fig. 6. (A,B,C) Immunoblot analysis of culture supernatant of transfectomas 13A5 (secretes chimeric antitransferrin receptor antibody) and 5B4 (secretes light chain and heavy chain-TNF fusion protein). Supernatant was immunoprecipitated with goat anti-human IgG-Sepharose beads, eluted and fractionated on 12.5% SDS-PAGE. The proteins were transferred to a membrane and antibodies were detected using anti-human IgG (B) or anti-TNF (A and C), as described in Materials and Methods. The positions of M_r markers are indicated ($M_r \times 10^{-3}$). (D) Immunoprecipitation analysis of in vivo labeled culture supernatant of 5B4 and 13A5. The samples were immunoprecipitated using goat anti-human IgG-Sepharose beads, eluted, reduced and fractionated on 12.5% SDS-PAGE, after which an autoradiogram of the gel was made. The position of the antibody heavy and light chains is indicated.

protein (Fig. 6D), pointing out that the antigen-binding domains are in the expected configuration.

TNF activity upon mouse and human cell lines

The cytotoxicity of the supernatant of the 5B4 transfectoma on various cell lines was analyzed. The cells were incubated in 200 μl medium containing a variable amount of supernatant of SP2/0 cells (non producer), 13A5 (chimeric antibody) or 5B4 (fusion protein). After 1, 2 or 3 days the amount of living cells was determined using the MTT-staining method. Fig. 7 depicts the growth curves of the mouse L929 fibroblast cell line and the relatively TNF-resistant human MCF-7 breast carcinoma. As shown in Fig. 7, only 5B4 supernatant has a growth inhibiting effect upon both cell lines. The antitransferrin receptor antibody f 13A5 does n t cause growth inhibition, because there is no competition with transferrin for binding to the receptor. Similar assays with cell lines HL-60 and MOLT-4 showed the same growth inhibitory effect of 5B4 supernatant (results not shown).

According to the L929-assay, the 5B4 supernatant contains approximately 10 U TNF/100 μl. However, the growth of MCF-7 cells, which can not be inhibited with 400 U TNF as tested with pure TNF, can be influenced with the 10 U TNF-containing 5B4 supernatant. This difference might be explained by the targeting effect of the antibody-TNF molecules to human cells due to the transferrin receptor binding. Since the antibody recognizes human transferrin receptor only, there is no targeting to the murine L929 cells. To gain insight into this hypothesis, a competition assay was performed: if targeting of the TNF molecule happens through the transferrin receptor, the intact chimeric antibody should be able to block the toxicity by competiting for the same receptor. L929 and MCF-7 cells were incubated with various amounts of 5B4 and 13A5 supernatants and combinations of both. Fig. 8 shows

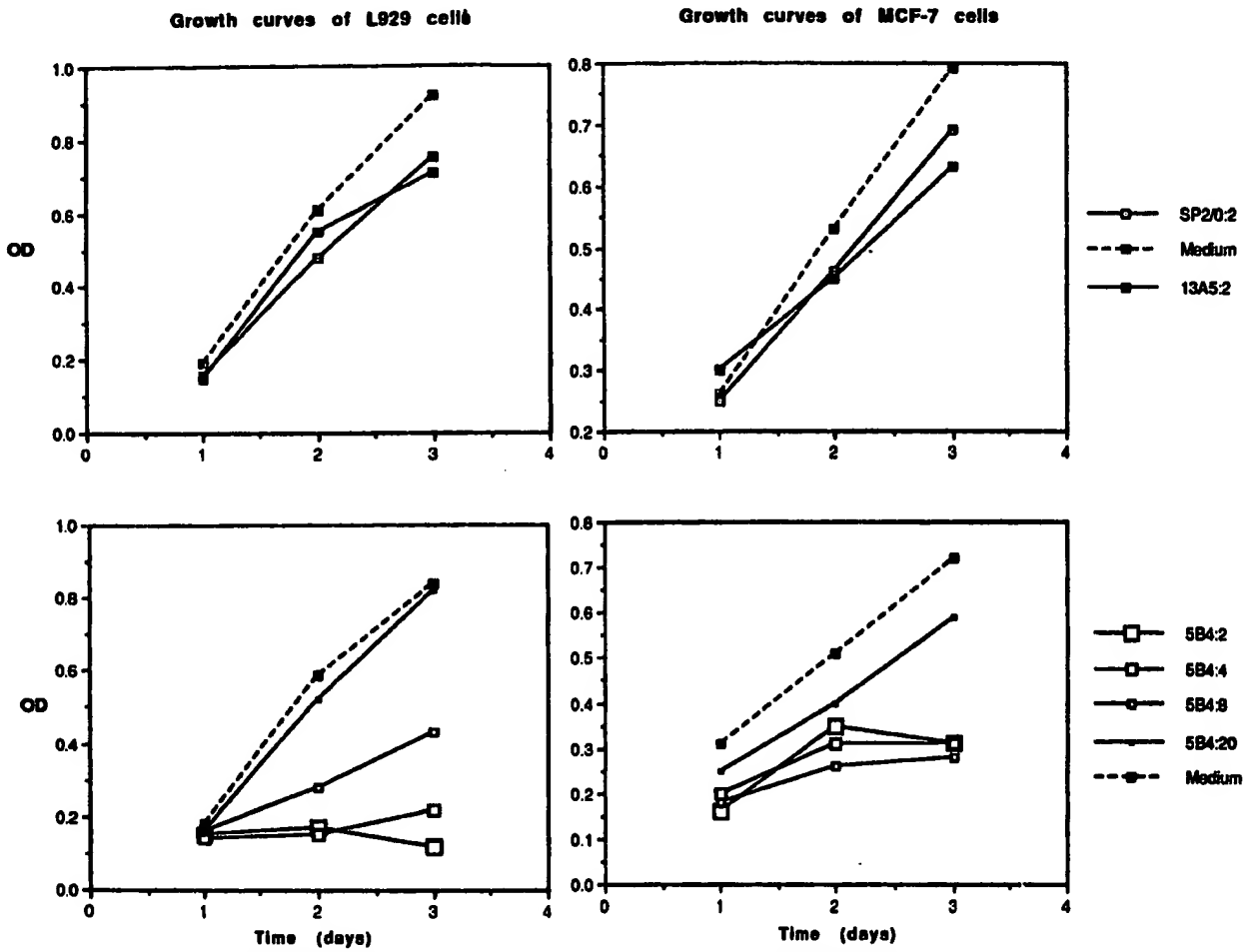

Fig. 7. Growth curves of L929 (left) and MCF-7 (right) cells, in the presence of culture supernatant of SP2/0 (non-producer) and transfectomas 13A5 (secretes chimeric antitransferrin receptor antibody) and 5B4 (secretes light chain and heavy chain-TNF fusion protein). Culture supernatant was added at the indicated dilution (:2, :4, etc.) and living cells were quantified in an MTT-assay after 1, 2 or 3 days.

Murine L929 cells			
13A5 \ 5B4	:2	:4	no
:2	-	-	+
:4	-	-	+
no	-	-	+
Human MCF-7 cells			
13A5 \ 5B4	:2	:4	no
:2	(+)	+	+
:4	+	+	+
no	-	-	+

Fig. 8. Growth of cells in the presence of culture supernatant of transfectomas 13A5 (secretes chimeric antitransferrin receptor antibody) and 5B4 (secretes light chain and heavy chain-TNF fusion protein), at a given dilution (:2, :4, no) and combination. '+' means no effect on growth, normal growth; '−' means growth inhibition.

that 13A5-supernatant can indeed block TNF-toxicity of 5B4-supernatant to the MCF-7 cells only. The results strongly support the hypothesis, suggesting the targeting of the antibody-TNF fusion protein to human cells has been accomplished.

Discussion

The data presented here describe the construction and expression of an antibody heavy chain-TNF gene. A cell line was obtained secreting light chain and detectable amounts of heavy chain-TNF fusion protein. Few genetically engineered antibody-enzymes have been described so far, using *Staphylococcus aureus* nuclease and c-*myc* [9], Klenow polymerase [28], tissue plasminogen activator [10] and the photoprotein aequorin [29]. In most cases the enzyme or other protein was linked with its N-terminal end t the C-terminal end of the mouse

gamma2b constant region, yielding a potential $F(ab')_2$-like molecule. We for the first time used the human gamma-1 gene and DNA encoding human TNF for the production of an antigen-binding fusion protein. So far, TNF has only been used nce in an N-terminal linked gene fusion, i.e. with human thymosin β_4 [30]. The fusion did not change the activity of TNF.

Alike the antibody-enzymes mentioned above, linkage of the non-antibody region (in the present study TNF) to the antibody moiety had no deleterious effect upon the secretory pathway followed by the antibody protein. The level of secretion (estimated to be in the ng/ml range: 15–25 ng/ml) was lower than for the antibody-enzymes previously described, although correct values can be obtained after purification of the recombinant protein only. To obtain higher expression levels of the hybrid molecule, amplification of the gene by the *dhfr* system can be tried out [31], or alternatively, expression in *E. coli* as a Fab-like or single-chain antibody-TNF protein, as was done for other molecules [32–34] can be envisaged.

The culture supernatant of the transfected cell line 5B4, producing light chain and heavy chain-TNF protein, contained growth inhibiting activity upon murine and human cell lines. Therefore, the fusion product has TNF-activity, but the specific activity was not yet determined. Whereas the active form of TNF is a compact trimer [35], the active native form of this Fab-like antibody-TNF protein and its possible trimerization remain to be elucidated. The TNF-activity of the supernatant of 5B4 upon human MCF-7 cells was inhibited by adding the antitransferrin receptor antibody, suggesting (i) competition between antibody and Fab-like antibody-TNF for the same receptor and correct assembly of the heavy and light chain regions of the protein, (ii) the initial goal, that is targeting of TNF towards human transferrin receptor rich cells, was achieved. The initial TNF-activity might result not only from the concentrating effect of direct binding to the plasma membrane, but also from the appropriate trafficking of the hybrid molecule.

The use of a mouse/human chimeric antibody linked to human TNF, is the first attempt to produce a more human immunotoxin-like molecule. Immunotoxins were long expected to become the magic bullets for treatment of cancers and other diseases [36]. However, the toxins used so far comprise the extremely toxic proteins isolated from bacteria and plants (diphtheria toxin, *Pseudomonas* exotoxin, ricin, etc.; for a review see Ref. 37). One of the problems with these proteins is that, since in the immunotoxins neither the toxins nor most of the antibodies are human, immunot xins evoke an immune response when used for human cancer therapy [38]. The use of chimeric [13], humanized [39] or human antibodies linked to human proteins with toxic properties like TNF would circumvent many problems seen with the classical immunotoxins. The results presented in this study indicate the potential of the antibody engineering technique to develop totally new, more human-like and more potent anticancer agents.

Work is in progress to purify and determine the native structure of the hybrid protein as well as the activity of the protein upon other cancer and normal cells. Purification of the new protein will also enable us to determine the affinity constants of the protein for the human transferrin receptor and the TNF receptor and to elucidate the mechanism of action of this new antibody-cytokine molecule.

Acknowledgements

We thank Dr. K. Ashman, Dr. M. Neuberger, Dr. G. Winter and Dr. J. Foote for their generous gifts of DNAs. H.R.H. was a research assistant of the Belgian Nationaal Fonds voor Wetenschappelijk Onderzoek (N.F.W.O.).

References

1 Carswell, E.A., Old, J., Kassel, R., Green, S., Fiore, N. and Williamson, B. (1975) Proc. Natl. Acad. Sci. USA 72, 3666.
2 Beutler, B. and Cerami, A. (1986) Nature 320, 584.
3 Fiers, W., Brouckaert, P., Devos, R., Franssen, L., Leroux-Roels, G., Remaut, E., Suffys, P., Tavernier, J., Van der Heyden, J. and Van Roy, F. (1986) Cold Spring Harbor Symp. Quant. Biol. LI, 587.
4 Goeddel, D.V., Aggarwal, B.B., Gray, P.W., Leung, D.W., Nedwin, G.E., Palladino, M.A., Patton, J.S., Pennica, D., Shepard, H.M., Sugarman, B.J. and Wong, G.H.W. (1986) Cold Spring Harbor Symp. Quant. Biol. LI, 597.
5 Creaven, P.J., Plager, J.E., Dupere, S., Huben, R.P., Takita, H., Mittelman, A. and Proefrock A. (1987) Cancer Chemother. Pharmacol. 20, 137.
6 Oi, V.T., Morrison, S.L., Herzenberg, L.A. and Berg, P. (1983) Proc. Natl. Acad. Sci. USA 80, 825.
7 Morrison, S.L., Johnson, M.J., Herzenberg, L.A. and Oi., V.T. (1984) Proc. Natl. Acad. Sci. USA 81, 6851.
8 Sharon, J., Gefter, M.L., Manser, T., Morrison, S.L., Oi, V.T. and Ptashne, M. (1984) Nature 309, 364.
9 Neuberger, M.S., Williams, G.T. and Fox, R.O. (1984) Nature 312, 604.
10 Schnee, J.M., Runge, M.S., Matsueda, G.R., Hudson, N.W., Seidman, J.G., Haber, E. and Quertermous, T. (1987) Proc. Natl. Acad. Sci. USA 84, 6904.
11 Trowbridge, I.S. and Omary, M.B. (1981) Proc. Natl. Acad. Sci. USA 78, 3039.
12 Heyligen, H., Thijs, C., Weber, W., Bosmans, E. and Raus (1985) J. Fed. Proc. 44, 787.
13 Hoogenboom, H.R., Raus, J.C.M. and Volckaert G. (1990) J. Immunol. 144, 3211.
14 Honjo, T., Obata, M., Yamawaki-Kataoka, Y., Kataoka, T., Kawakami, T., Takahashi., N. and Mano, Y. (1979) Cell 18, 559.
15 Neuberger, M.S. (1983) EMBO J. 2, 1373.
16 Orlandi, R., Güssow, D.H., Jones, P.T. and Winter, G. (1989) Proc. Natl. Acad. Sci. USA 86, 3833.
17 Ashman, K., Matthews, N. and Frank., R.W. (1989) Prot. Engin. 2, 387.
18 Maniatis, T., Fritsch, E.F. and Sambrook, J., Molecular Cloning.

A Laboratory Manual, Cold Spring Harbor Laboratory, Cold Spring Harbor, New York, 1982.
19 Sanger, F., Nicklen, S. and Coulson, A.R. (1977) Proc. Natl. Acad. Sci. USA 74, 5463.
20 Potter, H., Weir, L. and Leder, P. (1984) Proc. Natl. Acad. Sci. USA 81, 7161.
21 Laemmli, U.K. (1970) Nature 227, 680.
22 Ruff, M. and Gifford, G., Lymphokines 1,2: 235. E. Pick, Acadamic Press, New York 1981.
23 Mosmann, T. (1983) J. Immunol. Methods 65, 55.
24 Burton, D.R. (1981) in Molecular Genetics of Immunoglobulin. New Comprehensive Biochemistry (Calabi, F. and Neuberger, M.S., eds.), 17: 1, Londen.
25 Schneider, W.P., Wensel, T.G., Stryer, L. and Oi, V.T. (1988) Proc. Natl. Acad. Sci. USA 85, 2509.
26 Shirai, T., Yamaguchi, H., Ito, H., Todd, C.W. and Wallace, R.B. (1985) Nature 313, 803.
27 Weidle, U.H., Koch, S. and Buckel, P. (1987) Gene 60, 205.
28 Williams, G.T. and Neuberger, M.S. (1986) Gene 43, 319.
29 Casadei, J., Powell, M.J. and Kenten, J.H. (1990) Proc. Natl. Acad. Sci. USA 87, 2047.
30 Tsjui, Y., Kitahara-Tanabe, K., Noguchi, K., Gatanaga, T., Mizuno, D. and Soma, G-I. (1989) Biochem. Internat. 18, 501.
31 Hendricks, M.B., Luchette, C.A. and Banker, M.J. (1989) Biotechnol. 7, 1271.
32 Huston, J.S., Levinson, D., Mudgett-Hunter, M., Tai, M.-S., Novotny, J., Margolies, M.N., Ridge, R.J., Bruccoleri, R.E., Haber, E., Crea, R. and Oppermann, H. (1988) Proc. Natl. Acad. Sci. USA 85, 5879.
33 Chaudary, V.K., Queen, C., Junghans, R.P., Waldmann, T.A., Fitzgerald, D.J. and Pastan, I. (1989) Nature 339, 394.
34 Batra, J.K., Jinno, Y., Chaudary, V.K., Kondo, T., Willingham, M.C., FitzGerald, D.J. and Pastan, I., (1989) Proc. Natl. Acad. Sci. USA 86, 8545.
35 Jones, E.Y., Stuart, D.I. and Walker, N.P.C. (1989) Nature 338, 225.
36 Vitetta, E.S., Fulton, R.J., May, R.D., Till, M. and Uhr, J.W. (1987) Science 238, 1098.
37 Spooner, R.A. and Lord, J.M. (1990) TIBTECH 8, 189.
38 Schroff, R.W., Foon, A.F., Beatty, S.M., Oldham, R.K. and Walton, C.M. (1985) Cancer Res. 45, 879.
39 Riechmann, L., Clark, M., Waldmann, H. and Winter, G. (1988) Nature 332, 323.
40 Burton, D.R. (1985) Mol. Immunol. 22, 161.

Brief Definitive Report

T Cell–m diated Eradication of Murine M tastatic Melanoma Induc d by Target d Interleukin 2 Th rapy

By Jürgen C. Becker,* James D. Pancook,* Stephen D. Gillies,‡ Koichi Furukawa,§ and Ralph A. Reisfeld*

*From the *Department of Immunology, The Scripps Research Institute, La Jolla, CA 92037; ‡Fuji ImmunoPharmaceuticals Corp., Lexington, Massachusetts 02173; and §Department of Oncology, School of Medicine, Nagasaki University, 1-12-4 Sakamoto, Nagasaki 852, Japan*

Summary

Induction of a T–cell mediated antitumor response is the ultimate goal for tumor immunotherapy. We demonstrate here that antibody-targeted IL2 therapy is effective against established pulmonary and hepatic melanoma metastases in a syngeneic murine tumor model. The effector mechanisms involved in this tumor eradication are not dependent on NK cells, since the therapeutic effect of antibody-IL2 fusion protein was not altered in NK cell-deficient mice. In contrast, T cells are essential for the observed antitumor effect, since therapy with antibody-IL2 fusion proteins is unable to induce tumor eradication in T cell–deficient SCID mice. In vivo depletion studies characterized the essential effector cell population further as CD8+ T cells. Such CD8+ T cells, isolated from tumor bearing mice after antibody-directed IL2 therapy, exerted a MHC class I–restricted cytotoxicity against the same tumor in vitro. These data demonstrate the ability of antibody-targeted IL2 delivery to induce a T cell–dependent host immune response that is capable of eradicating established melanoma metastases in clinically relevant organs.

Most progressively growing neoplasms, e.g., melanoma, do not provoke antitumor immune responses that are capable of controlling the growth of malignant cells, in spite of the fact that these cells express tumor-associated, T cell epitopes. Almost two decades ago, Talmage et al. (1) first described a tumor cell line that failed to induce an allogeneic T cell response despite its apparently normal expression of MHC molecules. Furthermore, they demonstrated that this defective T cell activation could be restored by cytokines (1); thereby providing the rationale for cytokine based forms of immunotherapy.

A therapeutic approach currently receiving much attention is the ex vivo genetic modification of tumor cells to express various cytokines (2, 3). When produced by tumors, many of these cytokines induce a local inflammatory response which results in elimination of the injected tumor cells. In some cases, systemic immune responses are generated against challenge with the wild-type parental tumor. Since most cytokines are paracrine factors working physiologically at high concentrations within a few cell diameters from their cell of origin, this gene transfer approach, in general can not be replaced by systemic cytokine administration unless the cytokine is directed preferentially to the tumor site (4).

We recently demonstrated the feasibility of an alternative therapeutic approach for cancer that combines high local concentrations of cytokines in the tumor microenvironment, low systemic toxicities, and a technically simple modus operandi (5, 6). This goal was achieved by the construction of fusion proteins consisting of tumor-specific monoclonal antibodies and cytokines; thereby, employing the unique targeting ability of antibodies to direct cytokines to the tumor site. Here, we demonstrate the effectiveness of antibody-targeted IL2 therapy for established pulmonary and hepatic melanoma metastases in a syngeneic tumor model that enabled the analysis of effector mechanisms responsible for the therapy-induced tumor eradication. This analysis revealed CD8+ T cells as the essential effector population.

Materials and Methods

Cell Lines, Animals, and Reagents. The murine melanoma cell lines, B16 and B78-D14, have been described previously (7). B78-D14 was derived from B16 melanoma cells by transfection with genes coding for β-1,4-*N*-acetylgalactosaminyltransferase and α-2,8-sialyltransferase inducing a constitutive expression of the gangliosides G_{D2} and G_{D3}.

Mouse/human chimeric antibodies directed against the EGF receptor (ch225) or G_{D2} (ch14.18) were constructed by joining the cDNA for the variable region of the murine antibodies with the constant regions of the γ1 heavy chain and the κ light chain. The antibody-interleukin 2 fusion protein ch14.18-IL2 was constructed by fusion of a synthetic sequence coding for human IL2 to the carboxyl end of the human Cγ1 gene followed by inser-

 J. Exp. Med. © The Rockefeller University Press • 0022-1007/96/05/2361/06 $2.00
Volume 183 May 1996 2361–2366

tion into the eukaryotic expression vector pdHL2. The resulting vector was introduced into Sp2/0-Ag14 cells. Each μg of fusion protein corresponds to approximately 3,000 IU of IL-2 activity. (5).

C57BL/6J, C57BL/6J *bg/bg* and C57BL/6J *scid/scid* mice were obtained from Jackson Laboratory at the age of 4–6 wk and housed under specific pathogen-free conditions.

In Vivo Depletion with mAb. Rat IgG_{2b} anti-CD4 (clone H129.19) and rat IgG_{2a} anti-CD8 (clone 53-6.7) mAb were used for in vivo depletion of T cell subsets (8). Protocols yielding maximum depletion of T cell subsets, i.e., over 95% as determined by indirect immunofluorescence staining and cytofluometric analysis of lymph nodes and spleens, consisted of weekly i.p. injections of 500 μg of the respective mAb.

Experimental Lung Metastases. Single cell suspension of 5×10^5 tumor cells in 500 μl PBS were injected into the lateral tail vein. After 7 d micrometastases were present disseminated throughout the lungs and were invading into the pulmonary alveoli. At d 28 after tumor cell injection, grossly visible metastases were present on the surface of the organ.

Experimental Hepatic Metastases. Tumor cells (2.5×10^5) were injected in 100 μl RPMI 1640 with a 27-gauge needle beneath the splenic capsule over a period of 60 s, followed by ligation of the splenic pedicle with a 4.0 silk suture and the removal of the spleen. 35 d after this procedure the animals were sacrificed and examined for metastases.

Biodistribution. The ch14.18-IL2 fusion protein was labeled with ^{125}I as described (6). Experimental hepatic or pulmonary metastases were induced as described above. 10 d after tumor cell inoculation, animals received one i.v. injection of 5 mCi ^{125}I-labeled ch14.18-IL2 fusion protein. Animals were killed 12 h after injection.

Statistical Analysis. The statistical significance of differential findings between experimental groups of animals was determined by student's *t* test. The nonparametric Wilcoxon rank sum test was chosen when the data were not amenable for parametric tests as defined by the David-Pearson-Stephen's test. Findings were regarded as significant if two-tailed *P* values were ≤ 0.01.

Results

Therapeutic Efficacy of Antibody-IL2 Fusion Proteins. We previously demonstrated that the genetic fusion of IL2 to the carboxy-terminal end of an antibody heavy chain changes neither the biological activity of IL-2 nor the binding affinity of the monoclonal antibody (5, 6). To test the effect of these antibody-IL2 fusion proteins on melanoma metastases in vivo, we employed a number of different experimental tumor models using B16 melanoma cells, which had been transfected with genes coding for β-1,4-*N*-acetylgalactosaminyltransferase and α-2,8-sialyltransferase resulting in a constitutive expression of the gangliosides G_{D2}, the antigen recognized by ch14.18-IL2. These tumor cells form experimental pulmonary and hepatic metastases following intravenous or intrasplenic injection, respectively. After 1 wk these were present as disseminated, established micrometastases.

The first series of experiments addressed the effect of the antibody-IL2 fusion protein on disseminated, established pulmonary metastases. Treatment of mice 1 wk after tumor cell inoculation by i.v. administration of 8 μg ch14.18-IL2 fusion protein for 7 d completely eradicated pulmonary micrometastases in 14 of 16 animals (Table 1). This complete eradication of micrometastases was confirmed by histologic examination of serial sections of lung specimens (data not shown). For the remaining two animals the tumor load was dramatically reduced to one or two grossly visible pulmonary foci, as compared to control animals which suffered from more than 500 pulmonary metastases, after receiving either no treatment or the combination of equimolar amounts of recombinant IL2 (24,000 I.U.) and ch14.18 mAb (8 μg). Similar results were obtained when animals bearing disseminated hepatic metastases established for 7 d were treated i.v. with 8 μg ch14.18-IL2 fusion protein for 7 d (Table 1). This treatment resulted in complete regression of micrometastases in 87.5% of these animals. The specificity of the antitumor effect of ch14.18-IL2 fusion proteins was established, since a fusion protein that is not reactive with the tumor cells completely failed to exert any antitumor effects (Table 1). Differences in the number of metastatic pulmonary foci or the hepatic metastatic score between animals receiving the specific fusion protein and those subjected to other treatments were statistically significant ($P \leq 0.002$).

Although no metastatic foci could be detected by macroscopic and/or histologic examination in the animals following treatment with ch14.18-IL2 these mice could still suffer from minimal residual disease. Survival studies were performed to measure the extent of such a hypothetical residual disease. The mean survival time of mice after induction of experimental pulmonary metastases without further treatment was 41 d. This survival time was not significantly altered by the administration of ch14.18 antibody in combination with recombinant IL2 (mean = 44 d), but was more than doubled by treatment with the ch14.18-IL2 fusion protein. The same was true for mice suffering from hepatic metastases. These mice lived at least twice as long after therapy with ch14.18-IL2, than control animals (mean 51 or 55 d, respectively). Only one of the treated animals died within the observation period. At the end of the observation period a post mortem examination revealed no metastatic disease in any of the major peripheral organs or the central nervous system.

Biodistribution of ch14.18-IL2. We previously demonstrated that fusion proteins localize in antigen-expressing subcutaneous tumors in nude mice (6). However, the clinically more relevant question is whether the fusion protein is able to target micrometastases in affected organs of a syngeneic host. The biodistribution of ^{125}I-ch14.18-IL2 fusion protein in C57BL/6J mice suffering from either hepatic or pulmonary metastases, 10 d after experimental induction with B78-D14 melanoma cells, is shown in Fig. 1. The amount of radioactivity in livers and lungs of these or naive animals was determined 12 h after i.v. injection of ^{125}I-ch14.18-IL2. This analysis revealed a strong localization of the tumor specific fusion protein within the tumor bearing organs. Since only parts of the organs' tissue is involved in the metastatic process, the ratio of ^{125}I-ch14.18-IL2 fusion protein localizing to the tumor or to normal tissue can be ex-

Table 1. *Effect of the Tumor Specific Antibody-IL2 Fusion Protein on Established Pulmonary and Hepatic Metastases*

Pulmonary metastasis	Treatment*	No. of Foci
	None	254, >500, >500, >500, >500, >500, >500, >500‡
		>500, >500, >500, >500, >500, >500, >500
	rIL2 + ch14.18	96, 167, 231, >500, >500, >500, >500, >500
		82, 151, 154, 163, >500, >500, >500, >500
	ch225-IL2	113, 136, 200, >500, >500, >500, >500
	ch14.18-IL2	0, 0, 0, 0, 0, 0, 1, 2
		0, 0, 0, 0, 0, 0, 0, 0
Hepatic Metastasis	**Treatment**	**Metastatic Score§**
	None	2, 3, 3, 3, 3, 3, 3‡
	rIL2 + ch14.18	2, 2, 2, 3, 3, 3, 3, 3
	ch14.18-IL2	0, 0, 0, 0, 0, 0, 0, 1

*Experimental pulmonary and hepatic metastases were induced by i.v. injection of 5×10^5 or intrasplenic injection of 2.5×10^5 B78-D14 cells, respectively. Treatment was started 1 wk thereafter and consisted of daily i.v. administration of PBS, 8 μg chimeric monoclonal antibody ch14.18 and 24000 IU recombinant IL2, or 8 mg of either the non-specific fusion protein ch225-IL2 or the tumor-specific fusion protein ch14.18-IL2 as indicated for seven consecutive days.

‡All experimental groups were started with eight mice; animals found dead before the planned killing date were not included in the evaluation.

Differences in numbers of metastatic foci and scores between the fusion protein group and all control groups were statistically significant ($P \leq 0.001$).

§Results are given as metastatic score with 0 = no visible metastatic foci, 1 = less than 5% of the liver surface covered with metastatic foci, 2 = between 5 and 50% of the liver surface covered with metastatic foci, and 3 = more than 50% of the liver surface covered with metastatic foci.

pected to be even higher than the experimental results indicate.

T Cell Dependency of Fusion Protein-induced Tumor Rejection. To test whether NK cells are essential for the antitumor effect of antibody-IL2 fusion proteins, we induced experimental pulmonary metastases of B78-D14 cells in C57BL/6 *beige/beige* mice. Since these mice lack functional NK activity, any therapeutic host response induced is independent of NK cells. This was the case, as treatment of tumor bearing NK-deficient mice with ch14.18-IL2 caused a complete eradication of tumor micrometastases (Table 2). The second series of studies with immunodeficient mice addressed the relevance of T cells for the observed tumor eradication. B78-D14 cells were injected i.v. into T cell–deficient C57BL/6 *scid/scid* mice and therapy with ch14.18-IL2 was started 7 d thereafter. In the absence of T cells the therapeutic efficacy of the antibody-IL2 fusion protein is dramatically reduced. In fact, a complete eradication of micrometastases was not achieved in any of the animals (Table 2). This observation strongly suggests a T cell–dependent mechanism for the demonstrated antitumor effect. Thus, the participation of T cell subsets in the fusion protein-induced tumor regression was investigated by systemic in vivo depletion of T cell subpopulations with specific antibodies. Since NK cells might be able to substitute for some functions of depleted T cell populations, these studies were done in C57BL/6 *beige/beige* mice. These studies revealed that depletion of CD4+ T cells did not significantly interfere with the antibody-IL2 induced immune response (Table 2). In contrast, depletion of CD8+ or both CD4+ and CD8+ cells abrogates the therapeutic effect of the administered fusion protein. Provided that depletion of each T cell subset was effective and specific, these results indicate that

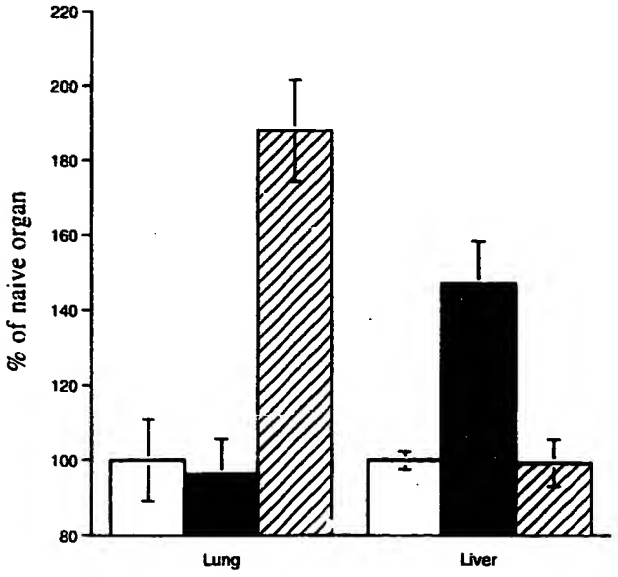

Figure 1. Biodistribution of ch14.18-IL2. C57BL/6 mice bearing either no (*white*), pulmonary (*striped*), or hepatic (*black*) metastases established for 14 d were injected with 5 μCi ^{125}I-labeled ch14.18-IL2 and the amount of radioactivity in lung or liver was measured 12 h thereafter. Each value represents the mean and standard deviation for three animals.

Table 2. *Effect of Antibody-IL2 Fusion Protein Therapy on Micrometastases in Immunodeficient and T Cell–depleted Mice*

Mice*	In vivo depletion‡	Treatment	No. of Foci
C57BL/6 *beige/beige*	None	None	>500, >500, >500, >500, >500, >500, >500
	None	rIL2 + ch14.18	149, 187, >500, >500, >500, >500, >500, >500
	None	ch14.18-IL2	0, 0, 0, 0, 0, 0, 3, 21
C57BL/6 *scid/scid*	None	None	>500, >500, >500, >500, >500, >500
	None	rIL2 + ch14.18	149, 187, >500, >500, >500, >500, >500, >500
	None	ch14.18-IL2	98, 131, 150, 171, 180, 180, 200, >500
C57BL/6 *beige/beige*	None	None	>500, >500, >500, >500
	None	ch14.18-IL2	0, 0, 0, 2
	CD4	ch14.18-IL2	0, 0, 22, 62
	CD8	ch14.18-IL2	56, 79, 126, >500
	CD4 + CD8	ch14.18-IL2	78, 142, >500, >500

*Experimental pulmonary metastases were induced in C57BL/6 *beige/beige* or *scid/scid* mice by i.v. injection of 5×10^5 B78-D14 cells; treatment was started 1 wk thereafter and consisted of daily i.v. administration of PBS, 8 μg chimeric monoclonal antibody ch14.18 and 24,000 IU recombinant IL2 or 8 μg of the tumor-specific fusion protein ch14.18-IL2 as indicated for 7 consecutive days.
‡C57BL/6 *beige/beige* mice were depleted of CD4+, CD8+ or both cell populations by weekly i.p. injections of 500 μg anti-CD4, anti-CD8 or both mAb starting 3 d before induction of tumors.
§All experimental groups were started with eight mice; animals found dead before the planned killing date were not included in the evaluation.

only the presence of CD8+ T cells is mandatory for tumor eradication.

The third line of evidence indicating the involvement of CD8+ T cells was provided by cytotoxicity studies. Spleen cells isolated from mice after induction of pulmonary metastases and subsequent treatment with ch14.18-IL2 displayed a high cytolytic activity against B78-D14 cells in a 4-h ^{51}Cr-release assay (Fig. 2 *A*). Enrichment for CD8+ T cells, demonstrated that this cell population provides the major contribution to the detected cytolytic activity (Fig. 2 *B*). Furthermore, blocking studies with antibodies against H-2K^b/H-2D^b antigens (clone 28-8-6, C3H IgG$_{2a}$, κ) proved that the killing of B78-D14 cells by either unselected primed lymphocytes or the CD8+ subset thereof is MHC class I restricted. In contrast, spleen cells from tumor bearing mice treated with the same amount of a fusion protein (ch225-IL2) not reacting with the tumor showed no specific lysis of tumor cells.

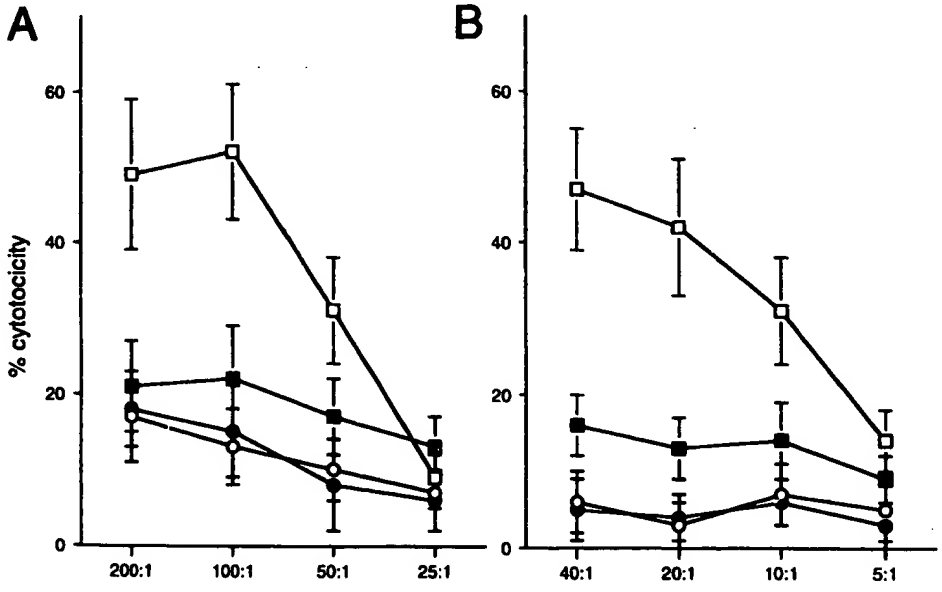

Figure 2. T cell mediated cytotoxicity against B78-D14 induced by antibody-IL2 fusion proteins. C57BL/6 mice bearing pulmonary metastases of B78-D14 melanoma cells, were treated 1 wk after tumor induction with 8 μg ch14.18-IL2 (*squares*) or nonspecific fusion protein ch225-IL2 (*circles*) for 7 d. Splenocytes (*A*) or CD8+ cells (*B*) were isolated 3 d after cessation of therapy and analyzed for their lytic activity against B78-D14 cells. Experiments were performed in the absence (*open symbols*) or presence (*closed symbols*) of an excess (50 μg/ml) of antibodies directed against H-2K^b/H-2D^b MHC class I antigens (clone 28-8-6, C3H IgG$_{2a}$, κ). Percentage of specific lysis is plotted on the y-axis for various effector to target rations. Each value represents the mean and standard deviation for three animals.

Discussion

Antibody-cytokine fusion proteins combine the unique targeting ability of antibodies with the multifunctional activity of cytokines. In the present report we demonstrate the therapeutic effectiveness of such constructs for the treatment of established hepatic and pulmonary melanoma metastases. Several lines of evidence, i.e., in vivo depletion studies and in vitro cytotoxicity assays, indicate that this antitumor effect is largely dependent on CD8+ T cells, which kill the tumor cells in an MHC class I–restricted manner.

Since becoming available in recombinant form, IL2 has been used as an in vivo T cell growth factor in the treatment of patients with advanced renal cell carcinoma or melanoma (4). The aim of this partially successful approach is to generate or propagate tumor-reactive lymphocytes. Forni et al. demonstrated that injection of a physiological dose of IL2 directly into tumors caused suppression of their growth (9). The major advantage of an in situ application is that it avoids certain forms of toxicity associated with the systemic use of cytokines. Recently, in situ cytokine therapy has been developed further by transferring cytokine genes into tumor cells (2, 3). We reasoned that by using the targeting ability of tumor-specific monoclonal antibodies we could develop a technically more simple strategy to achieve effective concentrations of IL2 in the tumor microenvironment (5). We demonstrate here that this approach is capable to induce and maintain effective IL2 concentrations at the tumor site. Analysis of the biodistribution of ^{125}I-ch14.18-IL2 demonstrated its localization in tumor bearing livers and lungs. Therefore, it seems feasible to achieve effective local cytokine concentrations at the tumor site in a non personalized way, which makes this approach more practicable for clinical applications than the ex vivo transfer of cytokine genes. Furthermore, antibody-targeted IL2 therapy is essentially different from such gene transfer approaches with regard to the order of events; the latter aims at the induction of an antitumor host immune response by re-inoculation of IL2-producing tumor cells, whereas antibody-IL2 fusion protein therapy directs IL2 to the microenvironment of established tumors. This is particularly noteworthy, not only because of the high clinical relevance of this setting, but also because it might change immune reactions in several ways. The host immune system has most likely encountered the tumor before the immune modulation is initiated. Therefore, priming of T cells may have already occurred via antigen presenting cells, e.g., macrophages or dendritic cells; especially, since tumor cells are more sensitive to the innate cytodestructive effects of these cells immediately after inoculation than after establishment in micrometastases. Another possibility is that some tumor cells might have metastasized to the draining lymph node during this period. This would overcome the problem that naive T cells are compartmentalized in blood and lymphoid organs (10).

Taking these considerations into account, there are a number of possible mechanisms by which antibody-IL2 fusion proteins can induce eradication of disseminated tumor metastases. First, the tumor cells themselves might interact with naive T cells with IL-2 acting as the second costimulatory signal in the activation of cytotoxic T cells. A recent model proposed by J. Sprent for the activation of naive T cells provides the rationale for this mechanism (11) . According to this model, high-avidity interactions oetween peptide-MHC class I complexes and the T cell receptor promotes strong cross-linking of T cell receptor-CD3 complexes, which in turn leads to strong signaling; thereby stimulating the production of cytokines, such as IL2, and receptors thereof; costimulation boosts the T cell receptor mediated signal. If the intensity of signaling is below a certain threshold, e.g., when the density of peptide-MHC complexes or the level of costimulation is low, the responding T cells express IL2 receptors, but no IL2. Hence, these T cells fail to proliferate unless exposed to exogenous IL2. The second possible scheme for the establishment of T cell activation is based on tumor antigens being processed by antigen-presenting cells that transfer to the lymph node, where T cell priming then occurs. It has been shown that preactivated macrophages, dendritic cells and granulocytes express receptors for IL2 and that in vitro culture with IL2 causes functional changes in these cells (12, 13). After arriving at the tumor site these cells may be activated by the antibody-targeted IL2 to kill these tumor cells and subsequently present the tumor antigens to T cells. One further possibility is that the CD8+ T cells act as non-specific IL2-activated killer cells. However, since the applied amounts of IL2-activity are too low to induce a generalized LAK cell phenomenon (4), and application of a tumor-unspecific fusion protein failed to show any therapeutic effect or to induce B78-D14 cytolytic cells, this possibility is rather unlikely. Furthermore, in vitro cytotoxicity studies confirmed the MHC class I restriction of the antibody-IL2 fusion protein-induced immune response.

In conclusion, we have demonstrated the efficacy of antibody targeted-IL2 in the treatment of established, disseminated melanoma metastases affecting clinically relevant organs. The fusion protein-induced eradication of the tumor is critically dependent on T cells, and is likely due to either priming of naive T cells, the activation of cytotoxic effector cells, or both.

We wish to express our appreciation for Jessica van Leeuwen's and Manuel Perez's skilled and dedicated care of the animals. J.C. Becker extends special thanks to Prof. Dr. Eva-Bettina Bröcker (Department of Dermatology, University of Würzburg) for her ongoing support and encouragement.

This work was supported by Outstanding Investigator Grant CA 42508-09. J.C. Becker was support by a training grant of the Deutsche Forschungsgemeinschaft. This is The Scripps Research Institute's manuscript number 9756-IMM.

Address correspondence to Ralph A. Reisfeld, The Scripps Research Institute, IMM13, 10666 North Torrey Pines Road, La Jolla, CA 92037.

Received for publication 1 December 1995 and in revised form 5 March 1996.

References

1. Talmage, D.W., J.A. Woolnough, H. Hemmingsen, L. Lopez, and K.J. Lafferty. 1977. Activation of cytotoxic T cells by non-stimulating tumor cells and spleen cell factor(s). *Proc. Natl. Acad. Sci. USA.* 74:4610–4614.
2. Schmidt-Wolf, G., and I.G.H. Schmidt-Wolf. 1995. Cytokines and clinical gene therapy. *Eur. J. Immunol.* 25:1137–1140.
3. Colombo, M.P., and G. Forni. 1994. Cytokine gene transfer in tumor inhibition and tumor therapy: where are we now? *Immunol. Today.* 15:48–51.
4. Maas, R.A., H.F.J. Dullens, and W.D. Otter. 1993. IL2 in cancer treatment. *Cancer Immunol. Immunother.* 36:141–148.
5. Gillies, S.D., E.B. Reilly, K.-M. Lo, and R.A. Reisfeld. 1992. Antibody-targeted interleukin 2 stimulates T-cell killing of autologous tumor cells. *Proc. Natl. Acad. Sci. USA.* 89: 1428–1432.
6. Becker, J.C., J.D. Pancook, S.D. Gillies, J. Mendelsohn, and R.A. Reisfeld. 1996. Eradication of human hepatic and pulmonary melanoma metastases in SCID mice by antibody-interleukin 2 fusion proteins. *Proc. Natl. Acad. Sci. USA.* In press.
7. Haraguchi, M., S. Yamashiro, A. Yamamoto, K. Furukawa, K. Takamiya, K.O. Lloyd, H. Shiku, and K. Furukawa. 1994. Isolation of GD3 synthase gene by expression cloning of GM3 α-2,8-sialtransferase cDNA using anti-GD2 monoclonal antibody. *Proc. Natl. Acad. Sci. USA.* 91:10455–10459.
8. Ledbetter, J.A., R.V. Rouse, H.S. Micklem, and L.A. Herzenberg. 1980. T cell subsets defined by expression of Lyt-1,2,3 and Thy-1 antigens. *J. Exp. Med.* 152:280–295.
9. Forni, G., G. Mirrella, A. Santoni, A. Modesti, and M. Forni. 1987. Interleukin 2 activated tumor inhibition in vivo depends on the systemic involvement of host immunoreactivity. *J. Immunol.* 138:4033–4041.
10. Mackay, C.R. 1993. Immunological Memory. *Adv. Immunol.* 53:217–265.
11. Sprent, J. 1995. Professionals and amateurs. *Curr. Biol.* 5: 1095–1097.
12. Steinman, R.M. 1991. The dentritic cell system and its role in immunogenicity. *Annu. Rev. Immunol.* 9:271–307.
13. Strobel, I., R. Rupec, A. Wollenberg, and T. Bieber. 1993. IL-2 receptor on human Langerhans cells lack the β-chain but mediates IL-2 dependent migration: evidence for a putative γ-chain? *Arch. Dermatol. Res.* 285:108.

Proc. Natl. Acad. Sci. USA
Vol. 89, pp. 1428–1432, February 1992
Immunology

Antibody-targeted interleukin 2 stimulates T-cell killing of autologous tum r cells

(recombinant antibody/cytokine fusion protein/tumor-infiltrating lymphocytes)

STEPHEN D. GILLIES*†, EDWARD B. REILLY*, KIN-MING LO*, AND RALPH A. REISFELD‡

*Research Department, Abbott Biotech, Inc., 119 Fourth Avenue, Needham Heights, MA 02194; and ‡Department of Immunology, The Scripps Research Institute, 10666 North Torrey Pines Road, La Jolla, CA 92037

Communicated by M. Frederick Hawthorne, November 14, 1991

ABSTRACT **A genetically engineered fusion protein consisting of a chimeric anti-ganglioside GD2 antibody (ch14.18) and interleukin 2 (IL2) was tested for its ability to enhance the killing of autologous GD2-expressing melanoma target cells by a tumor-infiltrating lymphocyte line (660 TIL). The fusion of IL2 to the carboxyl terminus of the immunoglobulin heavy chain did not reduce IL2 activity as measured in a standard proliferation assay using either mouse or human T-cell lines. Antigen-binding activity was greater than that of the native chimeric antibody. The ability of resting 660 TIL cells to kill their autologous GD2-positive target cells was enhanced if the target cells were first coated with the fusion protein. This stimulation of killing was greater than that of uncoated cells in the presence of equivalent or higher concentrations of free IL2. Such antibody–cytokine fusion proteins may prove useful in targeting the biological effect of IL2 and other cytokines to tumor cells and in this way stimulate their immune destruction.**

Much attention has been focused on the use of interleukin 2 (IL2) for cancer immunotherapy because of its stimulatory effect on a broad range of immune cell types, including both T and B cells, monocytes, macrophages, and natural killer cells. One class of cells resulting from *in vitro* or *in vivo* stimulation of immune cells has been called lymphokine-activated killer cells (1), and therapeutic approaches using such populations have shown clinical responses with some tumor types (2). Other, more refractory tumors may show greater responses if monoclonal antibodies directed against these tumors are used in combination with IL2 (3, 4). Such antibodies mediate antibody-dependent cellular cytotoxicity (ADCC) through their interactions with both the tumor cell antigen and the Fc receptor (CD16) present on certain subsets of natural killer cells, monocytes, granulocytes, and macrophages.

While IL2 treatment *in vivo* leads to increases in both natural killer and ADCC activities, the cytolytic activity of antigen-specific, major histocompatibility complex (MHC)-restricted T cells may actually be reduced (5). Treatment of T cells with anti-CD3 antibody prior to IL2 exposure greatly increases T-cell cytolytic activity (6). Likewise, expansion of tumor-infiltrating lymphocytes (TIL) by culture in the presence of high concentrations of IL2 with periodic target-cell stimulation leads to substantial increases in cytolytic activity (7). Both approaches involve costimulation of IL2 and T-cell antigen receptors for expansion and maintenance of T-cell cytolytic activity. Thus, an optimal therapy might combine IL2 activation and tumor antigen presentation together with a tumor-specific antibody that mediates both complement-dependent cyt t xicity (CDC) and ADCC activities. By combining a chimeric anti-ganglioside GD2 antibody (ch14.18) which has potent CDC and ADCC activities (8), with IL2, we hope to target this cytokine to tumors such as neuroblastoma (9, 10) and melanoma (11) expressing GD2. In this way, relatively large amounts of tumor antigens should be present during IL2 activation for expansion of cytotoxic T cells, since melanoma cell lines have been reported to express an average of 1.5×10^7 sites per cell for ch14.18 (8). Furthermore, the antibody would also be available to target Fc receptor-bearing cells that have been activated by the targeted IL2.

The ch14.18 antibody used in this report has already been shown to mediate potent ADCC activity by IL2-activated peripheral blood mononuclear cells from cancer patients (12). We have focused on the ability of a ch14.18–IL2 fusion protein to stimulate the proliferation and cytolytic activity of a human T-cell line against autologous melanoma targets. This cell line, 660 TIL, is $CD3^+$, $CD8^+$, antigen-specific, and MHC class I-restricted and was originally obtained by outgrowth from a human metastatic melanoma (13). A melanoma line, 660 mel, was derived from the same tumor and serves as a source for antigen stimulation and as an autologous target for 660 TIL (14). Results of this study show that tumor cells coated with a fusion protein in which IL2 is at the carboxyl terminus of the heavy-chain constant region 3 (CH3) exon of ch14.18 (CH3–IL2) efficiently stimulate resting 660 TIL cells to kill autologous targets. These coated cells serve as a model for tumors that have been targeted *in vivo*.

MATERIALS AND METHODS

Plasmid Constructs. The immunoglobulin–IL2 fusion protein expression vector was constructed by fusing a synthetic human IL2 sequence to the carboxyl end of the human $C_\gamma 1$ gene. A synthetic DNA linker, extending from the *Sma* I site near the end of the antibody coding sequence to the single *Pvu*II site in the IL2 sequence, was used to join the amino-terminal codon of mature IL2 to the exact end of the CH3 exon (CH3–IL2). The fused gene was inserted into the vector pdHL2-14.18 as described earlier for an antibody–lymphotoxin fusion protein construct (15). Additional constructs were made in which the IL2 sequence was fused to the *Sac* I site in the hinge region of the human $C_\gamma 3$ gene (Fab–IL2) or to the end of the CH2 exon at a *Taq* I site (CH2–IL2). In both cases synthetic linkers were used to fuse the antibody and IL2 sequences directly without introducing any additional amino acid residues.

Transfection and Purification. The expression plasmids were introduced into Sp2/0-Ag14 cells by protoplast fusion and selected in Dulbecco's modified Eagle's medium (GIBCO) containing 10% fetal bovine serum and 100 nM

The publication costs of this article were defrayed in part by page charge payment. This article must therefore be hereby marked "*advertisement*" in accordance with 18 U.S.C. §1734 solely to indicate this fact.

Abbreviations: ADCC, antibody-dependent cellular cytotoxicity; CDC, complement-dependent cytotoxicity; IL2, interleukin 2; MHC, major histocompatibility complex; TIL, tumor-infiltrating lymphocyte(s); C, constant; CH, heavy-chain C region; V, variable.

†To whom reprint requests should be addressed.

methotrexate. Clones secreting the fusion proteins were identified by ELISA (16). The highest producers were grown in increasing concentrations of methotrexate and subcloned in medium containing 5 μM methotrexate. The CH3–IL2 fusion protein was purified using protein A-Sepharose (Repligen, Cambridge, MA) as affinity adsorbent. Small amounts of the Fab–IL2 and CH2–IL2 proteins were purified using an anti-human κ chain immunoaffinity column.

Antigen-Binding Activity. The antigen-binding activity was measured in a solid-phase ELISA using a chloroform extract of human neuroblastoma cells as a source of GD2 (17). In some cases the fusion proteins were first treated with plasmin (0.125 casein unit/ml) in 50 mM Tris, pH 8/150 mM NaCl for 1–2 hours at 37°C. Aprotinin (Sigma) was added at the end of the digestion (200 kallikrein inhibitory units/ml) when the digested protein was tested for antigen binding or IL2 activity.

Human TIL Culture. The 660 TIL line and its autologous $GD2^+$ tumor line 660 mel were established from a human melanoma tumor sample and maintained in culture as described (14).

IL2 Assays. IL2 activity of antibody–IL2 fusion proteins was assayed in standard T-cell proliferation assays using either the mouse CTLL-2 line (18) or 660 TIL. After IL2 depletion for 48 hr, 3×10^4 CTLL-2 cells or 10^5 660 TIL cells were added to individual wells of a 96-well microtiter plate in a volume of 0.2 ml with various concentrations of fusion protein (normalized for IL2 content) or recombinant IL2 [either yeast-derived (Genzyme) or bacteria-derived (Hoffmann–La Roche)]. After 72 hr, 0.5 μCi (18.5 kBq) of [*methyl*-^{3}H]thymidine was added to each well, and plates were harvested 12 hr later. All samples were tested in duplicate.

Cytotoxicity Assays. Cytolytic activity of 660 TIL was measured in ^{51}Cr-release assays against 660 mel target cells. The 660 TIL cells were depleted of IL2 for 4 days prior to their use in assays except where noted. Target cells (3×10^6) were labeled with 300 μCi of $Na_2{}^{51}CrO_4$ (Amersham) for 1 hr at 37°C and washed in RPMI 1640 with 10% heat-inactivated fetal bovine serum. For experiments in which target cells were coated with antibody, ^{51}Cr-labeled target cells (10^6 in 1 ml) were incubated with ch14.18 or CH3–IL2 fusion protein (50 μg/ml in RPMI 1640 with 10% heat-inactivated fetal bovine serum). After 1 hr at 4°C with periodic mixing, cells were washed three times with serum-containing medium to remove excess antibody and were used in cytotoxicity assays. In some experiments the effect of adding either antibody or IL2 at the time of assay was determined. Duplicate assay mixtures were incubated at 37°C for 7–16 hr.

RESULTS

Characterization of Immunoglobulin–IL2 Fusion Proteins. Several forms of antibody–IL2 fusion proteins were constructed and expressed in transfected hybridoma cells. In initial studies we compared antigen-binding and IL2 activities of constructs consisting of a chimeric light chain, expressed in the same transfected cell with various truncated heavy chain–IL2 fusion proteins. In one case IL2 was fused to the beginning of the first hinge domain of the human $C_\gamma 3$ gene (deleting CH2 and CH3 exons) and in another construct IL2 was fused to the end of the CH2 exon (deleting CH3; Fig. 1*A*). These heavy-chain fusion protein constructs were expressed together with the variable (V) regions of the anti-GD2 antibody 14.18 and the human C_κ gene. Secreted heavy chains were found to associate with the chimeric light chain to form Fab–IL2 or CH2–IL2 fusion proteins, but the latter did not assemble into a whole antibody even though it contained an intact hinge region (Fig. 1*B*). The covalent disulfide bonds that are normally involved in inter-heavy-chain binding are contained in the hinge.

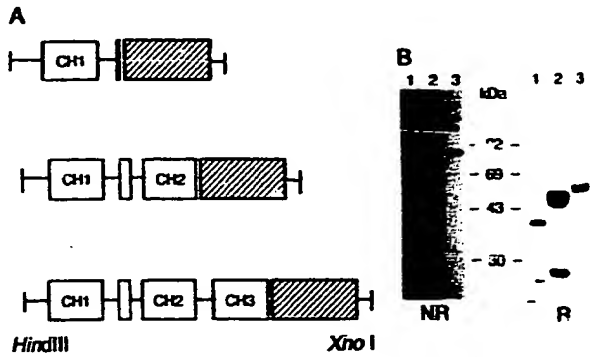

FIG. 1. Construction of fusion protein genes and analysis of the expressed proteins. (*A*) IL2 sequence (hatched box) was joined to the human $C_\gamma 3$ (Fab–IL2) or $C_\gamma 1$ heavy-chain gene by using synthetic DNA linkers, to express (from top to bottom) Fab–IL2, CH2–IL2, and CH3–IL2 constructs. Unlabeled open box represents the hinge region. (*B*) Gel electrophoretic analysis of Fab–IL2 expressed with B72.3 V regions (lanes 1), chimeric 14.18 whole antibody (lanes 2), and CH2–IL2 expressed with 14.18 V regions (lanes 3). Samples either were nonreduced (NR) or were reduced (R) with 2-mercaptoethanol. The gel was stained with Coomassie blue.

The antigen-binding and IL2 activities of these proteins are summarized in Table 1. The Fab–IL2 protein containing the 14.18 V regions had no antigen-binding activity (within the limits of our binding assay), whereas the CH2–IL2 protein was strongly positive. The 14.18 Fab, produced by genetic engineering, had greatly reduced antigen binding (data not shown), suggesting that bivalency is required for full activity. We then constructed a second Fab–IL2 fusion protein using the V regions of the anti-TAG 72 antibody B72.3 (19), to test whether such a molecule could be made that retained both IL2 activity and antigen binding. The B72.3 Fab–IL2 protein had normal antigen-binding activity, and all of the fusion proteins had IL2 specific activities ranging from 5 to 6.5×10^6 units/mg when normalized for IL2 content.

We next decided to construct a whole antibody–IL2 fusion protein by fusing the coding sequence of IL2 to the end of the heavy-chain CH3 exon (CH3–IL2). In this way we hoped to produce fully assembled IL2 fusion proteins that might also have more favorable pharmacokinetic properties *in vivo* and that could most likely be purified by protein A-Sepharose affinity chromatography. The CH3–IL2 protein constructed with the 14.18 anti-GD2 V regions was found to be expressed as a fully assembled antibody fusion protein (Fig. 2 *Inset*) with full IL2 activity (see below) and to have enhanced antigen-binding activity. Since the carboxyl-terminal lysine residue of the heavy chain was contained in this construct (just before the +1 residue of mature IL2), we tested whether this site would be accessible to cleavage with proteases such as plasmin, which cleaves after lysine or arginine. The CH3–IL2 protein was treated with plasmin and subsequently analyzed by SDS/polyacrylamide gel electrophoresis.

Table 1. IL2 activity of immunoglobin–IL2 fusion proteins

Construct	V region	Antigen binding	IL2 activity
Fab–IL2	14.18	–	5.0×10^6
Fab–IL2	B72.3	+	6.0×10^6
CH2–IL2	14.18	+	6.5×10^6

IL2 activity in culture supernatants (without methotrexate) was determined by thymidine incorporation into mouse CTLL-2 cells. The amount of each fusion protein was determined by ELISA and the activity is reported as units/mg of IL2. Antigen binding was determined using GD2-coated (14.18) or mucin-coated (B72.3) plates as described (13).

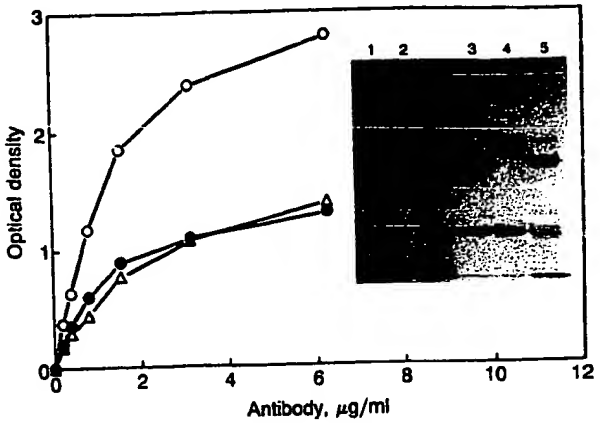

FIG. 2. Antigen-binding activity of CH3–IL2 (14.18) fusion protein before and after proteolytic cleavage to remove IL2. Purified CH3–IL2 was assayed for direct antigen-binding activity on GD2-coated plates before (○) and after (△) treatment with plasmin for 1 hr at 37°C. ●, Control. (*Inset*) Electrophoretic analysis of ch14.18 (lanes 1 and 3), CH3–IL2 (lanes 2 and 4), and plasmin-treated CH3–IL2 (lane 5) under nonreducing (lanes 1 and 2) or reducing (lanes 3–5) conditions. The unlabeled lane contained molecular size markers (see Fig. 1 for sizes).

The untreated CH3–IL2 protein had much higher binding activity in a direct antigen-binding assay than the chimeric antibody, and this enhanced activity was lost when IL2 was cleaved from the heavy chain with plasmin (Fig. 2). The gel analyses showed that the antibody itself was resistant to plasmin cleavage and that a heavy chain of the expected size was generated by cleavage at the antibody/IL2 junction. These results suggest that the fused IL2 domain actively interacts in some way with the antibody to alter antigen-binding activity. Upon removal of IL2, the normal level of activity is restored.

Since the CH3–IL2 construct was fully assembled into an antibody fusion protein, it is likely that this molecule has the most favorable properties for both *in vitro* and *in vivo* studies. It could also be readily purified by affinity chromatography on protein A-Sepharose. The availability of a matched set of TIL and its autologous tumor cell line, expressing the GD2 antigen, has allowed us to exploit this system as a model for testing the biological properties of antibody-targeted IL2. Such a system was not available for a tumor cell expressing the TAG 72 antigen. For these reasons we have focused our studies on the characterization of the ch14.18 CH3–IL2 fusion protein.

Biological Activities of Whole Antibody–IL2 Fusion Proteins. The IL2 activity of the CH3–IL2 (14.18) fusion protein was tested in a standard T-cell proliferation assay using either the mouse CTLL-2 line or a human TIL line (660 TIL) established from a metastatic melanoma. Both lines were cultured without IL2 for 48 hr prior to assay. The activity of the fusion protein was found to be somewhat less than that of a recombinant IL2 made in bacteria but was identical to that of a recombinant IL2 preparation produced in yeast (2.5×10^6 units/mg) when either the murine or the human T cells were used (Fig. 3). Thus, fusion of this cytokine at the carboxyl terminus of an antibody or antibody fragment does not significantly reduce its activity. We reported a similar result when we found that lymphotoxin (tumor necrosis factor β) retained its full activity when fused to the end of the CH3 domain (15). However, in that case some inactivation of lymphotoxin activity occurred during the elution from the protein A-Sepharose column. In contrast, the CH3–IL2 preparation used in this study was stable throughout the purification and during subsequent storage for up to 18

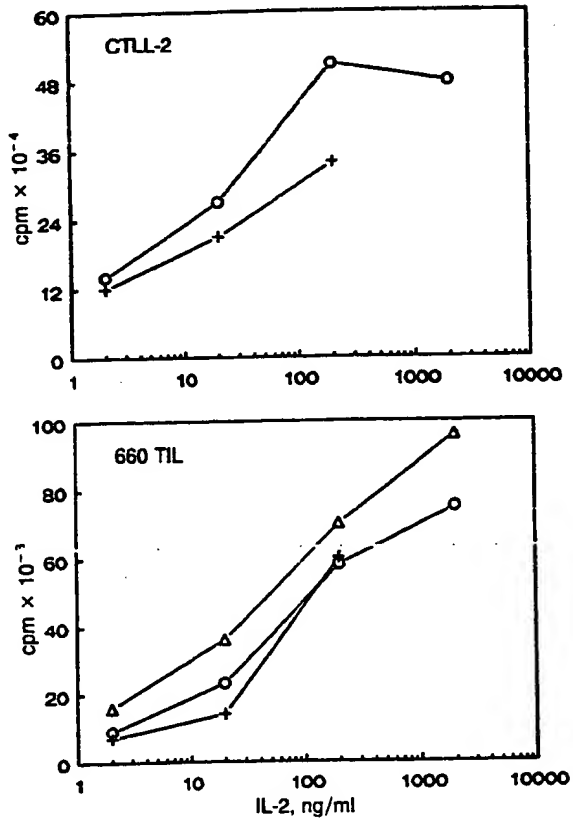

FIG. 3. IL2 activity of purified CH3–IL2 protein (○) as measured by [^{3}H]thymidine incorporation of mouse CTLL-2 (*Upper*) or human 660 TIL (*Lower*) T cells. Recombinant IL2 expressed in *Escherichia coli* (△) or in yeast (+) was used as control. Results were normalized to the IL2 content of the fusion protein.

months at −20°C. The effector functions of the CH3–IL2 protein—i.e., the ability to mediate complement and Fc receptor-dependent lysis—were also tested and found to be maintained (but somewhat decreased) when compared with that of the chimeric 14.18 antibody (data not shown). A similar result was reported for the CH3–lymphotoxin fusion protein (15).

Enhanced TIL Cytotoxic Activity of Autologous Tumor Targets. The human 660 TIL line was used to test the ability of the CH3–IL2 (14.18) fusion protein to stimulate the killing of GD2$^+$ autologous melanoma tumor cells (660 mel). The 660 TIL line is routinely cultured in serum-free medium containing IL2 (1000 units/ml) and is stimulated bimonthly with 660 mel to maintain killing activity (13). The lytic activity of this CD8$^+$ cell line for its target varies over time in culture as a function of antigen stimulation. For the purpose of this study we have also examined the effect of IL2 depletion on TIL cytotoxic activity and how this might be affected by subsequent addition of IL2 or the CH3–IL2 fusion protein. Consequently, the level of killing varies from one experiment to another, as does the ability of IL2 to enhance the killing in both normal and IL2-depleted cell cultures.

An example of a killing assay performed with 660 TIL shortly after antigen stimulation is shown in Fig. 4*A*. The tumor target cells were first coated with the fusion protein or with ch14.18 antibody and then used as targets in a 7-hr ^{51}Cr-release assay. At the higher effector/target ratio (50:1), the antibody alone stimulated killing, but to a much lesser extent than CH3–IL2. The effect of CH3–IL2 was more pronounced with TIL that had been deprived of IL2 for 4 days.

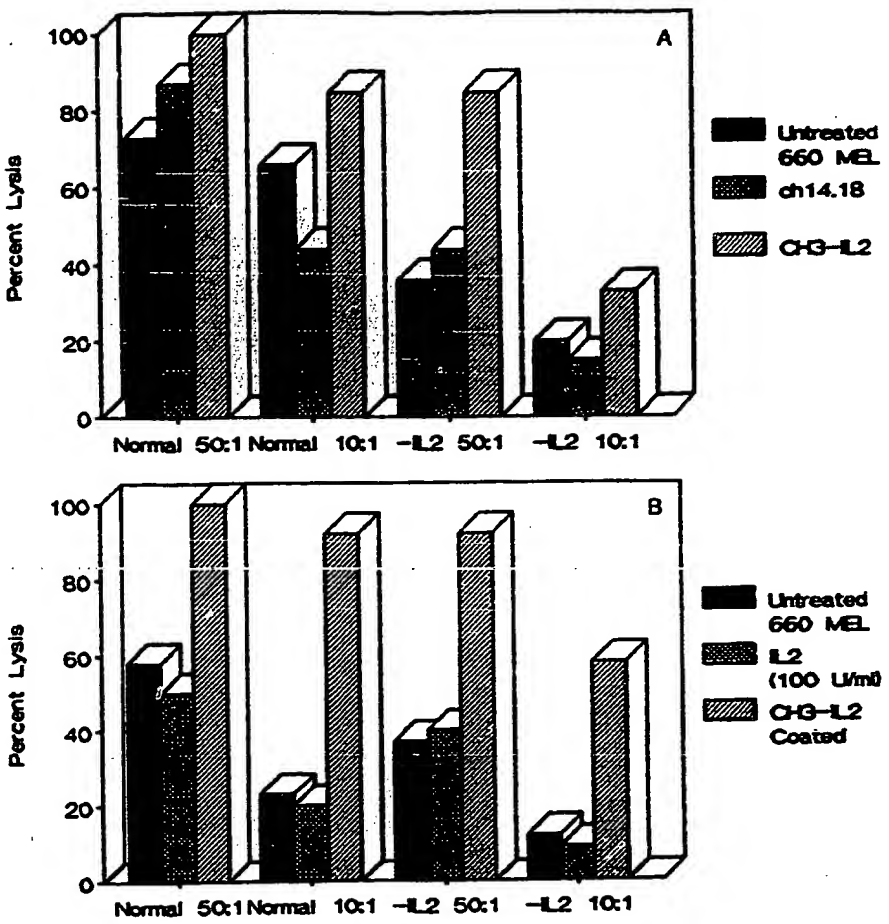

FIG. 4. Stimulation of autologous cytolytic activity by CH3–IL2-coated tumor cells. (*A*) Freshly stimulated 660 TIL cells were used as effectors against 660 mel targets in a 7-hr ^{51}Cr-release assay. Before the assay, the target cells were either untreated (filled bars) or coated with chi4.18 (cross-hatched bars) or CH3–IL2 (hatched bars). The effector cells (660 TIL) were taken from growing cultures (normal) or were cultured for 4 days without IL2 (−IL2) and were used at an effector/target ratio of 50:1 or 10:1. (*B*) Normal and IL2-depleted 660 TIL cells, 1 week after antigen stimulation, were used as effectors against untreated (filled bars) or CH3–IL2-coated (hatched bars) 660 mel targets at the indicated effector/target ratio in a 16-hr release assay. One set was incubated with added IL2 [100 units (U)/ml; cross-hatched bars].

A similar experiment comparing the fusion protein and exogenously added IL2 was performed 1 week later, when the autologous killing activity had declined. For this reason the duration of the cytotoxicity assay was extended to 16 hr. As seen in Fig. 4*B*, the addition of IL2 (100 units/ml) to the assay mixture had little effect. The stimulatory effect of CH3–IL2 in these experiments was quite striking, especially at the lower effector/target ratios and when IL2-depleted effector cells were used. The results were less pronounced once the TIL had been cultured without antigen stimulation with 660 mel tumor cells (data not shown). In all cases, the amount of stimulation obtained by coating the tumor cells exceeded that obtained by adding equivalent levels of IL2.

DISCUSSION

A fusion protein consisting of an intact tumor-specific chimeric antibody and human IL2 (CH3–IL2) has been shown to retain both antibody and IL2 functions. IL2 activity was measured by the ability of the fusion protein to stimulate the proliferation of resting human and mouse T cells. Constructs containing smaller portions of the antibody molecule were also found to retain full IL2 activity. These results contrast with an earlier report (20) in which a purified Fab–IL2 fusion protein was 200-fold less active than recombinant IL2 in a proliferation assay. Our constructs also differ from those reported by Fell *et al.* (20) in that we have directly fused antibody and IL2 sequences, without the introduction of artificial linker residues. In the case of our 14.18 Fab–IL2, we could not demonstrate antigen binding, but this was not likely due to the fusion of IL2, since a similar construct made with the V regions of B72.3 maintained both IL2 and antigen binding activities. Genetically engineered 14.18 Fab was also found to have greatly reduced antigen-binding activity.

Melanoma cells expressing GD2 that have bound the CH3–IL2 fusion protein serve as much better targets for cytotoxic T cells. This was demonstrated by using a TIL line (660 TIL) that had been maintained in culture in the presence of high concentrations of IL2 with periodic antigen stimulation by autologous melanoma cells (660 mel). The stimulatory effect was most pronounced when the TIL had been maintained without IL2 for several days. The amount of IL2 that would be bound to the 660 mel cells under saturating conditions would be equivalent to 50 units/ml in the assay, if these cells express $>10^7$ GD2 sites as was reported for M21 melanoma cells (8). These levels of IL2 added to the assay mixture were less effective than the fusion protein in stimulating cytolytic activity.

In the experiment depicted in Fig. 4*A*, there was some enhancement of killing of cells coated with chimeric antibody alone at the 50:1 effector/target ratio, suggesting some ADCC activity. However, the 660 TIL line does not contain detectable numbers of cells expressing Fc receptors as shown by immunofluorescence analyses (unpublished data).

The ability to combine the targeting of a tumor-specific antibody together with a potent cytokine such as IL2 should prove useful in directing and localizing its effect at tumor sites. In this regard, tumors secreting either IL2, tumor necrosis factor, or granulocyte colony-stimulating factor after transfection with genes encoding these molecules are rejected upon transplantation into syngeneic animals due to the establishment of cellular immunity (21–23). Antibody targeting of cytokines may achieve this same end by stimulating a cytotoxic T-cell response and in this way augment the helper T-cell function that may be lacking in cancer patients.

The use of a whole antibody–IL2 fusion protein may have advantages over antibody fragment–IL2 fusion proteins, since additional effector functions (ADCC and CDC) will be targeted to the same site. As discussed earlier, experiments using peripheral blood cells from patients treated with IL2 have already shown that the ch14.18 antibody can mediate ADCC against tumor cells (12). In this case the primary effector cells are Fc receptor-positive ($CD16^+$) natural killer cells. The work presented here suggests that cytotoxic T cells can also be stimulated to kill autologous antigen-positive cells that have been coated with the antibody–IL2 fusion protein.

We thank Giovanna Antognetti and Susan Foley for technical assistance. This work was supported, in part, by National Cancer Institute Grants RFA89-CA-03 and CA42508.

1. Grimm, E. A., Mazumder, A., Zhang, H. Z. & Rosenberg, S. A. (1982) *J. Exp. Med.* **155**, 1823–1841.
2. Rosenberg, S. A., Lotze, M. T., Muul, L. M., Chang, A. E., Avis, F. P., Leitman, S., Linehan, M., Robertson, C. N., Lee, R. E., Rubin, J. T., Seipp, C. A., Simpson, C. G. & White, D. E. (1987) *N. Engl. J. Med.* **316**, 889–897.
3. Eisenthal, A., Cameron, R. B., Uppenkamp, I. & Rosenberg, S. A. (1988) *Cancer Res.* **48**, 7140–7145.
4. Berinstein, N., Starnes, C. O. & Levy, R. (1988) *J. Immunol.* **140**, 2839–2845.
5. Hank, J. A., Sosman, J. A., Kohler, P. C., Bechhofer, R., Storer, B. & Sondel, P. M. (1990) *J. Biol. Response Modif.* **9**, 5–14.
6. Weil-Hillman, G., Schell, K., Segal, D. M., Hank, J. A., Sosman, J. A. & Sondel, P. M. (1991) *J. Immunother.* **10**, 267–277.
7. Rosenberg, S. A., Spiess, P. & Lafreniere, R. (1986) *Science* **223**, 1318–1321.
8. Mueller, B. M., Romerdahl, C. A., Gillies, S. D. & Reisfeld, R. A. (1990) *J. Immunol.* **144**, 1382–1386.
9. Schulz, G., Cheresh, D. A., Varki, N. M., Yu, A. L., Staffileno, L. K. & Reisfeld, R. A. (1984) *Cancer Res.* **44**, 5914–5920.
10. Cheung, N.-K., Saarinen, U. M., Neely, J. E., Landmeier, B., Donovan, D. & Coccia, P. F. (1985) *Cancer Res.* **45**, 2642–2649.
11. Cheresh, D. A., Harper, J. R., Schulz, G. & Reisfeld, R. A. (1984) *Proc. Natl. Acad. Sci. USA* **81**, 5767–5771.
12. Hank, J. A., Robinson, R. R., Surfus, J., Mueller, B. M., Reisfeld, R. A., Cheung, N.-K. & Sondel, P. M. (1990) *Cancer Res.* **50**, 5234–5239.
13. Reilly, E. B., Antognetti, G., Wesolowski, J. S. & Saikorafas, P. (1990) *J. Immunol. Methods* **126**, 273–279.
14. Reilly, E. B. & Antognetti, G. (1991) *Cell. Immunol.* **135**, 526–533.
15. Gillies, S. D., Young, D., Lo, K.-M., Foley, S. F. & Reisfeld, R. A. (1991) *Hybridoma* **10**, 347–356.
16. Gillies, S. D., Dorai, H., Wesołowski, J. S., Majeau, G., Young, D., Boyd, J., Gardner, J. & James, K. (1989) *Bio/Technology* **7**, 799–804.
17. Gillies, S. D., Lo, K.-M. & Wesolowski, J. A. (1989) *J. Immunol. Methods* **125**, 191–202.
18. Gillis, S., Ferm, M. M., Ou, W. & Smith, K. A. (1978) *J. Immunol.* **120**, 2027–2032.
19. Johnson, V. G., Schlom, J., Paterson, A. J., Bennet, J., Magnani, J. L. & Colcher, D. (1986) *Cancer Res.* **46**, 850–857.
20. Fell, H. P., Gayle, M. A., Grosmire, L. & Leibetter, J. A. (1991) *J. Immunol.* **146**, 2446–2452.
21. Fearon, E. R., Pardoll, D. M., Itaya, T., Golumbek, P., Levitsky, H. I., Simons, J. W., Karasuyama, H., Vogelstein, B. & Frost, P. (1990) *Cell* **60**, 397–403.
22. Asher, A. L., Mule, J. J., Kasid, A., Restifo, N. P., Salo, J. C., Reichert, C. M., Jaffe, G., Fendly, B., Kriegler, M. & Rosenberg, S. A. (1991) *J. Immunol.* **146**, 3227–3234.
23. Colombo, M. P., Ferrari, G., Stoppacciaro, A., Parenza, M., Rodolfo, M., Mavilio, F. & Parmiani, G. (1991) *J. Exp. Med.* **173**, 889–897.

1: J Neuroimmunol 1997 Feb;72(2):163-8 Related Articles, Links

TNF-alpha receptor fusion protein prevents experimental auto-immune encephalomyelitis and demyelination in Lewis rats: an overview.

Klinkert WE, Kojima K, Lesslauer W, Rinner W, Lassmann H, Wekerle H.

Department of Neuroimmunology, Max-Planck Institute for Psychiatry, Martinsried, Germany. klinkert@alf.biochem.mpg.de

To explore the therapeutic use of TNF-alpha inhibitors in human inflammatory demyelinating diseases we examined the effect of a recombinant TNFRp55 protein constructed by fusing TNFRp55 extracellular domain cDNA to a human IgG1 heavy gene fragment containing the hinge and constant domains CH2 and CH3 (TNFRp55-IgG1) in diverse experimental model systems representing inflammation and inflammatory demyelination of encephalitogenic T cells in vivo. In EAE actively induced by immunization of Lewis rats with MBP, a single dose of TNFRp55-IgG1 protected the recipient animals from clinical signs. Interestingly, the treatment neither prevented the formation CNS infiltrations, nor did it alter the cellular composition of the infiltrates. In EAE transferred by MBP specific activated T line cells, a model of inflammatory (not demyelinating) brain disease, the inhibitor's therapeutic effect on clinical disease was also striking achieving almost complete protection even after repeated transfers of encephalitogenic T cells. Finally, the recombinant inhibitor was also protective in Lewis rats with demyelinating experimental autoimmune panencephalitis produced by combined transfer of panencephalitogenic T cells and demyelinating monoclonal antibody specific for MOG. In this system, the T cells are of low encephalitogenic activity, but open the blood-brain barrier for the demyelinating immunoglobulins. The fusion protein treatment, however, prevented the formation of inflammatory lesions and demyelination. The strong therapeutic effect of the recombinant chimeric TNF-alpha inhibitor in three models of myelin specific autoimmunity raises hopes as to TNF-alpha directed therapy of human diseases like MS.

Publication Types:

THE JOURNAL OF BIOLOGICAL CHEMISTRY

Vol. 270, No. 8, Issue of February 24, pp. 3958–3964, 1995
Printed in U.S.A.

Interferon γ Receptor Extracellular Domain Expressed as IgG Fusion Protein in Chinese Hamster Ovary C lls

PURIFICATION, BIOCHEMICAL CHARACTERIZATION, AND STOICHIOMETRY OF BINDING*

(Received for publication, July 19, 1994, and in revised form, September 28, 1994)

Michael Fountoulakis‡§, Cecilia Mesa‡, Georg Schmid¶, Reiner Gentz‖, Michael Manneberg‡, Martin Zulauf, Zlatko Dembic‡, and Gianni Garotta‡**

*From F. Hoffmann-La Roche Ltd., Pharmaceutical Research, ‡Department of Gene Technology, ¶Department of Biotechnology, and **Department of Physics, CH-4002 Basel, Switzerland*

Agents that antagonize the functions of interferon γ (IFNγ) are potential pharmaceuticals against several immunological and inflammatory disorders. IFNγ receptor-immunoglobulin G fusion proteins (IFNγR-IgG) function as antagonists of endogenous IFNγ and have longer half-lives *in vivo* in comparison with soluble IFNγ receptors (sIFNγR), consisting of the extracellular region of the native sequence. A fusion protein comprising the extracellular domain of the human IFNγ receptor and the hinge, CH_2 and CH_3 domains of the human IgG3 constant region, was expressed in Chinese hamster ovary cells. The IFNγR-IgG3 fusion protein was secreted into the culture medium as a 175-kDa glycoprotein and was purified over Protein G-Sepharose, DEAE-Sepharose, and size exclusion chromatography. IFNγR-IgG3 bound IFNγ in solid phase assays and ligand blots, competed for the binding of radiolabeled IFNγ to the cell surface receptor of Raji cells, and inhibited the IFNγ-mediated antiviral activity with an efficiency at least one order of magnitude higher than that of the soluble receptor produced in the same expression system. Two IFNγR-IgG3 fusion proteins bound two IFNγ dimers forming a complex of approximately 380 kDa. In immunodiffusion assays, the IFNγR-IgG3 fusion protein did not precipitate IFNγ. Dissociation of bound IFNγ from IFNγR-IgG3 was 2-fold slower than from the sIFNγR produced in insect cells.

Interferon γ (IFNγ)[1] is a cytokine, produced by activated T lymphocytes and natural killer cells, that exerts complex functions in the control and modulation of nearly all phases of immunological and inflammatory responses (1–3). The active protein is a homodimer with a predominant α-helical structure, the two subunits showing an anti-parallel organization (4). IFNγ exerts its functions by interacting with a ubiquitous, specific cell receptor (5–7), a 90-kDa glycoprotein (8–10). In addition to IFNγ and IFNγR, accessory proteins are required for signal transduction (11–15). Recently the cloning of such an accessory factor or IFNγR β-chain was reported (16, 17). It is not clear at present whether the accessory protein participates in ligand binding. The IFNγR does not possess intrinsic tyrosine kinase activity, suggesting receptor association with specific kinases following ligand binding (18–20). The signal transduction pathway of IFNγ involves phosphorylation of p91, a subunit of the IFN-stimulated gene factor-3 (21, 22).

In certain immunological disorders, IFNγ acts as a disease-promoting agent, and substances that antagonize its functions are potential pharmaceuticals (23, 24). In order to obtain IFNγ antagonists, we engineered soluble forms of the IFNγ receptor (sIFNγR), comprising the extracellular domain of the native protein and retaining full capacity for binding IFNγ (25, 26). When administered to animals, the sIFNγRs inhibited the activity of IFNγ, but they showed relatively short half-lives of 1–3 h in the blood and 6 h in lymphoid organs (28, 29). Fusion proteins comprising the extracellular domain of the mouse IFNγ receptor and sequences of the mouse constant IgG region were active *in vivo* and showed an increased blood persistency (30, 31). Because administered human sIFNγR is expected to have a short half-life, we expressed in Chinese hamster ovary (CHO) cells a fusion protein comprising the extracellular domain of the human IFNγR and parts of the human IgG constant chain. Here we report on the purification and characterization of this human fusion protein and the stoichiometry of its interaction with IFNγ.

EXPERIMENTAL PROCEDURES

Materials—Reagents for the preparation of SDS-polyacrylamide gels and protein size markers were from Bio-Rad. ^{14}C-Protein markers and iodinated sheep anti-mouse Ig were from Amersham. Protein G- and DEAE-Sepharose were from Pharmacia Biotech Inc. Proteolytic enzymes were purchased from Boehringer Mannheim.

IFNγ—Human IFNγ was purified from *Escherichia coli* according to Döbeli *et al.* (32) and was iodinated utilizing the chloramine-T method (33) to 2 × 10^6 cpm/ng of protein. The monoclonal antibody γ69 was raised against recombinant IFNγ.

Soluble Human IFNγ Receptors Produced in CHO and Insect Sf9 Cells—The proteins were purified essentially like the soluble mouse IFNγR produced in insect cells (26, 34). The monoclonal antibody γR99 was raised against the native IFNγR (10), and the polyclonal 3891 was raised against the sIFNγR produced in *E. coli* (25).

Analytical Methods—The fusion protein and the soluble receptors were resolved on 7.5 and 12% SDS-polyacrylamide gels, respectively, and revealed by staining with Coomassie Blue. The purity of the proteins was estimated by densitometric analysis of the stained SDS gels. If not otherwise indicated, no reducing agent was present in the sample buffer. Where it is mentioned, the proteins were reduced by addition of 10% β-mercaptoethanol and heating at 95 °C for 5 min. Controlled reduction was performed in 5 mM dithiothreitol at room temperature for 30 min. The reaction was stopped by addition of iodoacetamide to 0.1 M final concentration. Analysis on native gels was performed as previously reported (35). The protein concentration was determined by amino acid analysis (36). Immunodiffusion assays were performed on

* The costs of publication of this article were defrayed in part by the payment of page charges. This article must therefore be hereby marked "*advertisement*" in accordance with 18 U.S.C. Section 1734 solely to indicate this fact.

§ To whom correspondence should be addressed: F. Hoffmann-La Roche Ltd., PRPG, Bldg. 15-16, CH-4002 Basel, Switzerland.

‖ Present address: Human Genome Sciences Inc., Rockville, MD.

[1] The abbreviations used are: IFNγ, interferon γ; CHO, Chinese hamster ovary; FBS, fetal bovine serum; IgG3, immunoglobulin G heavy chain γ3; sIFNγR, soluble interferon γ receptor; IFNγR-IgG3, interferon γ receptor-immunoglobulin G3 fusion protein; PBS, phosphate-buffered saline; PAGE, polyacrylamide gel electrophoresis; PCR, polymerase chain reaction.

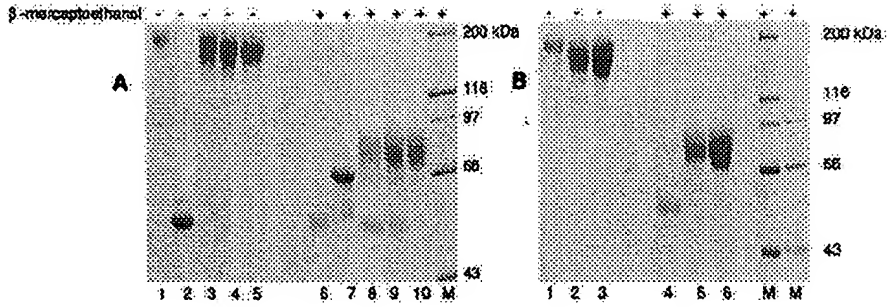

FIG. 1. **SDS-PAGE analysis of the human IFNγR-IgG3 fusion protein after each purification stage (*A*) and after a second size exclusion chromatography step (*B*).** The fusion protein was purified as described under "Experimental Procedures." Electrophoresis was in the presence or absence of 10% β-mercaptoethanol (as indicated) on 7.5% SDS gels stained with Coomassie Blue. *A*, *lanes 1* and *6*, bovine IgG (reference, 2 μg). In *lane 6* only the heavy chain of bovine IgG is seen. In *lanes 2–5* and *7–10*, 10 μg of total protein were loaded. *Lanes 2* and *7*, supernatant of culture medium. The strong band represents BSA, which shows a shift in mobility under reducing conditions (*lane 7*). *Lanes 3* and *8*, eluate from Protein G-Sepharose. *Lanes 4* and *9*, eluate from DEAE-Sepharose. *Lanes 5* and *10*, eluate from Superose-12 HR 10/30 column. *M*, high molecular mass markers. *B*, the eluate from the size exclusion step was concentrated by ultrafiltration and loaded a second time on the sizing column. *Lanes 1* and *4*, bovine IgG3 (reference). *Lanes 2–3* and *5–6*, eluate from the second Superose-12 step (*lanes 2* and *5*, 10 μg; *lanes 3* and *6*, 20 μg). *M*, high and low molecular mass markers.

1% agarose according to Ouchterlony (37).

Construction of Plasmids and Selection of Transfectant Cell Lines—Plasmid RCI 28.1-3A encoding the complete human IFNγ receptor (8) served as template for PCR. The amplified fragment contained DNA coding for the signal sequence and the extracellular domain of the receptor protein. The PCR was performed using *Taq* polymerase as described by the manufacturer (Perkin-Elmer). The pCD4-Hg3 (38) was used as the source of the immunoglobulin gene part. The open reading frame of the extracellular domain of the receptor cDNA was joined with that of the IgG3 gene hinge region. The human IFNγ receptor fragment-human IgG3 chimeric gene construct was introduced into the eukaryotic expression vector pN316 containing *Rous sarcoma* virus long terminal repeat promoter element and the polylinker region allowing integration of the genes of interest.[2] Downstream from the polylinker site, pN316 included the 3′-intron and the polyadenylation site of the rat preproinsulin gene, pSV40 enhancer, the mouse *dhfr* gene, and the ampicillin resistance gene. CHO cells were transfected with the expression vector, and stable clones were selected as described (27).

Fermentation of CHO Cells—Inoculum cells were cultivated in roller bottles using a mixture of Dulbecco's, Ham's F12, and Iscove's powdered media (25:25:50) with 3% fetal bovine serum (FBS). Additional medium supplements included insulin, transferrin, Pluronic F68, and Primatone RL, an enzymatic meat hydrolysate (Sheffield Products). Batch fermentations were performed in stirred tank and airlift bioreactors of up to 100 liters working volume. Cell-free supernatants were harvested by continuous centrifugation (Varifuge 20RS, Heraeus, Germany). Protease inhibitors, phenylmethylsulfonyl fluoride and benzamidine hydrochloride, were added to the culture supernatants after harvesting and to all buffers (except for the buffer used in the last purification step) to a final concentration of 1 mM and 10 mM, respectively. The culture supernatant was concentrated 10-fold by ultrafiltration using an Amicon SP20 ultrafiltration system.

Purification of the IFNγR-IgG3 Fusion Protein—The concentrated supernatant was mixed with 50 ml of Protein G-Sepharose equilibrated with 15 mM sodium phosphate buffer, pH 7.4, containing 150 mM NaCl (PBS) and stirred gently at 4 °C overnight. The protein solution was separated on a column from the gel, which was washed with five column volumes each of PBS and 0.1 M glycine-HCl, pH 5.0. The fusion protein was eluted with 0.1 M glycine-HCl, pH 3.0 and was neutralized with 1 M Tris-HCl, pH 8.0. The eluate was dialyzed against 20 mM sodium acetate, pH 6.0, and loaded onto a 25-ml DEAE-Sepharose column (2.5 × 5.0 cm) equilibrated with the same buffer. The ion exchanger was washed with 10 volumes of 50 mM sodium acetate, pH 4.0, and the fusion protein was eluted with 0.1 M glycine-HCl, pH 3.0. The eluate was concentrated by ultrafiltration and loaded onto a Superose-12 column HR 10/30 (Pharmacia) developed with PBS at 0.5 ml/min. One-ml fractions were collected and analyzed by SDS- and native-PAGE before pooling.

Ligand Binding and Antiviral Assays—The solid phase IFNγ binding assays, the ligand blots, the competition of binding of radiolabeled IFNγ to the cell surface receptor of Raji cells assays, and the inhibition of the IFNγ-mediated antiviral activity assays were performed as reported (10, 27).

Dissociation of IFNγ from sIFNγR and IFNγR-IgG3—The kinetics of IFNγ dissociation from sIFNγR, IFNγR-IgG3, or anti-IFNγ monoclonal antibody γ69 were performed according to Evans *et al.* (39) with minor modifications. In brief, 30 μg of sIFNγR (carrying one binding site), 40 μg of IFNγR-IgG3 (two binding sites), or 40 μg of γ69 (two binding sites) were incubated with 1 μg of IFNγ containing 200 ng of ^{125}I-IFNγ (3 × 10^6 cpm) in PBS *in ice* for 20 min. Unbound ^{125}I-IFNγ was separated on a Superose-12 column developed with PBS. The ^{125}I-IFNγ complexes in 750 μl were treated with 15 μg of unlabeled IFNγ at room temperature. At different times, 100-μl aliquots of complexes between IFNγ and IFNγR-IgG3 or γ69 were withdrawn and were added to 50 μl of Protein G-Sepharose beads, whereas complexes between IFNγ and sIFNγR were added to 50 μl of Protein G-Sepharose beads saturated with anti-IFNγR polyclonal antibody 3891, in FBS containing 2% fetal calf serum. After incubation for 4 min with gentle agitation, the beads were separated by filtering the sample through a 0.22-μm filter (Millipore Corp.). The radioactivity of the filtrate and of the beads was measured in a γ-counter. The time required for quantitative precipitation of the complexes (4 min) was added to the overall incubation time.

Amino Acid Analysis—Amino acid composition analysis was performed according to a modified method of Spackman *et al.* (40).

Analytical Ultracentrifugation—Analytical ultracentrifugation was performed as described previously (41).

Thermal Treatment—Soluble IFNγ receptor produced in insect cells (12 μg) and fusion protein (6 μg) in 1.2 ml of PBS were kept at 37 °C or were heated at 95 °C. At various times, 100-μl samples were withdrawn and kept *in ice* until they were analyzed for residual ligand binding capacity by ligand blots.

Proteolytic Digestion—Digestion of 1 μg of protein substrate in 1 ml of 0.1 M Tris-HCl, pH 7.4, in the presence or in the absence of 6 M urea, was performed as described (42).

RESULTS AND DISCUSSION

Expression of IFNγR-IgG Fusion Proteins—Two fusion proteins were constructed by fusing cDNA sequences encoding the extracellular domain of the human IFNγ receptor to sequences encoding parts of the human IgG γ1 or IgG γ3 heavy chains, including the hinge and constant regions CH2 and CH3. The construction of the eukaryotic expression vectors will be described elsewhere.[2] Transfected CHO cells were grown in the presence of 2–5% FBS, and the fermentation conditions were not optimized. Because the fusion proteins include cysteine residues of the hinge and constant domains of the IgG1 and IgG3 chains, they should have been produced as covalently linked homodimers. However, this happened only with the IFNγR-IgG3 fusion protein, whereas IFNγR-IgG1 was produced as a mixture of single chain and covalently linked homodimer in a ratio of approximately 2:1. The reasons for this discrepancy are under investigation. The purification and char-

[2] C. Kürschner, N. Knezevic, G. Garotta, and Z. Dembic, manuscript in preparation.

acterization of the IFNγR-IgG1 fusion protein was not followed further in this study.

Purification Scheme—IFNγR-IgG3 fusion protein was secreted into the culture medium, which was separated from the cells by centrifugation and concentrated by ultrafiltration. IFNγR-IgG3 was purified in three chromatographic steps, comprising (i) Protein G-Sepharose, (ii) DEAE-Sepharose, and (iii) size exclusion chromatography. Protein G is a Type III Fc receptor that binds to the Fc region of IgG. For binding to Protein G, both chains of the fusion protein are required. IFNγR-IgG3 recovered from Protein G-Sepharose was contaminated with bovine IgG, which was present in the FBS used for cell culture (Fig. 1*A*, *lanes 3* and *8*). When the FBS was passed through a Protein G-Sepharose column before fermentation, the amount of bovine IgG co-eluted with the human fusion protein was significantly reduced, but it was not completely eliminated (not shown). On nonreducing SDS-PAGE, the fusion protein migrated at approximately 175 kDa. Under the same conditions, bovine IgG co-migrated with IFNγR-IgG3, so that a discrimination between these proteins was not possible (Fig. 1*A*, *lanes 3–5*). Under reducing conditions, the proteins could be clearly discriminated, since bovine IgG was resolved in heavy and light chains of 50 and 25 kDa, respectively (Fig. 1*A*, *lanes 6* and *8–10*; the light chain co-migrated with the front on 7.5% SDS gels and is not seen), whereas the hybrid protein gave rise to a 90-kDa band corresponding to a single fusion chain (Fig. 1*A*, *lanes 8–10*).

Chromatography on DEAE-Sepharose, following the Protein G-Sepharose step, removed most of the bovine IgG, eluted at pH 4.5. The fusion protein was eluted at pH 3.5 and 3.0, and it still included small amounts of bovine IgG (Fig. 1*A*, *lanes 4* and *9*). Size exclusion chromatography, which followed the ion exchanger step, delivered two protein peaks, *a* and *b*, corresponding to proteins of apparent molecular masses 600 and 160 kDa, respectively (Fig. 2*A*). The protein bands of the fractions of *peak a* barely entered the native gel (Fig. 2*B*, *lanes 2–4*). When these fractions were analyzed on SDS-PAGE, the proteins co-migrated with the fusion protein of *peak b* (Fig. 2*C*, *lanes 7–9*), indicating that *peak a* included oligomeric forms of IFNγR-IgG3 (Fig. 2*C*, *lanes 2–4*). The oligomeric forms were noncovalently linked (nonreducing SDS-PAGE is not shown). The SDS-PAGE analysis additionally revealed the presence of bovine IgG in the fractions of *peak a* (Fig. 2*C*, *lanes 2–4*; the 55-kDa band). *Peak b* comprised highly purified fusion protein (Fig. 2*B*, *lanes 8–10*, and Fig. 2*C*, *lanes 7–9*), still contaminated, however, with approximately 2% bovine IgG (Fig. 1*A*, *lanes 5* and *10*). A second size exclusion chromatography cycle of the fusion protein of *peak b* yielded a more than 99% pure fusion protein preparation with less than 1% bovine IgG (Fig. 1*B*, *lanes 2–3* and *5–6*). The overall recovery was approximately 60%, as judged by ligand blots. The described method did not completely remove bovine IgG. Bovine IgG was completely removed when Protein G-pretreated FBS was used for cell culture and the fusion protein was purified following the described purification scheme over Protein G-Sepharose, DEAE-Sepharose, and sizing steps (data not shown).

Characterization of the IFNγR-IgG3 Protein—Amino acid sequence analysis from the N-terminal end revealed that the protein was processed properly and that the signal peptide sequence was cleaved off. The protein was heterogeneous at the N-terminus since 50% of the molecules started with Glu-Met-Gly-Thr-Ala-Asp- and the rest with Gly-Thr-Ala-Asp-. Amino acid composition analysis showed that the protein had the expected composition. A molecular mass of 114 kDa was calculated for IFNγR-IgG3 (comprising the two covalently linked chains). Gel filtration and analytical ultracentrifugation revealed a molecular mass of approximately 160 kDa for the fusion protein, suggesting that it exists as monomer in physiological buffer. The difference between the apparent and calculated mass is caused by glycosylation.[3] In immunoblots, the fusion protein was detected by specific antibodies raised against the native IFNγR. In immunodiffusion assays on agarose, the fusion protein was precipitated by the polyclonal antibody R3891 but not by the monoclonal γR99 (data not shown).

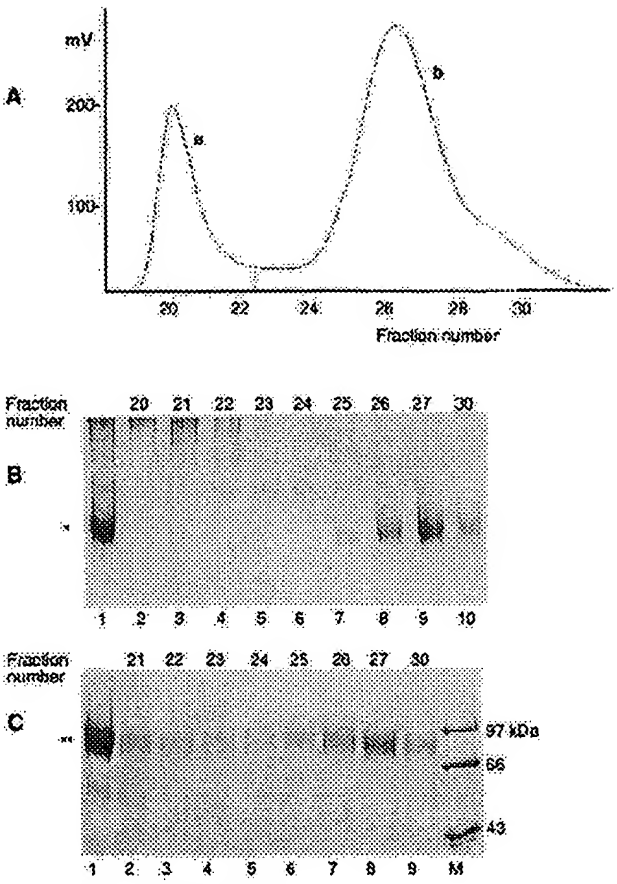

FIG. 2. **Protein elution profile (*A*), native (*B*), and SDS-PAGE analysis (*C*) of the proteins eluted from the sizing column.** *A*, the proteins were loaded on a Superose 12 HR 10/30 column developed with PBS. *B*, analysis of selected fractions on a 5% native gel stained with Coomassie Blue. *Lane 1*, starting material loaded; *lanes 2–10*, fractions eluted from the column. Fractions 20–22 (*lanes 2–4*) contained oligomeric forms of the fusion protein. *, fusion protein, homodimer. *C*, the proteins were analyzed under reducing conditions on a 7.5% SDS gel stained with Coomassie Blue. *Lane 1*, proteins loaded. The 55-kDa band represents bovine IgG (heavy chain). *Lanes 2–9*, fractions eluted from the sizing column. *M*, molecular mass markers. **, fusion protein, single chain.

Stability of IFNγR-IgG3—IFNγR-IgG3 retained full ligand binding capacity when incubated at 37 °C for 8 days and 20% of its activity when treated at 95 °C for 1 h, as judged by ligand blots. The ligand binding capacity of the fusion protein decreased after 10 freezing-thawing cycles to approximately 10% of the original value and then remained constant for up to 30 cycles. The resistance of IFNγR-IgG3 to proteolysis *in vitro* was similar to that of sIFNγRs (42, 43) during folding and in the folded state (data not shown).

Binding of IFNγ—IFNγR-IgG3 bound IFNγ on solid-phase

[3] Mesa, C., Dembic, Z., Garotta, G., and Fountoulakis, M. (1995) *J. Interferon Res.*, in press.

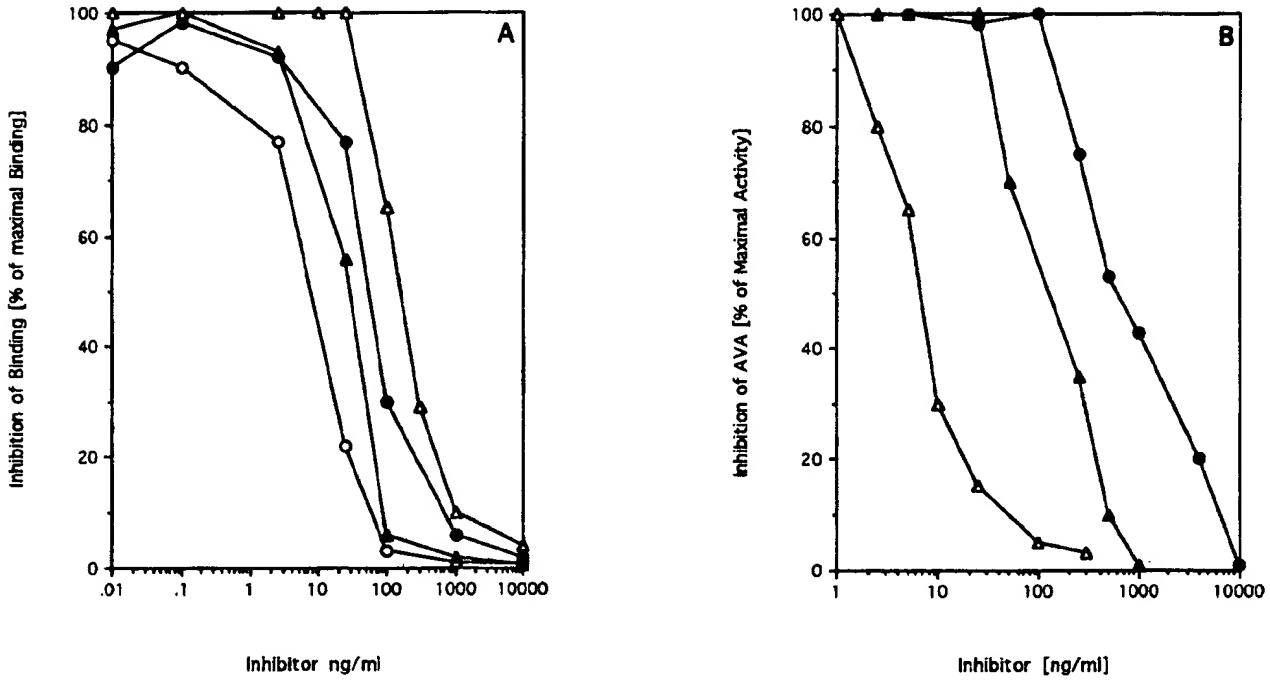

FIG. 3. **Competition of binding of radiolabeled IFNγ to Raji cells (*A*) and inhibition of IFNγ-mediated antiviral activity (*B*).** The assays were performed as described in Ref. 27. *A*, IFNγR-IgG inhibited the binding of 2 ng of ^{125}I-IFNγ to the receptor of 10^7 Raji cells with an IC_{50} of 0.17 nM (▲) and the sIFNγR from CHO cells inhibited with an IC_{50} of 2.30 nM (●). ○, inhibition by unlabeled IFNγ; ▲, inhibition by anti-IFNγ antibody γ69. *B*, the inhibition of antiviral activity was studied on human WISH fibrostast cells infected with encephalomyocarditis virus. IFNγR-IgG3 inhibited with an IC_{50} of 1.20 nM (▲), the CHO cell-derived sIFNγR with an IC_{50} of 23 nM (●), and the antibody γ69 with an IC_{50} of 0.05 nM (Δ). *AVA*, antiviral activity.

and protein blot assays (not shown). The bivalent IFNγR-IgG3 inhibited the ^{125}I-IFNγ binding to the natural receptor of Raji cells with an IC_{50} of approximately 0.17 nM (Fig. 3*A*). The molecular mass of the IFNγR-IgG3 was considered to be 114 kDa (glycosylation was not taken into account). Under the same conditions, unlabeled IFNγ also competed with an IC_{50} of 0.20 nM, whereas the monoclonal antibody γ69 competed with an IC_{50} of approximately 1.2 nM (Fig. 3*A*). Thus, the fusion protein competed at least one order of magnitude more efficiently (IC_{50} = 0.17 nM) in comparison with the sIFNγR produced in CHO cells (IC_{50} = 2.3 nM) (Fig. 3*A*) and the sIFNγRs produced in baculovirus-infected insect cells (IC_{50} = 8 nM) (27) or in *E. coli* (IC_{50} = 15 nM) (25). In inhibition of the cell cytopathic effect (Fig. 3*B*), IFNγR-IgG3 performed approximately 20-fold more efficiently (IC_{50} = 1.20 nM) than the sIFNγR from CHO cells (IC_{50} = 23 nM). In comparison, γ69 inhibited with an IC_{50} of 0.05 nM (Fig. 3*B*).

We investigated the exchange rate of IFNγ bound by IFNγR-IgG3 and for comparative reasons by sIFNγR and anti-IFNγ antibody γ69. The kinetics of dissociation were studied by mixing radiolabeled IFNγ with either of the three proteins, adding the excess of unlabeled IFNγ, and measuring the time-dependent release of the iodinated ligand. IFNγ complexed with IFNγR-IgG3 was released approximately 2-fold more slowly in comparison with that complexed with γ69 or the sIFNγR (Fig. 4). Table I summarizes the performance of the three proteins in ligand binding. The increased retention time may be essential if IFNγR-IgG3 will be used as antagonist of endogenous IFNγ. Similarly, the better performing *in vivo* tumor necrosis factor receptor p55 fusion protein had a significantly slower exchange rate for bound tumor necrosis factor α in comparison with the p75 fusion protein (39).

After reduction, IFNγR-IgG3 did not show IFNγ binding activity on ligand blots. Controlled reduction of the 175-kDa

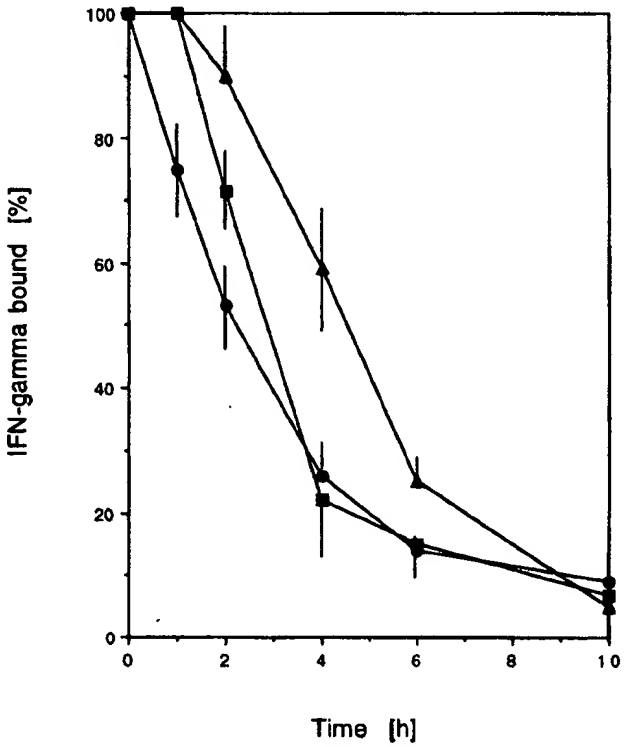

FIG. 4. **Dissociation of IFNγ bound to the IFNγR-IgG3 fusion protein.** The kinetics of dissociation of complexed ^{125}I-IFNγ (3×10^6 cpm) were performed as stated under "Experimental Procedures." Dissociation of ^{125}I-IFNγ bound to IFNγR-IgG3 (▲), to sIFNγR from insect cells ( ), and to monoclonal anti-IFNγ antibody γ69 (■). The *bars* represent standard error of the mean of four experiments.

TABLE I
Characteristics of binding of IFNγ to IFNγR-IgG3, sIFNγR, and anti-IFNγ monoclonal antibody γ69

The inhibition of binding and dissociation of binding studies were performed as stated under "Experimental Procedures." Unlabeled IFNγ (32-kDa homodimer) inhibited the binding of radiolabeled IFNγ to Raji cells with an IC_{50} of 7 ng/ml (0.2 nM). The K_d of the Raji cell receptor was calculated to be 0.22 nM.

Inhibitor	Molecular mass	Binding sites	IC_{50} of binding		K_d	Dissociation half-time
	kDa		*ng/ml*	*nM*	*nM*	*h*
sIFNγR	26	1	200	8.0	0.67	2.3
IFNγR-IgG3	114	2	20	0.17	0.9	4.6
Antibody γ69	150	2	180	1.2	0.96	3

fusion protein resulted in generation of a 90-kDa single-chain species with IFNγ binding capacity suggesting that the four disulfides of the extracellular domain of the IFNγR, all of which are essential for ligand binding (44, 45), are more stable than the disulfides connecting the two IgG3 heavy chains. Dialysis of the completely reduced fusion protein resulted in partial reconstitution of the biological activity of the 90-kDa single chain species only, but not of the 175-kDa IFNγR-IgG3. Thus, the disulfide bonds of the IFNγR domain of the fusion protein were reconstituted, whereas the disulfides between the two IgG3 constant domains were not formed (data not shown).

Stoichiometry of Binding—We investigated the stoichiometry of binding between IFNγR-IgG3 and IFNγ by native gels, gel filtration, amino acid composition analysis, and analytical ultracentrifugation. The components were mixed taking into consideration a molecular mass of 114 kDa for the fusion protein and 32 kDa for IFNγ, since this cytokine exists as a dimer in physiological buffer (41). Based on data of native gel analysis of different ligand-fusion protein ratios, IFNγR-IgG3 and IFNγ were mixed at a ratio of 1:1, and the complex was chromatographed on a size exclusion column. An apparent molecular mass of approximately 400 kDa was found for the complex (Fig. 5*A*). The complex, as eluted from the sizing column, as well as the nonmixed components were subjected to amino acid composition analysis. The observed amino acid ratios of the components and of their complex were introduced into a computer program (46), and an IFNγR-IgG3 fusion protein-IFNγ dimer molar ratio of 1:1 was found. Analytical ultracentrifugation delivered for the complex an apparent molecular mass of 360 kDa. Taking into consideration the results of the four analytical approaches, we conclude that IFNγR-IgG3 and IFNγ dimer interact at a molar ratio of 1:1 and that in physiological buffer they form a complex consisting of two IFNγR-IgG3 molecules and two IFNγ dimers ($(2 \times 160) + (2 \times 32) = 384$; the glycosylated fusion protein was detected as a 160-kDa species by size exclusion chromatography and analytical ultracentrifugation). The apparent molecular mass values of the complexes determined by the different approaches are in good agreement with each other. The minor deviations may be caused by the high glycosylation grade of the fusion protein (approximately 60 kDa).

We further studied whether the fusion protein and IFNγ dimer form complexes larger than the 380–400-kDa complex detected by gel filtration and analytical ultracentrifugation. IFNγR-IgG3 and IFNγ were mixed at different ratios, and the complexes were analyzed by nondenaturing gels (Fig. 5, *B* and *C*). Fusion protein and IFNγ dimer formed in all cases one major complex (*c*) for which amino acid analysis revealed a ratio of 1:1 (Fig. 5*B*, *lanes 2–8* and Fig. 5*C*, *lanes 2–8*). In excess of IFNγ, additional bands migrating between the fusion protein *f* and the complex *c* were visible, suggesting the formation of complexes in which two IFNγ dimers were bound by one bivalent IFNγR-IgG3 fusion protein (Fig. 5*B*, *lanes 4–5* and *8*, and Fig. 5*C*, *lane 4*; these bands are broad and not clearly seen).

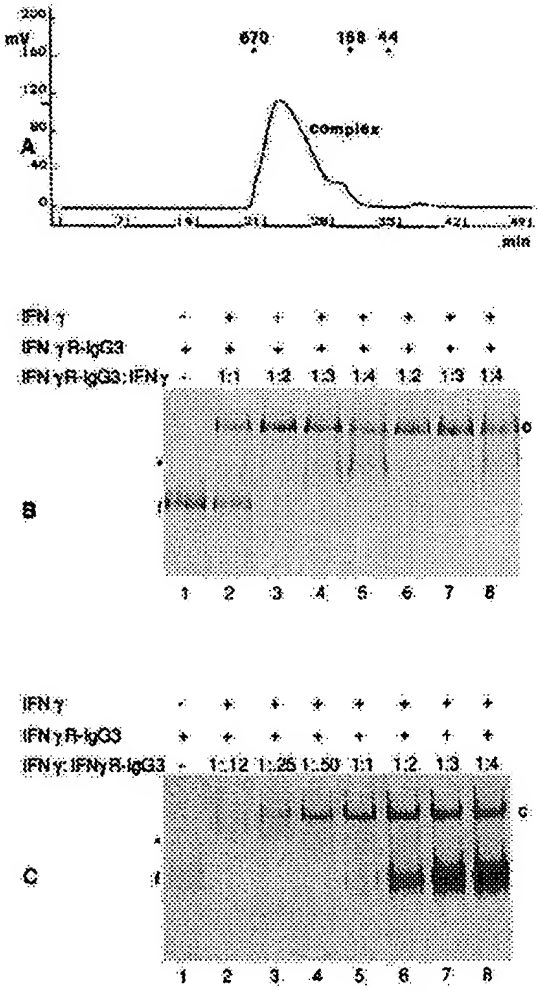

FIG. 5. **Size exclusion chromatography (*A*) and native gel analysis (*B* and *C*) of IFNγR-IgG3 fusion protein-IFNγ dimer complexes.** *A*, IFNγR-IgG3 (440 μg) and IFNγ (220 μg) were mixed and chromatographed on a Superose-12 column developed with PBS at 0.4 ml/min. The positions of elution of the peaks of standard proteins (670, 158, and 44 kDa) are indicated. *B*, 2 μg of IFNγR-IgG (*f*) were mixed with increasing amounts of IFNγΔ10 (*lanes 2–5*) or IFNγΔ0 (*lanes 6–8*) at the indicated ratios, and the complexes were analyzed on a 5% native gel stained with Coomassie Blue. One major complex (*c*) was formed. When IFNγ was added at ratios 1:3 and 1:4, additional broad bands were detected (*) (*lanes 4–5 and 7–8*). *C*, IFNγΔ10 (1.3 μg) was mixed with increasing amounts of IFNγR-IgG3 (*f*) as indicated. Analysis was as stated under *B*. One complex (*c*) was formed. In excess of IFNγ, additional weak bands (*) were visible (*lanes 2–4*). IFNγR-IgG3 added in excess remained uncomplexed (*f*, *lanes 6–8*).

Similar complexes were formed by one IFNγ dimer bound by one sIFNγR molecule when IFNγ was added in excess to the sIFNγR, although when the sIFNγR was available in adequate amounts, two soluble receptor molecules always bound one IFNγ dimer (41).

When IFNγR-IgG3 was added in excess, again one complex *c* was formed. The excess of IFNγR-IgG3 remained uncomplexed (Fig. 5*C*, *lanes 6–8*). Thus, no complexes larger than complex *c* were detected. Formation of such complexes would suggest an agglutination-like situation in which the fusion protein and IFNγ could form precipitate. In immunodiffusion assays on agarose, IFNγR-IgG3 did not precipitate IFNγ, behaving like a nonprecipitating monoclonal antibody. IFNγ was not precipitated by the anti-IFNγ monoclonal antibody γ69 either (data not shown).

In previous studies, using sIFNγRs produced in eukaryotic

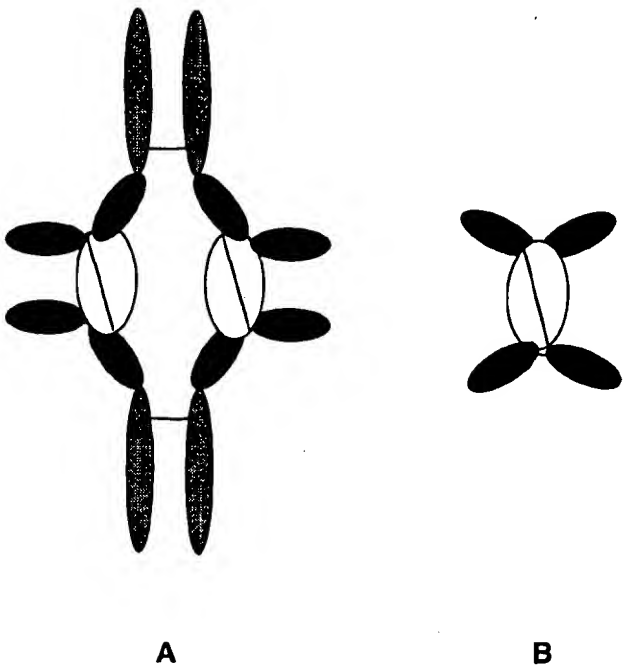

FIG. 6. **Schematic representation of the interaction between IFNγR-IgG3 fusion protein and IFNγ (*A*) and sIFNγR and IFNγ (*B*).** *A*, two IFNγR-IgG3 fusion protein molecules bind two IFNγ dimers, forming a complex of approximately 380 kDa. For such a complex to be formed, each IFNγ dimer should be bound by one of the ligand binding domains of either of the two bivalent fusion protein molecules. *B*, two sIFNγR molecules bind one IFNγ dimer (Refs. 35 and 41). *A* and *B*, the two Ig-like domains of the IFNγR part of each fusion protein (*A*) or soluble receptor (*B*) are shown in *black*. The IgG3 part is shown in *gray* (*A*). The *connecting line* between the IgG3 domains represents disulfides. The two subunits of the IFNγ dimer are shown in *white* (*A* and *B*).

expression systems, we found that one IFNγ dimer is bound by two receptor molecules (35, 41). The one human IFNγ dimer-two receptor relation was confirmed later by other groups (47). Applying chemical cross-linking and using high concentrations of two cross-linkers simultaneously, they showed the generation of a 240-kDa product, likely consisting of one IFNγ dimer bound by two native receptor molecules, thus confirming dimerization of the native receptor in the presence of ligand.

Based on predicted homology between IFNγR and members of the hematopoietic receptor family (48) and in analogy to the crystal structure of the human growth hormone receptor (49), we proposed a model for the IFNγ ligand-receptor interaction (45). According to that model, the extracellular part of the IFNγ receptor consists of two Ig-like domains linked in a V-shaped structure. The two domains are connected with one essential disulfide (Cys^{105}-Cys^{150}). The region at the convergence of the two Ig-like domains most likely includes the ligand binding domain of the receptor. That this region is essential for ligand binding was confirmed by studies with mutant IFNγ receptors carrying domains of both the human and mouse species (50).

In this study, applying four approaches, we found that two IFNγR-IgG3 molecules, carrying two ligand binding sites each, bind two IFNγ dimers. Such a complex could be formed if each IFNγ dimer interacts with one of the IFNγ binding regions of one fusion protein and one of the binding regions of a second fusion protein (Fig. 6*A*). The model of the IFNγR-IgG3 fusion protein-IFNγ dimer binding (Fig. 6*A*) shows that the stoichiometry of interaction is responsible for the higher ligand binding affinity of the fusion protein and for the better performance in competition of binding and inhibition of antiviral activity, in comparison with soluble receptors, in which case two receptor molecules bind only one ligand dimer (Fig. 6*B*).

Conclusion—We produced in CHO cells a human IFNγR-IgG3 fusion protein comprising the extracellular domain of the IFNγ receptor and parts of the human IgG γ3 heavy chain and worked out a purification method that delivered homogeneous IFNγR-IgG3. We investigated the stoichiometry of its interaction with the ligand, finding that two molecules of IFNγR-IgG3 bind two IFNγ dimers and explaining its superior performance in comparison with soluble receptors. The fusion protein has a slower IFNγ-exchange rate and is expected to have a longer half-life *in vivo* in comparison with the sIFNγRs; therefore, it may prove useful as an antagonist of endogenous IFNγ in the treatment of immunological and inflammatory diseases.

Acknowledgments—We thank M.-C. Boy, J.-F. Juranville, K. DiPadova, and N. Wild for technical assistance, A. Friedlein for sequence analysis, and Dr. H. Lötscher for critical reading of the manuscript.

REFERENCES

1. Landolfo, S., and Garotta, G. (1991) *J. Immunol. Res.* **3**, 81–94
2. Sen, G. C., and Lengyel, P. (1992) *J. Biol. Chem.* **267**, 5017–5020
3. Farrar, M., and Schreiber, R. D. (1993) *Annu. Rev. Immunol.* **11**, 571–611
4. Ealick, S. E., Cook, W. J., Vijay-Kumar, S., Carson, M., Nagabhushan, T. L., Trotta, P. P., and Bugg, C. E. (1991) *Science* **252**, 698–702
5. Langer, J. A., and Pestka, S. (1988) *Immunol. Today* **9**, 393–400
6. van Loon, A. P. G. M., Ozmen, L., Fountoulakis, M., Kania, M., Haiker, M., and Garotta, G. (1991) *J. Leukocyte Biol.* **49**, 462–473
7. Valente, G., Ozmen, L., Novelli, F., Geuna, M., Palestro, G., Forni, G., and Garotta, G. (1992) *Eur. J. Immunol.* **22**, 2403–2412
8. Aguet, M., Dembic, Z., and Merlin, G. (1988) *Cell* **55**, 273–280
9. Fountoulakis, M., Kania, M., Ozmen, L., Lötscher, H., Garotta, G., and van Loon, A. P. G. M. (1989) *J. Immunol.* **143**, 3266–3276
10. Garotta, G., Ozmen, L., Fountoulakis, M., Dembic, Z., van Loon, A. P. G. M., and Stüber, D. (1990) *J. Biol. Chem.* **265**, 6908–6915
11. Gibbs, V. C., Williams, S. R., Gray, P. W., Schreiber, R. D., Pennica, D., Rice, G., and Goeddel, D. V. (1991) *Mol. Cell. Biol.* **11**, 5860–5866
12. Hibino, Y., Kumar, C. S., Mariano, T. M., Lai, D., and Pestka, S. (1992) *J. Biol. Chem.* **267**, 3741–3749
13. Pellegrini, S., and Schindler, C. (1993) *Trends Biol. Sci.* **18**, 338–342
14. Kalina, U., Ozmen, L., DiPadova, K., Gentz, R., and Garotta, G. (1993) *J. Virology* **67**, 1702–1706
15. Soh, J., Donnelly, R. J., Mariano, T. M., Cook, J. R., Schwartz, B., and Pestka, S. (1993) *Proc. Natl. Acad. Sci. U. S. A.* **90**, 8737–8741
16. Soh, J., Donnelly, R. J., Kotenko, S., Mariano, T. M., Cook, J. R., Wang, N., Emanuel, S., Schwartz, B., Miki, T., and Pestka, S. (1994) *Cell* **76**, 793–802
17. Hemmi, S., Böhni, R., Stark, G., Di Marco, F., and Aguet, M. (1994) *Cell* **76**, 803–810
18. Müller, M., Briscoe, J., Laxton, C., Guschlin, D., Ziemiecki, A., Silvennoinen, O., Harpur, A. G., Barbieri, G., Witthuhn, B. A., Schindle, C., Pellegrini, S., Wilks, A. F., Ihle, J. N., Stark, G. R., and Kerr, I. M. (1993) *Nature* **366**, 129–135
19. Silvennoinen, O., Ihle, J. N., Schlessinger, J., and Levy, D. E. (1993) *Nature* **366**, 583–585
20. Shuai, K., Stark, G. R., Kerr, I. M., and Darnell, J. E., Jr. (1993) *Science* **261**, 1744–1746
21. Greenlund, A. C., Farrar, M. A., Viviano, B. L., and Schreiber, R. D. (1994) *EMBO J.* **13**, 1591–1600
22. Montminy, M. (1993) *Science* **261**, 1694–1695
23. Garotta, G., Ozmen, L., and Fountoulakis, M., (1989) *Pharmacol. Res.* **21**, Suppl. 2, 5–17
24. Nicoletti, F., Meroni, P. L., Landolfo, S., Gariglio, M., Guzzardi, S., Darcellini, W., Lunotta, M., Mughini, L., and Zanussi, C. (1990) *Lancet* **336**, 319
25. Fountoulakis, M., Juranville, J.-F., Stüber, D., Weibel, E. K., and Garotta, G. (1990) *J. Biol. Chem.* **265**, 13268–13275
26. Fountoulakis, M., Schlaeger, E.-J., Gentz, R., Juranville, J.-F., Manneberg, M., Ozmen, L., and Garotta, G. (1991) *Eur. J. Biochem.* **198**, 441–450
27. Gentz, R., Hayes, A., Grau, N., Fountoulakis, M., Lahm, H.-W., Ozmen, L., and Garotta, G. (1992) *Eur. J. Biochem.* **210**, 545–554
28. Ozmen, L., Gribaudo, G., Fountoulakis, M., Gentz, R., Landolfo, S., and Garotta, G. (1993) *J. Immunol.* **150**, 2698–2705
29. Ozmen, L., Fountoulakis, M., Gentz, R., and Garotta, G. (1993) in *International Review of Experimental Pathology* (Richter, G. W., Solez, K., and Ryffel, B., eds), Vol. 34B, pp. 137–147, Academic Press, San Diego, CA
30. Kürschner, C., Garotta, G., and Dembic, Z. (1992) *J. Biol. Chem.* **267**, 9354–9360
31. Kürschner, C., Ozmen, L., Garotta, G., and Dembic, Z. (1992) *J. Immunol.* **149**, 4096–4100
32. Döbeli, H., Gentz, R., Jucker, W., Garotta, G., Hartmann, W. D., and Hochuli, E. (1988) *Bio/Technology* **7**, 199–216
33. Greenwood, F. C., Hunter, W. M., and Glover, J. S. (1963) *Biochem. J.* **89**, 114–123
34. Schmid, G., Wild, N., Fountoulakis, M., Gallati, H., Gentz, R., Ozmen, L., and Garotta, G. (1994) in *Animal Cell Technology: Products for Today, Prospects for Tomorrow* (Spier, R. E., Griffiths, B. J., and Berthold, W. eds), pp. 625–631, Butterworth-Heinemann, Oxford
35. Fountoulakis, M., Takacs-di Lorenzo, E., Juranville, J.-F., and Manneberg, M.

(1993) *Anal. Biochem.* **208,** 270–276
36. Fountoulakis, M., Juranville, J.-F., and Manneberg, M. (1992) *J. Biochem. Biophys. Methods* **24,** 265–274
37. Ouchterlony, O. (1958) *Prog. Allergy* **5,** 1–78
38. Traunecker, A., Oliveri, F., and Karjalainen, K. (1991) *Trends Biotechnol.* **9,** 109–113
39. Evans, T. J., Moyes, D., Carpenter, A., Martin, R., Loetscher, H., Lesslauer, W., and Cohen, J. (1994) *Eur. Cytokine Network* **5,** 203
40. Spackman, D. H., Stein, W. H., and Moore, S. (1958) *Anal. Chem.* **30,** 1190–1206
41. Fountoulakis, M., Zulauf, M., Lustig, A., and Garotta, G. (1992) *Eur. J. Biochem.* **208,** 781–787
42. Fountoulakis, M. (1995) *J. Chem. Technol. Biotechnol.*, in press
43. Fountoulakis, M., and Gentz, R. (1992) *Bio/Technology* **10,** 1143–1147
44. Fountoulakis, M. (1992) *J. Biol. Chem.* **267,** 7095–7100
45. Stüber, D., Friedlein A., Fountoulakis, M., Lahm, H.-W., and Garotta, G. (1993) *Biochemistry* **32,** 2423–2430
46. Antoni, G., and Presentini, R. (1989) *Anal. Biochem.* **179,** 158–161
47. Greenlund, A. C., Schreiber, R. D., Goeddel, D. V., and Pennica, D. (1993) *J. Biol. Chem.* **268,** 18103–18110
48. Bazan, J. F. (1990) *Proc. Natl. Acad. Sci. U. S. A.* **87,** 6934–6938
49. de Vos, A. M., Ultsch, M., and Kossiakoff, A. A. (1992) *Science* **255,** 306–312
50. Axelrod, A., Gibbs, V. C., and Goeddel, D. V. (1994) *J. Biol. Chem.* **269,** 15533–15539

Proc. Natl. Acad. Sci. USA
Vol. 93, pp. 5512–5516, May 1996
Immunology

The protection receptor for IgG catabolism is the β_2-microglobulin-containing neonatal intestinal transport receptor

(Brambell receptor/Fc receptor/IgG survival/recycling/differential catabolism)

R. P. JUNGHANS*† AND C. L. ANDERSON‡

*Biotherapeutics Development Lab, Department of Medicine, Harvard Medical School, New England Deaconess Hospital, Boston, MA 02215; and ‡Departments of Internal Medicine, Molecular Genetics, and Medical Biochemistry, The Ohio State University, Columbus, OH 43210

Communicated by Henry Metzger, National Institutes of Health, Bethesda, MD, April 23, 1996 (received for review March 5, 1996)

ABSTRACT **More than 30 years ago, Brambell published the hypothesis bearing his name [Brambell, F. W. R., Hemmings, W. A. & Morris, I. G. (1964) *Nature (London)* 203, 1352–1355] that remains as the cornerstone for thinking on IgG catabolism. To explain the long survival of IgG relative to other plasma proteins and its pattern of increased fractional catabolism with high concentrations of IgG, Brambell postulated specific IgG "protection receptors" (FcRp) that would bind IgG in pinocytic vacuoles and redirect its transport to the circulation; when the FcRp was saturated, the excess unbound IgG then would pass to unrestricted lysosomal catabolism. Brambell subsequently postulated the neonatal gut transport receptor (FcRn) and showed its similar saturable character. FcRn was recently cloned but FcRp has not been identified. Using a genetic knockout that disrupts the FcRn and intestinal IgG transport, we show that this lesion also disrupts the IgG protection receptor, supporting the identity of these two receptors. IgG catabolism was 10-fold faster and IgG levels were correspondingly lower in mutant than in wild-type mice, whereas IgA was the same between groups, demonstrating the specific effects on the IgG system. Disruption of the FcRp in the mutant mice was also shown to abrogate the classical pattern of decreased IgG survival with higher IgG concentration. Finally, studies in normal mice with monomeric antigen-antibody complexes showed differential catabolism in which antigen dissociates in the endosome and passes to the lysosome, whereas the associated antibody is returned to circulation; in mutant mice, differential catabolism was lost and the whole complex cleared at the same accelerated rate as albumin, showing the central role of the FcRp to the differential catabolism mechanism. Thus, the same receptor protein that mediates the function of the FcRn transiently in the neonate is shown to have its functionally dominant expression as the FcRp throughout life, resolving a longstanding mystery of the identity of the receptor for the protection of IgG. This result also identifies an important new member of the class of recycling surface receptors and enables the design of protein adaptations to exploit this mechanism to improve survivals of other therapeutic proteins *in vivo*.**

Thirty-two years ago, Brambell published the hypothesis (1) bearing his name that remains as the cornerstone for thinking on IgG catabolism. To explain the long survival of IgG relative to other plasma proteins and its pattern of increased fractional catabolism with high concentrations of plasma IgG (2–4), Brambell and colleagues (1) proposed that specific IgG "protection receptors" (FcRp) bind IgG in pinocytic vacuoles and redirect its transport to the circulation; when the FcRp is saturated, the excess unbound IgG then passes to unrestricted lysosomal catabolism. Brambell similarly characterized the neonatal gut transport receptor (FcRn) and established its saturable nature (5) which was confirmed by others (6–8). The connection was made early and often between these two systems in which the same mechanism or receptor system was postulated (5, 6, 8), although it could not be demonstrated directly. Common features include IgG saturation and transendosomal transport (1–8), acid-enhanced binding (5–9), a shared site on the Fc for binding (10, 11), and widespread expression of both the heavy and light chain of the cloned FcRn in normal adult tissues (9, 12) that corresponds generally to diverse sites of IgG catabolism (13, 14). In 30 years, the FcRp has not been identified, and the problem has attracted little further attention in the absence of genetic markers to define its activity.

The intestinal receptor was cloned and characterized by Simister and colleagues (15, 16). It is a heterodimer of a membrane-integral class I-like heavy chain and a β_2-microglobulin (β_2m) light chain (15) in which both chains make essential contacts with Fc (11). When Fc is mutated in the domains contacting either FcR heavy or light chain (11), survival and transport are both adversely affected (10). In mice with a light chain deletion ($\beta_2m^{-/-}$), FcRn surface expression is lost and neonatal pups are devoid of maternal IgG transport (16). The same study noted that older $\beta_2m^{-/-}$ mice had autologous IgG levels 1/10th that of normal mice, which was proposed to reflect decreased IgG synthesis. We considered that this could instead be due to increased catabolism from parallel impairment of the IgG protection mechanism. Using a genetic knockout that disrupts the FcRn and intestinal IgG transport, we demonstrate that this lesion similarly disrupts the IgG protection receptor activity of these mice, providing genetic and functional links to support the identity of these two molecules.

MATERIALS AND METHODS

Animals. Wild-type and β_2m knockout ($\beta_2m^{-/-}$) mice were purchased from The Jackson Laboratory, with either a mixed C57BL/6 × 129/Ola background or an inbred C57BL/6J background. Animals were raised under low pathogen conditions (3, 4) to yield low endogenous IgG levels.

Proteins. Purified murine anti-Tac antibody was a gift of T. A. Waldmann (National Institutes of Health). Anti-Tac is an IgG2a,κ antibody against human interleukin 2 receptor α subunit and is not reactive with any mouse proteins or tissues. Isotype matched control antibody UPC was purified from ascites by protein A chromatography. Affinity-purified soluble Tac protein was a gift of J. Hakimi (Hoffmann–La Roche). Murine albumin was obtained from Inter-Cell (Hopewell, NJ). Proteins were radiolabeled with ^{125}I or ^{131}I with Iodobeads (Pierce) and separated from free iodide by size exclusion on a Sephadex PD10 G-25 column (Pharmacia). Final specific activities were 0.1–3 μCi/μg (1 Ci = 37 GBq), depending upon the experiment. Radioactivity was determined in a Beckman

The publication costs of this article were defrayed in part by page charge payment. This article must therefore be hereby marked "*advertisement*" in accordance with 18 U.S.C. §1734 solely to indicate this fact.

Abbreviation: β_2m, β_2-microglobulin.

†To whom reprint requests should be addressed.

model 5500 dual channel gamma counter, with corrections applied for radioactive crossover and decay.

In Vivo **Studies.** Mice were injected by tail vein for pharmacokinetic studies. Blood was sampled at indicated times and processed for protein-bound counts by trichloroacetic acid precipitation as described (17). Rapidly catabolized proteins require confirmation of the protein-bound fraction of radioactivity to distinguish protein from radioactive catabolites in serum. Some animals were injected i.p. with ^{125}I-labeled human immunoglobulin (Miles) on schedules to maintain different steady-state blood levels of IgG for the duration of the experiment. Mice received 1–3 i.p. doses of human IgG before i.v. injection of ^{131}I-labeled anti-Tac, and 0–8 i.p doses after the i.v. injection of ^{131}I-labeled anti-Tac. Mice were injected i.v. with a single dose of ^{131}I-labeled anti-Tac, six hours subsequent to the last prior i.p. dose of human IgG. Blood levels of administered human IgG were determined from ^{125}I counts and IgG specific activity, and added to the estimated total murine IgG.

Monomeric Antigen-Antibody Complexes. ^{131}I-soluble Tac [0.3 μg (10 pmol)] was mixed with 100 μg (1200 pmol binding site) of nonspecific (UPC) or specific (anti-Tac) ^{125}I-antibody and injected i.v. as above. The concentration of specific antibody binding site ranged from 1200 to 300 nM in the plasma over the duration of the experiment, ≥1000× the antibody K_d, thus ensuring that antigen binding is essentially complete. Antibody survival is unaffected by antigen binding (17) and "antigen excess" is accordingly not represented in these tests. Samples were collected and processed for protein-bound counts as above.

Pharmacokinetic Modeling. Kinetic parameters were obtained by two-compartment modeling of the composite data of each group using PCNONLIN 4.2 (SCI, Durham, NC). The reported catabolic rate constant is k_{10} (± fitting error) in standard pharmacokinetic nomenclature (catabolic $t_{1/2} = ln2/k_{10}$). The reported ratio of catabolic constants is between ^{131}I-labeled IgG and ^{125}I-labeled albumin as internal control. (It was previously noted that albumin catabolism is modestly faster in the mixed $\beta_2m^{-/-}$ than in wild-type mice; R.P.J., unpublished work.) For Fig. 2, the plasma loss kinetics of the administered ^{131}I-labeled anti-Tac antibody were analyzed for each group as above, except that the beta phase $t_{1/2}$ is shown that parallels previous representations (1–4) of the wild-type curve. A different experimental design including more early points (e.g., see Fig. 1) is required for accurate assessment of catabolic rates; however, it may be inferred from the extremes represented in the Fig. 1 data sets that the catabolic $t_{1/2}$ is 0.6 to 0.75 × the beta phase $t_{1/2}$ under the conditions of Fig. 2.

Immunoglobulin Levels. Plasma was prepared from blood obtained by cardiac puncture of anesthetized mice and measured by ELISA relative to purified mouse antibodies [UPC (an IgG monoclonal; Sigma) and bulk IgA (Sigma)]. Plates (Costar) were coated with polyvalent goat anti-(total mouse Ig) antibody, incubated with dilutions of plasma, and then developed with horseradish peroxidase-conjugated polyvalent antibodies specific to IgG or IgA and read against a standard curve.

RESULTS

Mice with the deletion for the FcRn β_2m light chain lose expression of the receptor on neonatal intestine and are devoid of maternal IgG transport (16). To test the hypothesis that the protection receptor (FcRp) and transport receptor (FcRn) are the same, we examined the impact of this same mutation on the survival of IgG in adult mice. Comparison of administered IgG in wild-type and $\beta_2m^{-/-}$ mice confirmed a marked acceleration of clearance in the latter (Fig. 1) (17). Compartmental modeling revealed catabolic rate constants of 0.14 ± 0.01 day^{-1} for wild-type (■) and 1.5 ± 0.12 day^{-1} for mutant (□)

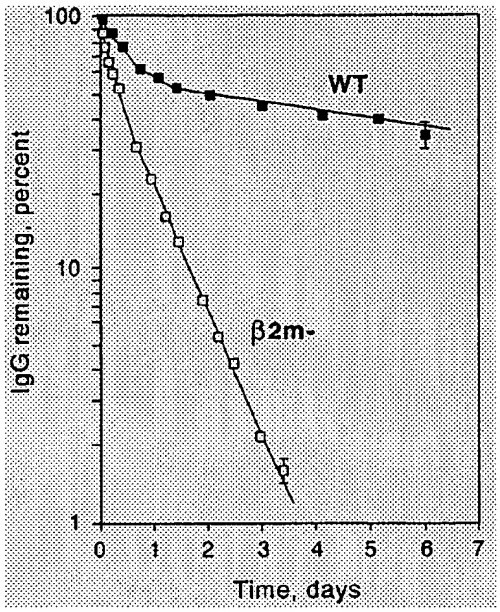

FIG. 1. Abbreviated IgG survival in $\beta_2m^{-/-}$ mice. Animals were injected with mixtures of ^{131}I-labeled murine anti-Tac antibody (■, wild-type mice; □, mutant mice) and ^{125}I-labeled murine albumin (Inter-Cell) (data not shown), and blood samples were processed for protein bound counts. Five mice were used per group. Error bars = ±1 SE, shown only on last points; fractional errors of other points are similar or less.

mice.§ When normalized to albumin coadministered in these tests, the wild-type mice catabolized IgG at a rate of 0.15 relative to albumin, reflecting an ≈7-fold relative protection of IgG, whereas the mutant mice catabolized IgG and albumin at identical rates (ratio = 0.97 ± 0.05), hence displaying no protection of IgG.

These results thus confirm disruption of the protection receptor (FcRp) that parallels FcRn disruption. Further, these data allow quantitation of the protection by the FcRp: the IgG in these normal mice was recycled through cellular endosomes an average of seven times (relative to albumin) before it was finally catabolized.

These studies were repeated in wild-type and mutant mice of inbred C57BL/6 background in which plasma immunoglobulin levels were also assayed. Similar to the data of the mice of mixed background in Fig. 1, the catabolic rate constants for IgG were 8-fold faster in the knockout (1.34 day^{-1}) than in the wild-type mice (0.18 day^{-1}). Correspondingly, plasma IgG levels were measured as 7-fold lower in mutant than in wild-type mice, which is comparable to the difference reported previously (16), whereas IgA was similar between groups (Table 1). This direct relation of decreased steady state blood levels and increased catabolism of IgG in FcRp-deleted mice is compatible with pharmacokinetic predictions with an unaltered IgG synthetic rate (17).

As a corollary of its role in protecting IgG from catabolism, the disruption of the FcRp is predicted to disrupt the classical pattern of decreased IgG survival with higher IgG concentration (1–6). An experiment was undertaken to examine this hypothesis. We recapitulated procedures developed by Fahey and Sell (3, 4) using human IgG, which competes equally for

§The catabolic $t_{1/2}$ values for IgG were 4.9 ± 0.4 days in wild-type versus 0.47 ± 0.02 day in the mutant mice. The $t_{1/2}$ values of the beta phase of the curves were longer for both (8.2 and 0.64 days, respectively) but beta phase constants are a complex composite of distribution and catabolism and are not appropriate for judging catabolic rates or steady states.

Table 1. Selective depression of plasma IgG concentration in $\beta_2m^{-/-}$ mice

	IgG	IgA
Wild-type	2200 ± 100	110 ± 20
Mutant	260 ± 30	110 ± 20
Ratio	8.4:1 ± 0.9	1.0:1 ± 0.2

Plasma was prepared from blood obtained by cardiac puncture of anesthetized mice and measured by ELISA. In this series, inbred C57BL/6J mice were used. Values are averages of five mice ± SE. Two significant figures are reported but all calculations were done with complete figures. The ratio standard errors were obtained by standard formulas. The catabolic $t_{1/2}$ values were measured in these animals as 3.78 ± 0.21 and 0.52 ± 0.02 days (k_{10} of 0.18 and 1.34 day^{-1}) for wild-type and mutant mice, predicting steady state IgG ratios of 7.3 ± 0.5, which is not significantly different from the observed ratio of 8.4 ± 0.9 ($P > 0.3$ by t test).

the protection mechanism as mouse IgG. ^{125}I-labeled human IgG was injected i.p., which transports to blood over several hours; by the dose quantity and frequency, different mean levels of plasma IgG were maintained. The catabolism of tracer ^{131}I-labeled mouse IgG injected i.v. was then evaluated. The expected survival pattern was confirmed (Fig. 2). Wild-type mice exhibited suppression of IgG survival with increased total IgG as shown previously (1–4, 6). The mutant mice showed no similar effect, with IgG behaving essentially as expected for subunit albumin, which does not share the IgG protection receptor and whose clearance is unaffected by IgG concentration (1–5).

Finally, studies were performed with monomeric antigen-antibody complexes. Our previous metabolic studies (17) with soluble Tac antigen (soluble interleukin 2 receptor α) and anti-Tac antibody showed that antibody binding greatly prolonged antigen survival by blocking renal glomerular filtration—the principal mode of catabolism of free soluble Tac—whereas antigen binding had no influence on antibody survival. However, these studies also noted that antigen-in-complex clears faster than antibody-in-complex in normal mice, termed "differential catabolism." This was interpreted (17) as antigen dissociation in the acidic endosome, where Fc-FcRp binding is stabilized, with return of antibody to circulation through the protection receptor but passage of antigen to lysosomal catabolism. The results of Fig. 3*A* confirm the observation of differential catabolism in the wild-type mice of this experiment, with longer survival of antibody than antigen associated with antibody. When performed with mutant mice (Fig. 3*B*), bound antigen was now cleared at the same accelerated rate as (unprotected) antibody. These results confirm that the protection receptor is central to the differential catabolic mechanism for antigen-in-complex and antibody-in-complex.

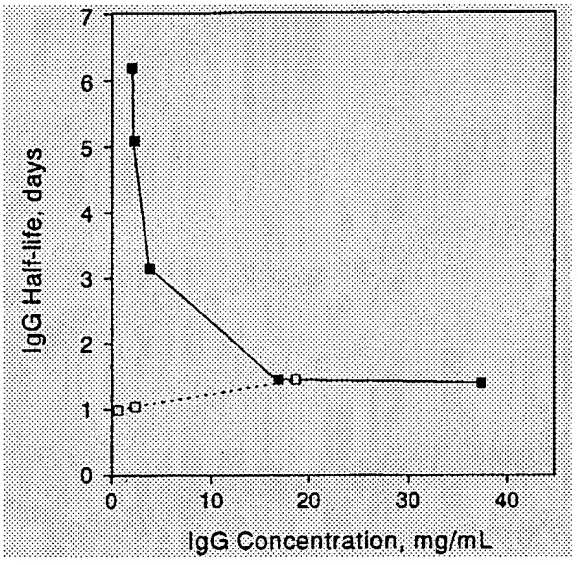

FIG. 2. Suppression of antibody survival by increased IgG concentration in wild-type but not in $\beta_2m^{-/-}$ mice. The survival $t_{1/2}$ for wild-type (■) or mutant (□) mice is plotted against plasma concentration of IgG, represented as the sum of human and endogenous murine IgG. Each point represents the average of two to five mice. Error bars not shown: fitting error of the $t_{1/2}$ was 10% or less, and the midquartile range for the IgG concentrations over the duration of the experiments was approximately ±25%.

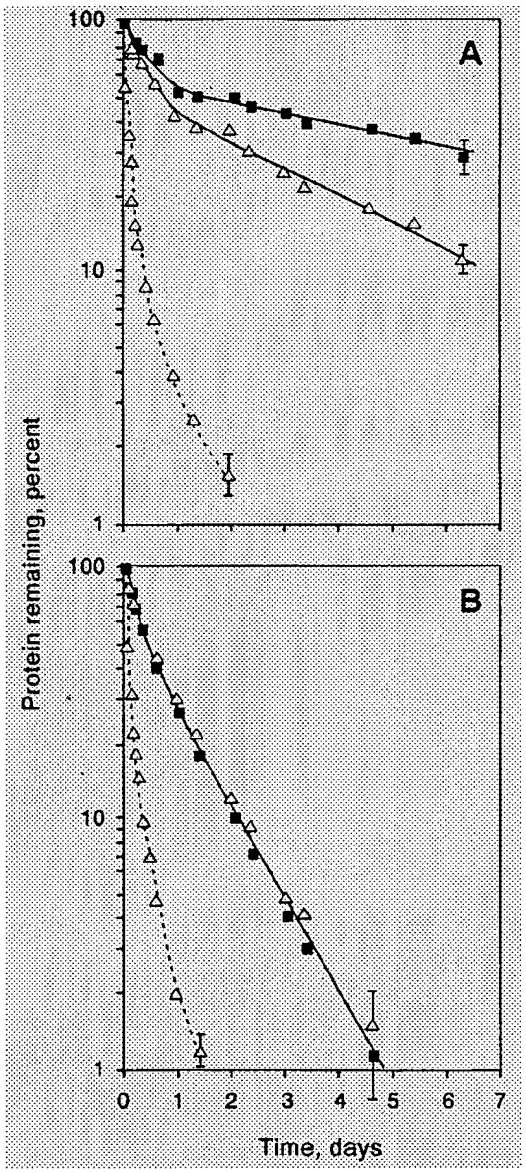

FIG. 3. Abrogation of differential catabolism mechanism for antigen-in-complex and antibody-in-complex in $\beta_2m^{-/-}$ mice. Monomeric antigen-antibody complexes were prepared and injected. Both panels show the survival in wild-type (*A*) or $\beta_2m^{-/-}$ (*B*) mice of soluble Tac antigen in the presence of nonspecific (·–△–·) or specific (—△—) antibody. Also shown is the survival of specific antibody (anti-Tac, ■) The nonspecific isotype control antibody (UPC) is not shown. Five mice were used in each group. Samples were collected and processed for protein-bound counts. Error bars = ±1 SE, shown only on last points; other points are similar or less.

DISCUSSION

IgG has a much prolonged survival relative to other serum proteins, but this survival decreases at higher concentrations of IgG (2–4). To explain this, Brambell *et al.* (1) proposed in 1964 that there was a saturable IgG protection receptor (FcRp) in cellular endosomes that selectively recycles endocytosed IgG back to the circulation. This concept, called the "Brambell hypothesis," remains as the cornerstone of thinking on IgG catabolism. Brambell subsequently demonstrated a neonatal intestinal receptor (FcRn) that transported maternal IgG with similar saturation behavior (5). Waldmann later showed preferential binding of IgG to an FcR at low pH using neonatal intestine (FcRn) or eviscerated adult carcasses (FcRp) (6, 7). Following cloning of the FcRn (15), both chains of the dimer were shown to be expressed much more broadly than neonatal gut (9), corresponding to the similarly wide distribution of sites of IgG catabolism previously shown (13). Other studies showed that mutations in IgG Fc at sites of contact with the FcRn (11) that suppressed intestinal transport also increased IgG catabolism (10).

Historically, the identity of the intestinal and protection receptors was suggested by these several features, prompting the hypothesis underlying the present study; however, the FcRp was never previously identified with any specific protein species. The common functional disruption of the FcRp and FcRn from genetic deletion of a subunit of the molecule is the most concrete evidence that the FcRp and FcRn are one and the same, which, by now, represents the most straightforward interpretation of these accumulated data. As the heavy chain and light chain (β_2m) subunits are each encoded by single copy genes, the expression of this FcR in these two contexts should be regulated from the same loci by temporal and tissue-specific factors. As FcRn, the receptor is expressed in intestinal tissue only in the first 2 weeks of neonatal life and then is down-regulated (5, 7, 8, 15, 16), in contrast to its systemic expression that persists through life (8, 9). Of these two settings, therefore, it is as the FcRp that this FcR has its broadest and most durable expression. Further studies will be needed to define aspects of cellular expression that differentiate its transient superexpression in neonatal gut from the constitutive expression observed in the majority of other tissues.

The unifying feature of the FcRn and the protection receptor is high affinity binding at low pH, present both in bowel and in the endosome, and low affinity at normal plasma pH. In the protection setting, we expect that IgG is not bound to FcRp on the cell surface at all, but only after IgG is passively internalized by ongoing pinocytosis into endosomes where low pH levels (5–6.5) foster tight binding to the FcRp, which then redirects the IgG to the cell surface where it is returned to circulation with reversal of binding at neutral physiologic pH. It is noted finally that the other known FcγRs, which mediate diverse effector and clearance functions (18) and also recycle (19), by inference do not participate importantly in the bulk catabolism of monomeric IgG, confirming previous data (20). The present studies show that normal IgG catabolism is regulated principally through the Brambell receptor because deletion of a subunit of the receptor renders its catabolism indistinguishable from that of albumin in the same mice.

These studies also provide further information on the differential catabolism mechanism for antigen-in-complex and antibody-in-complex (17), and establish the central role of the FcRp in the expression of this function, which now merits explicit representation (Fig. 4). The acidic endosome environment promotes dissociation of antigen from antibody and stimulates binding of IgG to FcRp, with return of IgG to circulation and passage of dissociated antigen to the lysosome, thus yielding the different catabolic rates. This mechanism thus "cleanses" the antibody of antigen and harvests antigen for presentation without antibody destruction, as occurs with mIg on B cells (21). That vesicles may be thus topologically "divided" was previously demonstrated with transferrin and horseradish peroxidase: both colocalize in early endosomes, but transferrin returns to the surface bound to its receptor, whereas horseradish peroxidase proceeds to the late endosomes and lysosomes (22).

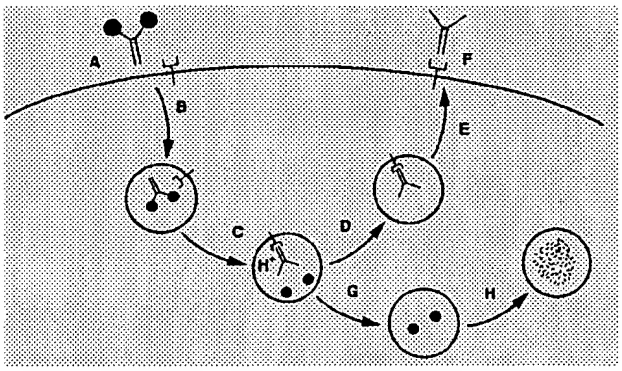

FIG. 4. Differential catabolism model incorporating Brambell receptor function. Circulating monomeric IgG plus antigen (*A*) is internalized into endosomes passively (*B*), without prior FcRp binding. In the low pH of the endosome (*C*), antigen dissociates from antibody, whereas binding of IgG to FcRp is promoted. The endosome then divides into two pathways. (*D–F*) Antibody retained by the FcRp is recycled to the cell surface and dissociates in the neutral pH of the extracellular fluid, returning IgG to circulation, free of antigen. (*G* and *H*) Unbound antigen is shunted with the endosomal contents to the lysosomes for degradation. When the Brambell receptor is deleted, the antigen and antibody pass together to lysosomal catabolism.

The survival of Tac-in-complex in wild-type (catabolic $t_{1/2}$ 1.7 days) versus β_2m$^{-/-}$ mice ($t_{1/2}$ 0.55 day) (Fig. 3) suggests that Tac bound to antibody in normal animals recycles through the endosome an average of three times before it is dissociated and passed to the lysosome for catabolism versus eight times for the antibody itself in this experiment. By this model, the survival of other antigens traversing the endosome will depend on antigen-antibody affinity (off-time) at acidic endosomal pH levels and on the endosomal transit time, expected to be of the order of a few minutes from data on other recycling receptors (22). The normal off-time for Tac from anti-Tac complexes is $t_{1/2}$ 100 min under physiologic conditions (23); the endosome environment evidently accelerates this dissociation rate to account for the 50% catabolism of Tac-in-complex on a few brief passages through the cell.

It is notable that the catabolic $t_{1/2}$ of 0.43 ± 0.06 day previously estimated for the 10% nonrenal fraction of Tac catabolism (90% is renally filtered) (17) approximates the value of 0.47 ± 0.02 day for IgG and albumin in the β_2m$^{-/-}$ mice (Fig. 1), and is also comparable with the nonrenal component of L chain and Fab catabolism (24) and to total catabolism for IgM (6), which is not filtered. This correspondence suggests that the dispersed pinocytotic activities of virtually all cells capture and process all soluble plasma proteins at a rate of ≈2× per day with equivalent degradative rates unless they are protected by specific mechanisms, as studied here with the FcRp and as available to transferrin and other recycled proteins through their cognate receptors (22). Although all nucleated cells perform pinocytosis, our data show that cells of the compartment in rapid equilibrium with the blood are relatively more active in this catabolism on a volume basis than is the extravascular compartment. This is apparent by the difference in the beta and catabolic rate constants for IgG: they would be identical if intravascular and extravascular catabolism were the same.

As a final point, there is apparently no feedback mechanism to regulate synthesis of IgG to maintain specific blood levels.

Although catabolism of IgG is 7- to 10-fold faster in mice deleted for the FcRp, resulting in markedly diminished blood levels, the direct correspondence of IgG blood level changes to catabolic changes implies a constant rate of synthesis (17) of IgG despite wide differences in plasma concentration.

Pharmacokinetic models of bulk metabolic processes in live animals with controlled genetic defects have enabled our correlation of long-established observations with newer information on these processes. In all respects, these data support the wisdom of early insights by Brambell, Waldmann, Fahey, and others who pioneered these concepts more than 30 years ago. The recent decade has been marked by major advances in understanding of the molecular features of this receptor and its intestinal expression. The present studies rejoin the link between these systems governing the transport and catabolism, respectively, of IgG and thereby provide the basis for a renewed examination of this receptor in the dominant metabolic role of its systemic expression. With the increased use of therapeutic antibodies in humans, the understanding of mechanisms of catabolism of the administered IgG will enable improvements in the design and application of these new clinical modalities. Other therapeutic non-Ig proteins may even be modified by "surface reshaping" to adapt to this recycling protection receptor system and thereby adopt a correspondingly long survival.

In this field, it was said, we are "standing on the shoulders of a giant" (8). In honor of the late Professor Brambell, who defined both the FcRp and FcRn activities, we propose that the generic and genetic names for this molecule be assigned as FcRB, and FcRBα or FcRB heavy chain for the class I-related subunit, with the specific designations of FcRn and FcRp preserved to distinguish its separate expressions as transporter or protection receptor for this most important of all immunoglobulins.

Note Added in Proof: We wish to call attention to concurrent efforts we learned of after completing our own studies, which also show faster IgG clearance in $\beta 2m^{-/-}$ mice (ref. 25; E. J. Israel, D. F. Wilsker, K. C. Hayes, D. Schoenfield & N. E. Simister, unpublished work). We note, however, that a conclusion of reduced IgG biosynthesis in these mice (25) contrasts with our analysis that it is essentially unaltered.

We are grateful to G. Zheng (Biotherapeutics Development Lab) for expert technical assistance throughout this project, to J. Watters (Biotherapeutics Development Lab) for laboratory assistance in diverse aspects, to K. Nieforth (Hoffmann–La Roche) for discussions on the kinetics data, and to T. Waldmann (National Institutes of Health) for comments on the manuscript. We also thank V. Ghetie and N. Simister for personal communications of their work before publication. This work is supported by grants from the Milheim Foundation for Cancer Research (R.P.J.), the American Cancer Society (R.P.J.), the Food and Drug Administration (R.P.J.), and the National Institutes of Health (C.L.A.).

1. Brambell, F. W. R., Hemmings, W. A. & Morris, I. G. (1964) *Nature (London)* **203,** 1352–1355.
2. Humphrey, J. H. & Fahey, J. L. (1961) *J. Clin. Invest.* **40,** 1696–1705.
3. Sell. S. & Fahey, J. L. (1964) *J. Immunol.* **93,** 81–87.
4. Sell, S. (1964) *J. Exp. Med.* **120,** 967–986.
5. Brambell, F. W. R. (1966) *Lancet* **ii,** 1087–1093.
6. Waldmann, T. A. & Strober, W. (1969) *Prog. Allergy* **13,** 1–110.
7. Jones, E. A. & Waldmann, T. A. (1972) *J. Clin. Invest.* **51,** 2916–2927.
8. Waldmann, T. A. & Jones, E. A. (1973) *Protein Turnover,* CIBA Foundation Symposium 9 (Elsevier, Amsterdam), pp. 5–18.
9. Story, C. M., Mikulska, J. E. & Simister, N. E. (1994) *J. Exp. Med.* **180,** 2377–2381.
10. Kim, J. K., Tsen, M. F., Ghetie, V. & Ward, E. S. (1994) *Eur. J. Immunol.* **24,** 2429–2434.
11. Burmeister, W. P., Huber, A. H. & Bjorkman, P. J. (1994) *Nature (London)* **372,** 379–383.
12. Chamberlain, J. W., Nolan, J. A., Conrad, P. J., Vasavada, A., Ganguly, S., Janeway, C. A. & Weissman, S. M. (1988) *Proc. Natl. Acad. Sci. USA* **85,** 7690–7694.
13. Henderson, L. A., Baynes, J. W. & Thorpe, S. R. (1982) *Arch. Biochem. Biophys.* **215,** 1–11.
14. Junghans, R. P. Dobbs, D., Brechbiel, M. W., Mirzadeh, S., Raubitscheck, A. A., Gansow, O. A. & Waldmann, T. A. (1990) *Cancer Res.* **53,** 5683–5689.
15. Simister, N. E. & Mostov, K. E. (1989) *Nature (London)* **337,** 184–187.
16. Israel, E. J., Patel, V. K., Taylor, S. F., Marshak-Rothstein, A. & Simister, N. E. (1995) *J. Immunol.* **154,** 6246–6251.
17. Junghans, R. P. & Waldmann, T. A. (1996) *J. Exp. Med.,* **183,** 1587–1602.
18. Ravetch, J. V. (1994) *Cell* **78,** 553–560.
19. Mellman, I., Plutner, H. & Ukkonen, P. J. (1984) *Cell Biol.* **98,** 1163–1169.
20. Wawrzynczak, E. J., Cumber, A. J., Parnell, G. D., Jones, P. T. & Winter, G. (1992) *Mol. Immunol.* **29,** 221–227.
21. Mamula, M. J. & Janeway, C. A. (1993) *Immunol. Today* **14,** 151.
22. Schmid, S. L., Fuchs, R., Male, P. & Mellman, I. (1988) *Cell* **52,** 73–83.
23. Robb, R. J., Greene, W. C. & Rusk, C. M. (1984) *J. Exp. Med.* **160,** 1126–1146.
24. Wochner, R. D., Strober, W. & Waldmann, T. A. (1967) *J. Exp. Med.* **126,** 207–221.
25. Ghetie, V., Hubbard, J. G., Kim, J.-K., Tsen, M.-F., Lee, Y. & Ward, E. S. (1996) *Eur. J. Immunol.* **26,** 690–696.

1: Mol Immunol 1993 Mar;30(4):379-86 Related Articles, Links

Entrez PubMed

PubMed Services

Related Resources

Insertion of constant region domains of human IgG1 into CD4-PE40 increases its plasma half-life.

Batra JK, Kasturi S, Gallo MG, Voorman RL, Maio SM, Chaudhary VK, Pastan I.

Laboratory of Molecular Biology, National Cancer Institute, National Institutes of Health, Bethesda, MD 20892.

CD4-PE40 is a recombinant toxin containing the binding domain of CD4 and a mutant form of Pseudomonas exotoxin A from which the cell binding domain has been removed. To increase the serum half-life of CD4-PE40, we have inserted various portions of the constant domain of human IgG1 into CD4-PE40. The constructs made include CD4-CH2-PE40, CD4-CH3-PE40, CD4-CH1-CH2-PE40 and CD4-CH2-CH3-PE40. The fusion proteins were expressed and purified from E. coli. Insertion of various domains from the constant region of IgG1 did not alter the cytotoxic activity of CD4-PE40; all these molecules were equally cytotoxic to cells expressing gp120 on their surface. However, there was a marked increase in the serum mean residence time of CD4-CH2-PE40 which was 115 min as compared to 47 min for CD4-PE40. Insertion of other domains also increased the half-life of CD4-PE40, however, CD4-CH2-PE40 was found to have the longest mean residence time in the circulation. One possible explanation for the increase in plasma half-life is diminished susceptibility of proteins to proteolysis. It was found that CD4-CH2-PE40 was much more resistant to proteolysis by trypsin than CD4-PE40. We proposed that insertion of the CH2 domain into CD4-PE40 covers up the protease sensitive sites in the molecule, thereby making the molecule less susceptible to degradation. The increase in size and reduced sensitivity to proteases could both be responsible for the increased plasma half-life of CD4-CH2-PE40.

PMID: 8455638 [PubMed - indexed for MEDLINE]

Proc. Natl. Acad. Sci. USA
Vol. 88, pp. 9036–9040, October 1991
Immunology

Identification of the Fc_γ receptor class I binding site in human IgG through the use of recombinant IgG1/IgG2 hybrid and point-mutated antibodies

M. SUZANNE CHAPPEL*, DAVID E. ISENMAN*†, MARGARET EVERETT*, YUAN-YUAN XU*, KEITH J. DORRINGTON*, AND MICHEL H. KLEIN*†‡§

Departments of *Immunology and †Biochemistry, University of Toronto, Toronto, ON, Canada M5S 1A8; and ‡Connaught Centre for Biotechnology Research, Willowdale, ON, Canada M2R 3T4

Communicated by David R. Davies, June 24, 1991 (received for review May 9, 1991)

ABSTRACT **To characterize the region on human IgG1 responsible for its high-affinity interaction with the human Fc_γ receptor class I ($Fc_\gamma RI$), we have analyzed the binding properties of a series of genetically engineered chimeric anti-dinitrophenyl antibodies with identical murine antibody combining sites and hybrid IgG1/IgG2 human constant (C) regions. In addition, we have investigated a panel of reciprocally point-mutated IgG1 and IgG2 chimeric antibodies to identify the amino acid residues that confer cytophilic properties to human IgG1. Our data unambiguously indicate that cytophilic activity of IgG1 is an intrinsic property of its heavy-chain C region 2 (C_H2) domain. We report that the entire sequence spanning residues 234–237 (LLGG) is required to restore full binding activity to IgG2 and IgG4 and that individual amino acid substitutions failed to render IgG2 active. Nevertheless, the reciprocal single point mutations in IgG1 either significantly lowered its activity or abolished it completely. Finally, we observed that an IgG2 antibody containing the entire ELLGGP sequence (residues 233–238) was more active than wild-type IgG1. This finding suggests that in addition to the primary contact site identified in the N terminus of the γ1 C_H2 domain, secondary sites involving residues from the C-terminal half of the domain may also contribute to the IgG1–$Fc_\gamma RI$ interaction.**

Fc receptors for human IgGs ($Fc_\gamma R$) form a family of integral membrane proteins that specifically bind to immunoglobulin Fc regions.¶ The interaction of $Fc_\gamma Rs$ with IgG trigger critical host effector functions such as phagocytosis of immune complexes (1), antibody-dependent cell-mediated cytotoxicity (2–4), and the release of inflammatory mediators (5).

Three classes of human $Fc_\gamma R$ have been defined on the basis of their reactivity with monoclonal antibodies (6). The high-affinity $Fc_\gamma RI$ (CD64) is a 72-kDa glycoprotein expressed on mononuclear phagocytes (7) and interferon γ-activated neutrophils (2). $Fc_\gamma RI$ displays a hierarchy of affinities for monovalent human IgG subclasses. IgG1 and IgG3 bind with high affinity (K_a 10^8–10^9 M^{-1}), whereas IgG4 is 10-fold less cytophilic and IgG2 is devoid of any significant binding activity (8).

Several indirect approaches suggest that the primary site that mediates the IgG1–$Fc_\gamma RI$ interaction resides within the heavy-chain constant region 2 (C_H2) domain. Monoclonal antibodies directed against a C_H2 domain N-terminal epitope including the isotype-specific residue K274, inhibited the IgG1–$Fc_\gamma RI$ interaction (9). Furthermore, the C_H2 domain-deleted IgG1 myeloma protein TIM failed to bind $Fc_\gamma RI$ (10). Results obtained with isolated C_H2 domains remain controversial since dimeric, but not monomeric, domains possess cytophilic activity (11, 12). In the context of a hybrid molecule, however, only a single cytophilic H chain is required for binding activity (13). More recently, the functional analysis of a panel of genetically engineered human IgG1/IgE hybrid antibodies indicated that the $Fc_\gamma RI$ binding site was essentially a property of the IgG1 C_H2 domain (14).

Several observations suggest that the C_H2 N terminus forms at least part of the IgG1 $Fc_\gamma RI$ recognition site. Comparative primary sequence analysis revealed that an LLGGP motif spanning residues 234–238 is conserved in all cytophilic IgGs (15). Site-directed mutagenesis of E235 in noncytophilic mouse IgG2b to L235 produced the LLGGP motif on an IgG2b background, rendering this molecule fully active (16). This was not predicted to be the only critical residue in the human site since IgG1 and IgG4 are identical at this position, yet IgG4 is 10-fold less active. Finally, whereas IgG1 Fc fragments obtained by digestion with papain retain cytophilic activity, those obtained with thermolysin, which cleaves between residues 234 and 235, do not (11). This indicates that $Fc_\gamma RI$ binding activity requires the presence of residues N-proximal to L235 but not that of the hinge disulfide bonds, since reduction and alkylation of IgG1 has no significant effect on its binding affinity for $Fc_\gamma RI$ (15).

We have engineered a panel of chimeric IgG1/IgG2 hybrid molecules and a set of reciprocally point-mutated IgG1 and IgG2 antibodies to identify the region(s) and ultimately the amino acids that are essential for IgG1–$Fc_\gamma RI$ recognition and are sufficient to restore full activity to IgG2. We report that IgG2 molecules containing only an IgG1 C_H2 domain are as cytophilic as wild-type IgG1 and that the amino acids that are critical for this activity are L234, L235, and G237.

MATERIALS AND METHODS

Cell Lines. The murine myeloma λ-chain-producing mutant cell line MOPC 315.26 was maintained as described (17). U937 cells were grown in RPMI 1640 medium supplemented with 2% fetal calf serum, 2 mM glutamine, and antibiotics.

Plasmid Constructs. The pSV2neoV_H315 mammalian expression vector has been described (18). The 3.2-kilobase *Hin*dIII/*Bam*HI IgG1 and IgG2 C_H gene fragments were kindly provided by L. Hood (California Institute of Technology). All molecular cloning techniques were performed according to Sambrook *et al.* (19). The human IgG1, IgG2, and IgG4 C region genes were cloned into pEMBL-19, where all

The publication costs of this article were defrayed in part by page charge payment. This article must therefore be hereby marked "*advertisement*" in accordance with 18 U.S.C. §1734 solely to indicate this fact.

Abbreviations: C, constant; H, H chain; $Fc_\gamma RI$, high-affinity Fc_γ receptor class I.

§To whom reprint requests should be addressed at: Department of Immunology, Medical Sciences Building, University of Toronto, Toronto, ON, Canada M5S 1A8.

¶Nomenclature Subcommittee, Oral Presentation, FASEB Summer Research Conference on Fc Receptors & Immunoglobulin Binding Factors, June 15–19, 1987, Saxton's River, VT.

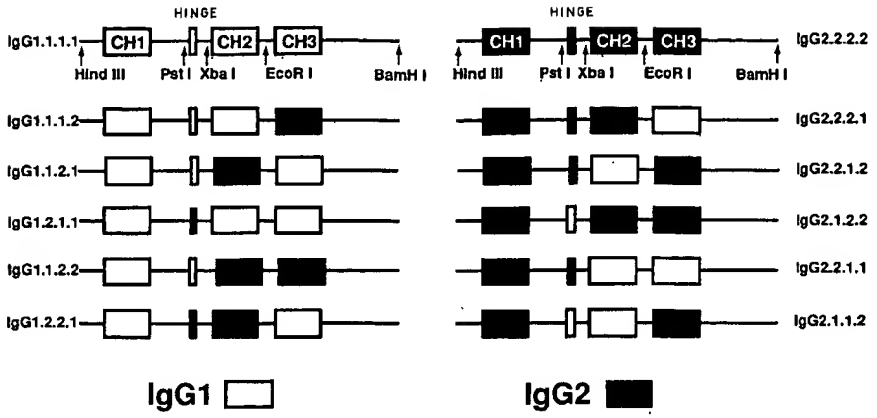

FIG. 1. Schematic representation of wild-type, hybrid IgG1/IgG2 (*Left*) and hybrid IgG2/IgG1 (*Right*) C region gene constructs. Genes were subcloned into pEMBL-19 between its *Hin*dIII and *Bam*HI sites. Unique *Xba* I and *Eco*RI sites were introduced by site-directed mutagenesis in the hinge–C_H2 and the C_H2–C_H3 introns, respectively. Hybrid genes were constructed by exchange of exons excised with the appropriate restriction enzymes.

subsequent genetic manipulations were done. Oligonucleotide-directed mutagenesis was performed by the Eckstein method (20) (Amersham) to introduce unique *Xba* I and *Eco*RI sites in the hinge–C_H2 and C_H2–C_H3 introns, respectively, and to substitute amino acids. Hybrid IgG1/IgG2, IgG2/IgG1, and IgG1/IgG4 genes were constructed by reciprocally exchanging exons excised with the appropriate restriction enzymes. The transfer of native and modified IgG1, IgG2, and IgG4 genes into the pSV2neoV_H315 expression vector was performed as described (18). The resulting expression vector encodes an entire H chain composed of a human IgG C region and the murine MOPC 315 H-chain variable region (V_H) domain. The identity of each construct was confirmed in both pEMBL-19 and in pSV2neoV_H315 by restriction map analysis and DNA sequencing.

Electroporation. The pSV2neoV_H315 IgG1, IgG2, and IgG4 H-chain constructs were transfected into the λ-chain-producing cell line MOPC 315.26 by electroporation according to the method of Baker *et al.* (21). The electroporated cells were grown and selected in G418 (GIBCO) (17). Antibody production was quantified by IgG-specific capture ELISA, using myeloma human IgG1 and IgG2 as standards.

Assembly of Chimeric Molecules. The assembly of the chimeric antibodies was evaluated by SDS/polyacrylamide gradient (4–15%) gel electrophoresis under nonreducing conditions. Culture supernatants containing ≈5 μg of chimeric immunoglobulin were incubated with 50 μl of a 10% suspension of formalin-treated *Staphylococcus aureus* bacteria for 1 hr at 4°C. The pellets were washed six times in phosphate-buffered saline (PBS) containing 0.5% Triton X-100, 0.25% deoxycholate, 0.5% SDS, 10 mM EDTA, and 2 mM phenylmethylsulfonyl fluoride and then boiled for 3 min in 2× sample buffer containing 4% SDS and 1 mM iodoacetamide to prevent disulfide interchange.

Preparation of Culture Supernatants for Binding Inhibition Assays. Culture supernatants were concentrated 10-fold using Centriprep-30 microconcentrators (Amicon). The concentrated culture supernatants were then subjected to ultracentrifugation for 30 min at 100,000 × *g* at 4°C to remove potential IgG aggregates. The final concentration of chimeric antibodies was assessed by triplicate ELISA determinations.

Binding Inhibition Studies. Purified human IgG1 myeloma protein was radioiodinated using Iodobeads (Pierce) to a specific activity of 1×10^6 cpm/μg. Bound ^{125}I was separated from free material by gel filtration through a Biogel P4 spin column. IgG concentration was measured spectrophotometrically at 280 nm using an extinction coefficient $E_{280}^{0.1\%}$ of 1.4. U937 cells were washed once in PBS containing 0.02% sodium azide and bovine serum albumin (1 mg/ml) and resuspended in the same buffer. Direct binding and inhibition assays were carried out in 96-well U-bottom microtiter plates essentially as described by Raychaudhuri *et al.* (22). In brief, for the inhibition assay, 2.5×10^6 U937 cells were incubated per well with 10 nM radiolabeled IgG1 and increasing concentrations of chimeric inhibitor for 2 hr at room temperature and then spun through a dibutyl phthalate oil cushion; cellular pellets were assayed for bound radioactivity. Nonspecific binding was determined from the residual bound radioactivity in the presence of 10 μM unlabeled IgG1 and never exceeded 2% of total binding. All values were corrected for nonspecific binding. The association constants of the chimeric antibodies were estimated from the displacement of the inhibition curve (at 50%) obtained with chimeric inhibitor relative to that obtained with myeloma IgG1 for which the K_a was determined in a direct binding assay (23). Three independent determinations were obtained in triplicate for each chimera species.

RESULTS

Construction, Expression, and $Fc_\gamma RI$ Binding Properties of Hybrid IgG1 and IgG2 Antibodies. The role of individual domains in the cytophilic activity of human IgG isotypes was analyzed by exon-shuffling experiments. The panel of hybrid genes is depicted schematically in Fig. 1. An IgG1 molecule with an IgG4 hinge was also constructed (data not shown). Hybrid molecules are described by four digit numbers indicating the subclass origin of the C_H1, hinge, C_H2, and C_H3 exons, respectively.

Chimeric immunoglobulins from clones secreting in the range of 5–10 μg of IgG per ml were affinity isolated with *S. aureus* cells and analyzed by SDS/PAGE. Nonreduced SDS/PAGE revealed that all molecules migrated as a single band with an apparent molecular mass of 150 kDa corresponding to a covalently assembled H_2L_2 molecule that could be dissociated into its constituent H and L chains upon reduction (data not shown). Representative electrophoretic patterns obtained with wild-type chimeric IgG1 and IgG2 and hybrid IgG1-1-2-1, IgG2-2-1-2 molecules are shown in Fig. 2.‖

The binding properties of the exon-shuffled antibodies were assessed by competitive inhibition assays. To validate the use of chimeric IgGs as inhibitors, we confirmed that the cytophilic activity of the IgG1 chimera was indistinguishable from that of myeloma IgG1. Representative binding inhibition curves obtained for these molecules are depicted in Fig. 3*A*. The curves demonstrate a typical sigmoidal shape and are superimposable. This indicated that the K_a value for the chimeric IgG1 molecule was the same as that of myeloma IgG1, which was determined in an independent direct binding

‖Example of nomenclature for hybrid molecules: IgG1-1-2-1 refers to C_H1, hinge, and C_H3 exons of IgG1 origin, and a C_H2 exon of IgG2 origin.

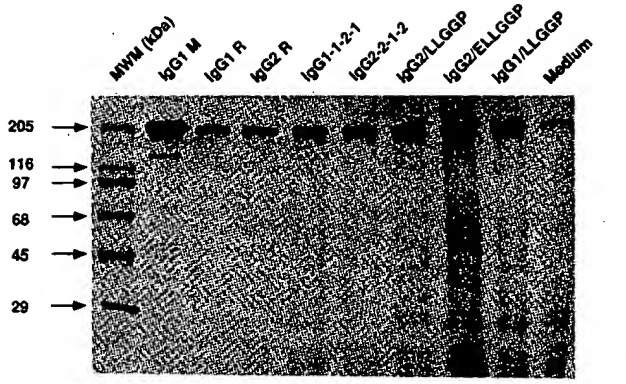

FIG. 2. SDS/PAGE analysis of hybrid and point-mutated chimeric IgGs. Samples were analyzed as described. IgG1 M, IgG1 R, and IgG2 R, IgG1 myeloma and recombinant IgG1 and IgG2 proteins, respectively. Immunoprecipitated supernatant from mock-transfected MOPC 315.26 cells (Medium) shows a faint 150-kDa band likely corresponding to bovine IgG.

experiment to be 4.30×10^8 M^{-1}. A similar experiment confirmed that chimeric IgG2 was devoid of any cytophilic activity at molar concentrations up to 10^{-7} M (Fig. 3*A*). Myeloma IgG2 displayed ≈30-fold lower activity than did IgG1, probably reflecting a small amount of contaminating cytophilic isotypes in the IgG2 preparation.

To assess the relative contribution of the Fc C region domains and the genetic hinge, combinations of domain and hinge exons were reciprocally exchanged (Fig. 1). Table 1 summarizes the $Fc_\gamma RI$ binding properties of these molecules as assessed by competitive inhibition assays. Neither the hinge nor the C_H3 domain was shown to contribute significantly to the IgG–$Fc_\gamma RI$ interaction, since grafting of an IgG1 hinge or C_H3 domain on an IgG2 background did not restore measurable activity to the IgG2 subclass within the range of concentrations tested. Conversely, IgG1 hybrid molecules containing either an IgG2 hinge or C_H3 domain retained full cytophilic activity. In marked contrast, the insertion of an IgG1 C_H2 domain conferred full cytophilic properties to IgG2 (Fig. 3*B*). Indeed, the IgG2-2-1-2 hybrid immunoglobulin was found to bind to the U937 $Fc_\gamma RI$ with an affinity ($K_a = 3.77 \times 10^8 \pm 0.86$ M^{-1}) comparable to that of wild-type IgG1, whereas the reciprocal hybrid molecule IgG1-1-2-1 was totally inactive. All molecules containing an IgG1 C_H2 domain were active regardless of the isotypic origin of the hinge or other γ-chain C domains. Conversely, all hybrids containing an IgG2 C_H2 domain were functionally inactive. In addition, we also observed that the replacement of an IgG1 hinge with its IgG4 counterpart did not affect the activity of the IgG1 chimera (Table 1).

Table 1. Apparent K_a values of hybrid IgG–U937 $Fc_\gamma RI$ interactions

IgG species	K_a, $\times 10^{-8}$ M^{-1}	SD, $\times 10^{-8}$ M^{-1}	*n*
IgG1 (myeloma)	4.30*	—	1
IgG1-1-1-1	4.30	0.49	3
IgG2-2-2-2	≪0.05	—	3
IgG1-1-1-2	5.04	0.46	3
IgG2-2-2-1	≪0.05	—	3
IgG1-1-2-1	≪0.05	—	3
IgG2-2-1-2	3.77	0.86	3
IgG1-2-1-1	3.51	0.40	3
IgG2-1-2-2	≪0.05	—	3
IgG1-1-2-2	≪0.05	—	3
IgG2-2-1-1	3.52	0.13	3
IgG2-1-1-2	≪0.05	—	3
IgG2-1-1-2	6.83	1.57	3
IgG1-4-1-1	3.45	—	1

*This K_a value was obtained by Scatchard analysis of data from a direct binding experiment. All other apparent K_a values were obtained from binding inhibition experiments as described in *Materials and Methods* and are expressed as the means from independent determinations (*n*) performed in triplicate.

Construction, Expression, and $Fc_\gamma RI$ Binding Properties of IgG1, IgG2, and IgG4 C_H2 Domain Point Mutants. The existence of striking primary sequence differences in the lower hinge region of IgG1 and IgG2 C_H2 domains (Table 2) and the indirect evidence that this region may be structurally important for $Fc_\gamma RI$ recognition led us to concentrate on residues 233–238 (Eu numbering) for more detailed analyses. Individual IgG1 residues E233, L234, and L235 of the ELLGGP sequence were systematically substituted with the corresponding IgG2 residues P233, V234, and A235, respectively. In addition, IgG1 G237 was deleted, since there is no corresponding residue at position 237 in IgG2. A similar mutagenesis strategy was also used to modify the N-terminal region of the IgG2 C_H2 domain. Residues P233, V234, and L235 of the IgG2 PVAG–P sequence were replaced with the corresponding IgG1 residues E, L, and L, respectively. In addition, a glycine residue was inserted at position 237. Multiple substitutions were also performed such that in all, a panel of 12 IgG1 and IgG2 analogues with mutated C_H2 domains were generated. The amino acid sequences of these variants, and an additional IgG4 F234 to L234 mutant molecule, are shown in Table 2. SDS/PAGE analysis revealed covalent H_2L_2 assembly in all cases. The electrophoretic patterns for three critical mutants are shown in Fig. 2. The relative binding activities of the mutated molecules obtained from two independent transfections were compared in binding inhibition assays at two different concentrations of chimeric inhibitor (2.3 and 6.7 nM) and equimolar concentra-

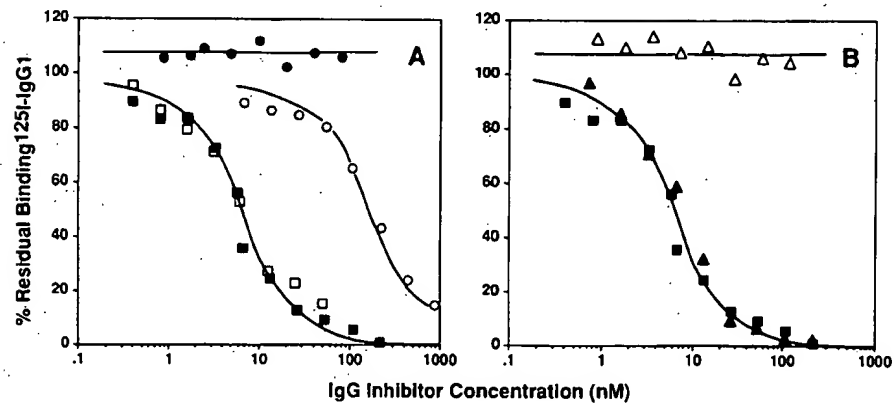

FIG. 3. Inhibition of ^{125}I-IgG1 binding to U937 cell $Fc_\gamma RI$ receptors by myeloma and recombinant wild-type IgG1 and IgG2 and by γ1/γ2 hybrid molecules. The assay was performed as described in ref. 22 using 2.5×10^6 U937 cells per assay and 10 nM ^{125}I-IgG1 in the presence of increasing concentrations of IgG inhibitors. (*A*) The inhibitors are myeloma IgG1 (□), wild-type recombinant IgG1 (■), myeloma IgG2 (○), and wild-type recombinant IgG2 (●). (*B*) The inhibitors are wild-type recombinant IgG1 (■), hybrid IgG1-1-2-1 (△), and hybrid IgG2-2-1-2 (▲).

Table 2. Apparent K_a values of the $Fc_\gamma RI$–IgG interaction obtained with IgG1 and IgG2 point mutants

IgG background	Sequence (amino acids 231–238)	K_a, $\times 10^{-8}$ M^{-1}	SD, $\times 10^{-8}$ M^{-1}	n
IgG1 WT	APELLGGP	4.30	0.49	3
IgG2 WT	APPVAG-P	—	—	3
IgG1	APPLLGGP	—	—	3
IgG2	APEVAG-P	—	—	3
IgG1	APEVLGGP	2.26	0.36	3
IgG2	APPLAG-P	—	—	3
IgG1	APELAGGP	—	—	3
IgG2	APPVLG-P	—	—	3
IgG1	APELLG-P	—	—	3
IgG2	APPVAGGP	—	—	3
IgG1	APELAG-P	—	—	3
IgG2	APPVLGGP	—	—	3
IgG2	APPLLGGP	5.17	0.39	4
IgG2	APELLGGP	16.5	5.51	4
IgG4	APELLGGP	3.44	—	1
IgG4 WT	APEFLGGP	0.04	—	1

Underlined letters indicate point mutations. All apparent K_a values were obtained from binding inhibition experiments and are expressed as the means of independent determinations (n) performed in triplicate. WT, wild type.

tions of the myeloma ^{125}I-labeled IgG1 (^{125}I-IgG1) tracer (Fig. 4*A*). Single substitutions at positions 233 (P for E) or 235 (A for L) completely abolished IgG1 cytophilic activity, as did the deletion of G237. The relatively conservative V for L substitution at position 234 yielded a molecule with reduced activity. This molecule, when examined more closely in a full binding-inhibition assay, displayed a 2-fold decrease in apparent K_a (Fig. 4*B*; Table 2). Although single mutations introduced in IgG1 between residues 233 and 238 reduced or abolished its functional activity, interestingly, none of the reciprocal mutations conferred any significant binding affinity to IgG2 (Fig. 4*A*; Table 2). Consequently, progressive mutations were sequentially introduced in IgG2 to gradually reconstruct the IgG1 ELLGGP sequence. Only simultaneous substitutions of L at positions 234 and 235, along with the insertion of G at position 237 (PLLGGP) restored binding affinity to a level comparable to that of wild-type IgG1. A representative binding inhibition curve obtained for this triple mutant is shown in Fig. 4*B*. The K_a was estimated to be $5.17 \times 10^8 \pm 0.39$ M^{-1}. Reconstruction of the IgG1-like ELLGGP sequence on an IgG4 background through the single F234 to L234 substitution yielded a cytophilic molecule with a binding affinity indistinguishable from that of IgG1 (Fig. 4*A*; Table 2). Finally, grafting of the entire IgG1 ELLGGP motif on an IgG2 background yielded a mutated molecule that was ≈4 times more active than wild-type IgG1 ($K_a = 1.65 \times 10^9 \pm 0.55$ M^{-1}; Fig. 4*B*; Table 2).

DISCUSSION

Human IgG subclasses differ with respect to their cytophilic properties. The objective of this study was to identify the amino acid residues that play a critical role in the IgG1–$Fc_\gamma RI$ interaction.

As a first step, we engineered a panel of IgG1/IgG2 antibodies by reciprocal exon shuffling to identify the homology region of IgG1 responsible for its interaction with $Fc_\gamma RI$ on U937 cells. We first demonstrated that the binding affinities of the chimeric IgG1 and IgG2 molecules were indistinguishable from those of their human myeloma counterparts (8).

The genetic hinges of IgG1 (15 residues) and IgG2 (12 residues), which include the upper and core regions of the "functional hinge" differ by three amino acids in length and by their primary sequences. However, reciprocal shuffling of hinge regions between IgG1 and IgG2 subclasses and the grafting of an IgG4 hinge onto an IgG1 background did not affect the $Fc_\gamma RI$ binding properties of the parent molecules. These findings strongly suggest that neither the length of the upper hinge, which restricts segmental flexibility (24), nor the amino acid sequence of the core hinge modulates cytophilic activity. In addition, it has been shown that this effector function is not affected by reduction of the hinge disulfide bridges (15). However, it requires the presence of a spacer between the Fab arms and the Fc region since the hinge-deleted IgG1 paraprotein Dob does not bind to $Fc_\gamma RI$ on monocytes (10).

Reciprocal exchange of C_H3 domains, which differ by only one conservative substitution, did not affect the binding properties of the native molecules. Our results are in agreement with the findings that noncovalent pFc' dimers (10) and monoclonal anti-C_H3 antibodies are unable to inhibit the binding of IgG1 to the monocyte $Fc_\gamma RI$ (9).

Reciprocal shuffling of C_H2 domains between the IgG1 and IgG2 subclasses unambiguously revealed that the $Fc_\gamma RI$ binding site is an intrinsic property of the IgG1 C_H2 domain, since all IgG2 hybrid molecules containing an IgG1 C_H2 domain are as active as wild-type IgG1. Furthermore, cytophilic activity was abolished in all IgG1 hybrids containing an IgG2 C_H2 domain. These results are consistent with indirect evidence that the C_H2 domain is the primary site for $Fc_\gamma RI$

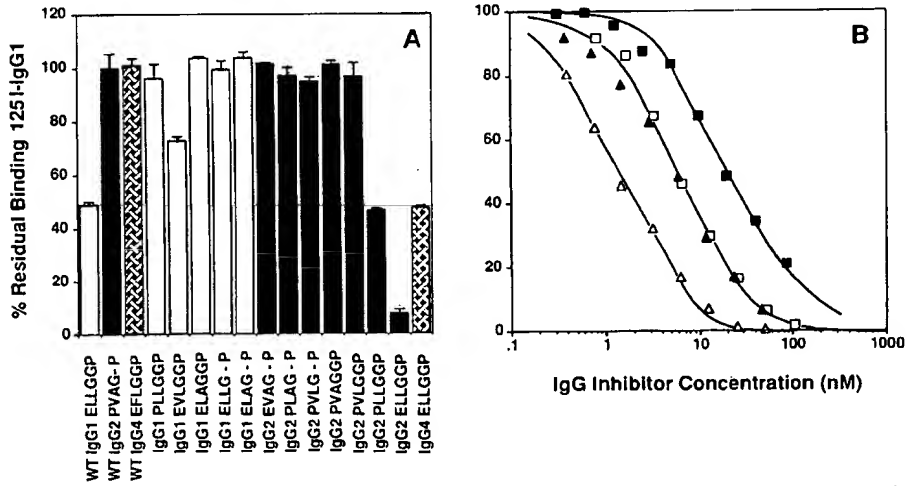

FIG. 4. Inhibition of ^{125}I-IgG1 binding to U937 $Fc_\gamma RI$ receptors by recombinant native and point-mutated IgG1, IgG2, and IgG4 molecules. (*A*) Bar graph representation of an experiment in which the concentrations of both ^{125}I-IgG1 and recombinant inhibitor were kept constant at 6.67 nM. The inhibitor used in the assay is indicated at the base of its corresponding bar. WT, wild type. (*B*) Binding inhibition curves using 10 nM ^{125}I-IgG1 and increasing concentrations of the following inhibitors: wild-type recombinant IgG1 (▲), IgG1/EVLGGP (■), IgG2/PLLGGP (□), and IgG2/ELLGGP (△).

recognition. Covalent IgG1 C_H2 domain dimers retain 85% of the cytophilic activity of the parent molecule (11), whereas the C_H2 domain-deleted paraprotein IgG1 TIM is devoid of activity (10). Furthermore, monoclonal anti-C_H2 antibodies inhibit the IgG1–Fc_γRI interaction (9). Recently, reciprocal domain and hinge exchange experiments between human IgG1 and IgE showed that both the IgG1 C_H2 and C_H3 domains were required to restore full Fc_γRI binding activity to IgE (14). Based on free energy calculations, it was concluded that the IgG1 C_H2 domain contributes ≈75% of the free energy gain associated with the IgG1–Fc_γRI interaction.

Several lines of evidence suggest that the activity of the Fc_γRI binding site depends on its conformation. Grafting an IgG1 C_H2 domain onto an IgE background did not restore Fc_γRI binding activity to IgE (14) despite its free energy contribution to the Fc_γRI interaction. The affinity of bispecific mouse IgG2a/IgG2b hybrid antibodies suggests that only one cytophilic H chain is required for the IgG1–Fc_γRI interaction (13). However, the findings that only dimeric isolated C_H2 domains are cytophilic (12) and that the C_H3 domain-deleted IgG1 paraprotein SIZ fails to bind Fc_γRI (10) infer that quaternary interactions between the domains are required to stabilize the active conformation of the IgG1 effector site. Furthermore, inactive aglycosylated IgG1 displays significantly enhanced sensitivity to pepsin and chymotrypsin (25). Since these enzymes cleave within the C_H2 domain, these findings suggest that carbohydrates maintain its conformation and stabilize the Fc_γRI binding site (8).

The most striking primary sequence differences between IgG1 and IgG2 C_H2 domains are clustered in the lower hinge region (residues 233–238) encoded by the C_H2 exon. A conserved LLGGP motif between positions 234 and 238 is found in all cytophilic IgG subclasses. The functional importance of the crystallographically defined "upper region" of the C_H2 domain is supported by the finding that inactive aglycosylated IgG3 Fc fragments show structural perturbations, as assessed by ^1H NMR, in the vicinity of the H268 reporter group located in the spatial proximity of the lower hinge (25). In addition, full Fc_γRI binding activity was restored to the inactive mouse IgG2b subclass by reconstructing the LLGGP motif with a single L for E substitution at position 235 (16). Moreover, recent reports (26, 27) showed that the binding activity of human IgG3 was lost in a panel of single point mutants where L234, L235, and G237 were replaced with A residues. Together, these observations led us to engineer a panel of IgG1 and IgG2 chimeras containing single and sequential point mutations in this region. Full binding activity was restored to an IgG2 molecule in which G was inserted at position 237, and V234 and A235 were replaced with their IgG1 counterparts L234 and L235 (IgG2/PLLGGP), respectively. Interestingly, within the limits of the binding-inhibition assay, none of the individual mutations could restore even partial activity to IgG2, although the single reciprocal mutations in IgG1 significantly diminished or abolished it completely. Our results confirm the prediction that the LLGGP motif is essential for Fc_γRI recognition (15). Indeed, an IgG4 mutant containing the ELLGGP motif was found to be as active as wild-type IgG1. Since only a single H chain is required for the Fc_γRI interaction (13), it is likely that at least the "docking" portion of the binding site is located on a loop or a single flexible strand at the N terminus of the C_H2 domain. Unfortunately, the protein segment containing the LLGGP sequence yielded no electron density in the x-ray crystallographic structure of human IgG1 Fc (28).

Interestingly, grafting of the ELLGGP motif onto IgG2 resulted in a molecule 4-fold more active than native IgG1. Although both the PLLGGP and the ELLGGP motifs restored activity to IgG2, only the ELLGGP sequence conferred full binding activity to IgG1. To rationalize these observations, it is necessary to propose the existence of "secondary" IgG2 Fc_γRI binding sites, which are either nonexistent in IgG1 or are more active than their IgG1 counterparts. These sites probably reside in the IgG2 C_H2 domain, since none of the shuffled IgG1 constructs displayed enhanced binding activity. IgG1 and IgG2 C_H2 domains diverge at five residues in their C-terminal halves. Whether these divergent residues contribute to a "secondary" interaction site between C_H2 and Fc_γRI remains to be investigated.

We would like to thank Dr. Leroy Hood for providing the original γ1, γ2, and γ4 C region gene segments and Cathy Horne for engineering the *Eco*RI site in the C_H2–C_H3 introns. We are also grateful to Dr. Aline Rinfret for providing the pSV2neoV_H315 expression vector and William Bradley for synthesizing the oligonucleotides used in this study. We also thank Dr. Alex Marks for donating the MOPC 315.26 variant cell line. This work was supported by Grant MT-4259 from the Medical Research Council of Canada. D.E.I. is the recipient of a Medical Research Council Grant (MT-7081) and M.S.C. is the recipient of an Ontario Graduate Scholarship.

1. Silverstein, S. C., Steinman, R. M. & Cohn, Z. A. (1977) *Annu. Rev. Biochem.* **46**, 699–722.
2. Shen, L., Guyre, P. M. & Fanger, M. W. (1987) *J. Immunol.* **139**, 534–538.
3. Graziano, R. F. & Fanger, M. W. (1987) *J. Immunol.* **139**, 3536–3541.
4. Karpovsky, B., Titus, J. A., Stephany, D. A. & Segal, D. M. (1984) *J. Exp. Med.* **160**, 1686–1701.
5. Rouzer, C. A., Scott, W. A., Kempe, J. & Cohn, Z. A. (1980) *Proc. Natl. Acad. Sci. USA* **77**, 4279–4282.
6. Anderson, C. L. & Looney, R. J. (1986) *Immunol. Today* **7**, 381–405.
7. Anderson, C. L. (1982) *J. Exp. Med.* **156**, 1794–1806.
8. Burton, D. R. (1985) *Mol. Immunol.* **22**, 161–206.
9. Partridge, L. J., Woof, J. M., Jefferis, R. & Burton, D. R. (1986) *Mol. Immunol.* **23**, 1365–1375.
10. Woof, J. M., Nik Jaafar, M. I., Jefferis, R. & Burton, D. R. (1984) *Mol. Immunol.* **21**, 523–527.
11. Ratcliffe, A. & Stanworth, D. R. (1983) *Immunology* **50**, 93–100.
12. Barnett Foster, D. E., Dorrington, K. & Painter, R. (1980) *J. Immunol.* **124**, 2186–2190.
13. Koolwijk, P., Spierenburg, G. T., Frasa, H., Boot, J. H., van de Winkel, J. G. J. & Bast, B. J. (1989) *J. Immunol.* **143**, 1656–1662.
14. Shopes, B., Weetal, M., Holowaka, D. & Baird, B. (1990) *J. Immunol.* **145**, 3842–3848.
15. Woof, J. M., Partridge, L. J., Nik Jaafar, M. I., Jefferis, R. & Burton, D. R. (1986) *Mol. Immunol.* **23**, 319–330.
16. Duncan, A. R., Woof, J. M., Partridge, L. J., Burton, D. R. & Winter, G. (1988) *Nature (London)* **332**, 563–566.
17. Mosmann, T. R., Baumal, R. & Williamson, A. R. (1979) *Eur. J. Immunol.* **9**, 511–517.
18. Rinfret, A., Horne, C., Dorrington, K. & Klein, M. (1989) *Mol. Immunol.* **26**, 431–434.
19. Maniatis, T., Fritsch, E. F. & Sambrook, J. (1982) *Molecular Cloning: A Laboratory Manual*, (Cold Spring Harbor Lab., Cold Spring Harbor, NY).
20. Taylor, J. W., Ott, J. & Eckstein, F. (1985) *Nucleic Acids Res.* **13**, 8764–8785.
21. Baker, M. D., Pennell, N., Bosnoyan, L. & Shulman, M. (1988) *Proc. Natl. Acad. Sci. USA* **85**, 6432–6436.
22. Raychaudhuri, G., McCool, D. & Painter, R. (1985) *Mol. Immunol.* **22**, 1009–1019.
23. Berzofsky, J. & Schechter, A. N. (1981) *Mol. Immunol.* **18**, 751–763.
24. Tan, L. K., Shopes, B. J., Oi, V. T. & Morrison, S. L. (1990) *Proc. Natl. Acad. Sci. USA* **87**, 162–166.
25. Lund, J., Tanaka, T., Takahashi, N., Sarmay, G., Arata, Y. & Jefferis, R. (1990) *Mol. Immunol.* **27**, 1145–1153.
26. Woof, J. M. (1990) *Biochem. Soc. Trans.* **18**, 217–218.
27. Jefferis, R., Lund, J. & Pound, J. (1990) *Mol. Immunol.* **27**, 1237–1240.
28. Deisenhofer, J. (1981) *Biochemistry* **20**, 2361–2370.

Delineation of the Amino Acid Residues Involved in Transcytosis and Catabolism of Mouse IgG1[1]

Corneliu Medesan,[2] Diana Matesoi, Caius Radu, Victor Ghetie, and E. Sally Ward[3]

The MHC class I-related receptor, FcRn, is involved in both the transcytosis of serum γ-globulins (IgGs) and in regulating their serum persistence. The interaction site of FcRn on the Fc region of rodent IgG has been mapped to residues at the CH2-CH3 domain interface using site-directed mutagenesis and x-ray crystallographic analyses. In the current study, the role of individual residues (H310, H433, and N434) at this interface in mediating the Fc-FcRn interaction has been investigated using recombinant, mutated Fc hinge fragments derived from mouse IgG1. In addition, two highly conserved Fc histidines (H435 and H436) have been mutated to alanine, and the resulting mutated Fc hinge fragments were analyzed in both transcytosis and pharmacokinetic studies in mice and in competition binding assays using recombinant, soluble FcRn. The analyses indicate that mutation of H310, H435, and, to a lesser extent, H436 to alanine results in reduced activity of the Fc hinge fragments in both in vivo and in vitro assays. Thus, in addition to the previously defined role of I253 in the FcRn-IgG interaction, these histidines play a key role in mediating the functions conducted by this Fc receptor. The effects of these mutations on binding of Fc hinge fragments to staphylococcal protein A have also been analyzed and demonstrate a partial, but not complete, overlap of the FcRn and staphylococcal protein A interaction sites on mouse IgG1. *The Journal of Immunology,* **1997, 158: 2211–2217.**

Recent studies have indicated that for mouse IgG, the MHC class I-related receptor FcRn[4] is involved in both the control of serum half-life and transcytosis across neonatal intestinal/maternofetal barriers (1–3). Site-directed mutagenesis has been used to identify amino acid residues of mouse IgG1 (mIgG1) that regulate these processes (4–7). These residues are located at the CH2-CH3 domain interface and are highly conserved in both human and murine IgGs (8). To identify these amino acids, recombinant Fc hinge fragments with double mutations of amino acid residues in the CH2 domain (H310A/Q311N) and CH3 domain (H433A/N434Q), and a single mutation in the CH2 domain (I253A) have been characterized in pharmacokinetic studies (4, 5) and in transcytosis across yolk sac and neonatal small intestine (6, 7). These studies demonstrated that mutation of the CH2 domain residues had a more marked effect on both serum half-life and transcytosis than the CH3 domain mutations. Furthermore, the mutants were also impaired in binding to recombinant, soluble FcRn (9). However, these analyses did not exclude a role for other conserved amino acid residues in the CH3 domain. In addition, for the H310A/Q311N and H433A/N434Q mutants, two simultaneous mutations were made in both the CH2 and CH3 domains, and it was, therefore, not possible to identify which of the four amino acids (H310, Q311, H433, and N434) are directly involved in building the FcRn interaction site of mIgG1. The aim of this work was to identify which of these four amino acid residues are involved in the regulation of IgG transcytosis/catabolism and to investigate a possible role for other CH3 domain residues (H435 and H436) that are highly conserved in IgGs (8).

Materials and Methods

Generation of mutated Fc hinge fragments derived from mIgG1

Mutations were made using designed mutagenic oligonucleotides and either splicing by overlap extension (10) or site-directed mutagenesis (11, 12). The mutants are described in Table I, and the generation of mutants I253A and H285A has been described previously (4, 5). For other mutants, mutagenic oligonucleotides used in site-directed mutagenesis were as follows: I1433A, 5′-GGTGGTTGGCCAGGCCCT-3′; H435A, 5′-CAGTAT GGGCGTTGTGCA-3′; and H436A, 5′-CTCAGTAGCGTGGTTGTG-3′. Mutants H310A, N434A, and N434Q were made using splicing by overlap extension (10) with the following mutagenic oligonucleotides: H310A, 5′-CCCATCATGGCCCAGGACTGG-3′ and 5′-CCAGTCCTGGGC CATGATGGG-3′; N434A, 5′-GGCCTGCACGCGCACCATACT-3′ and 5′-AGTATGGTGCGCGTGCAGGCCCTC-3′; and N434Q, 5′-AGTATG GTGTTGGTGCAG-3′ and 5′-CTGCACCAACACCATACT-3′. For each oligonucleotide, percent underlining indicates mutated bases. For all mutants, the corresponding genes were sequenced using the dideoxynucleotide method (13) and Sequenase before functional analysis.

Expression and purification of the recombinant proteins

Wild-type (wt) and mutant Fc hinge fragments tagged with carboxyl-terminal hexahistidine peptides were purified using Ni^{2+}-NTA-agarose (Qiagen, Chatsworth, CA) as described previously (4). After dialysis against 15 mM phosphate buffer/50 mM NaCl, pH 7.5, the mutants were either kept at 4°C for short term storage (<10 days) or freeze dried for longer term storage. Recombinant soluble mouse FcRn was expressed and purified using the baculovirus system as described previously (9) and stored at 4°C.

Department of Microbiology and Cancer Immunobiology Center, University of Texas, Southwestern Medical Center, Dallas, TX 75235

Received for publication September 13, 1996. Accepted for publication December 2, 1996.

The costs of publication of this article were defrayed in part by the payment of page charges. This article must therefore be hereby marked *advertisement* in accordance with 18 U.S.C. Section 1734 solely to indicate this fact.

[1] This work was supported in part by grants from the National Institutes of Health (AI39167), the Welch Foundation, and the Texas Advanced Research Program (Texas Higher Education Coordinating Board). This work was performed while Dr. Corneliu Medesan was a visiting fellow in the Department of Microbiology and Cancer Immunobiology Center, University of Texas Southwestern Medical Center (Dallas, TX).

[2] Current address: Institute of Virology, Center of Immunology, sos. Mihai Bravu 285, 79650 Bucharest, Romania.

[3] Address correspondence and reprint requests to Dr. E. Sally Ward, Department of Microbiology and Cancer Immunobiology Center, University of Texas Southwestern Medical Center, 5323 Harry Hines Blvd., Dallas, TX 75235-8576.

[4] Abbreviations used in this paper: FcRn, neonatal Fc receptor; Fc, immunoglobulin constant region fragment; mIgG1, mouse immunoglobulin G1; wt, wild type; CD, circular dichroism; PB-6, 50 mM phosphate buffer with 250 mM NaCl and 5 mM Na_2EDTA, pH 6.0; SpA, staphylococcal protein A; PB-7.5, 50 mM phosphate buffer containing 250 mM NaCl, 5 mM Na_2EDTA, pH7.5.

0022-1767/97/$02.00

Table I. *Recombinant Fc-hinge derivatives used in this study*

Designation	Mutation	Domain
WT Fc-hinge	None	
I253A[a]	Ile 253 to Ala	CH2
H285A	His 285 to Ala	CH2
H310A	His 310 to Ala	CH2
H433A	His 433 to Ala	CH3
H433A/N434Q[a]	His 433 to Ala and Asn 434 to Gln	CH3
N434A	Asn 434 to Ala	CH3
N434Q	Asn 434 to Gln	CH3
H435A	His 435 to Ala	CH3
H436A	His 436 to Ala	CH3

[a] Mutants described previously (4, 5).

Analysis of the mutant Fc hinge fragments using SDS-PAGE and circular dichroism (CD)

SDS-PAGE (14) and CD analyses were conducted as described previously (4).

Radiolabeling of the proteins

Monoclonal mIgG1, recombinant mouse Fcγ_1 hinge fragments, and recombinant mouse FcRn (mFcRn) (9) were radiolabeled with [^{125}I]Na (Amersham, Arlington Heights, IL) using the Iodogen reagent (15) as described previously (4). Free iodine was removed by centrifugation on MicroSpin G-25 columns (Pharmacia, Piscataway, NJ). The specific activities of the radiolabeled proteins were approximately 5×10^6 cpm/μg, with <5% free iodine. The radioactive proteins were stored at 4°C for not more than 1 wk before injection into mice.

Chromatographic analysis

All radiolabeled Fc hinge fragments were analyzed on an s-250 column (Bio-Rad, Hercules, CA) by permeation HPLC. The sera collected from mice injected with radiolabeled Fc hinge fragments at 24 h were pooled and analyzed by HPLC on an s-250 column (Bio-Rad). The radioactivities of the chromatographic fractions were measured with a gamma counter, and the molecular mass and heterogeneity of the radioactive peak were determined.

Determination of serum IgG concentration

The concentration of serum IgG was determined using radial immunodiffusion with Nanorid and Bindarid kits (The Binding Site, Birmingham, UK). Precipitin ring diameters were measured electronically.

Pharmacokinetic analyses

Pharmacokinetics of radioiodinated Fc hinge fragments were determined in 6-wk-old BALB/c mice (Harlan Sprague-Dawley Laboratory, Indianapolis, IN) as described previously (4, 5).

Maternofetal transmission

Previously described methodology (7) was used with pregnant outbred SCID mice (Taconic Co., Germantown, NY) near term (15–18 days). In brief, mice were fed 0.01% NaI in drinking water and then 1 day later injected with radiolabeled protein (2×10^7 to 5×10^7 cpm) in the tail vein. Mice were bled with a 20-μl capillary 3 min postinjection, and 24 h later fetuses were delivered by cesarean section. The fetuses of a litter were pooled (discarding the placenta), washed in saline, weighed, frozen in liquid nitrogen, and homogenized in 10 vol of 10% TCA. The suspension was centrifuged, and the radioactivity of the precipitate was determined in a gamma counter. The percentage of transmission was calculated with the formula: % transmission (%T) = (R3)/[(R1 − R2) × (W × 0.72)/0.02], where R1 is radioactivity in maternal blood at 3 min, R2 is radioactivity in maternal blood at 24 h, W is body weight (grams), and R3 is radioactivity of the fetuses.

The total weight and number of fetuses in a given litter varied from litter to litter, and therefore, the transmission data are presented per unit weight of fetuses rather than the amount transferred per litter (%T/g) (7). The blood volume of pregnant mice was considered to be 7.2% of body weight (16). The radioactivity in the maternal blood available for transmission to the fetus was calculated by deducting the radioactivity remaining at 24 h from that measured at 3 min after the injection of radiolabeled protein.

Inhibition of transintestinal transfer

BALB/c neonatal mice (10–14 days old) from the Animal Resource Center, University of Texas Southwestern Medical Center (Dallas, TX), were intubated with a mixture of [^{125}I]mIgG1 and Fc hinge fragment at a Fc/IgG molar ratio of approximately 2000 as described previously (6). The percentage of inhibition was calculated relative to the transfer of the same amount of [^{125}I]mIgG1 without inhibitor.

Inhibition of FcRn binding to mIgG1-Sepharose

All Fc hinge derivatives were dialyzed into 50 mM phosphate buffer with 250 mM NaCl and 5 mM Na_2EDTA, pH 6.0 (PB-6), and adjusted to a concentration of 1 mg/ml. Three hundred microliters of Fc hinge (wt or mutant) or PB-6 was incubated in Eppendorf tubes with rotation for 30 min at 25°C with 150 μl of mIgG1-Sepharose (1 mg/ml packed gel, 50% suspension), 50 μl of PB-6 containing 10 mg/ml OVA (Sigma Chemical Co., St. Louis, MO), and 10 μl of [^{125}I]FcRn (0.1 μg/200,000 cpm). Following incubation, 500 μl of ice-cold PB-6 was added, and the gel was washed three times by centrifugation at 12,000 × *g* for 3 min using ice-cold PB-6 (plus 1 mg/ml OVA). The radioactivity bound to the gel was determined. The gel pellet was resuspended in 1 ml of PB-7.5 (with 1 mg/ml OVA), and the supernatant was discarded after centrifugation. The remaining radioactivity bound to the gel was determined. The radioactivity specifically bound to the mIgG1-Sepharose gel was calculated by subtracting the remaining radioactivity from the bound radioactivity. The inhibition of binding of FcRn to mIgG1-Sepharose by Fc derivatives was calculated using the equation: % inhibition = 100 − 100 *A*/*B*, where *A* is the specific radioactivity bound to mIgG1-Sepharose in the presence of Fc hinge fragment, and *B* is the specific radioactivity bound in the absence of Fc hinge fragment.

Analysis of binding to staphylococcal protein A (SpA)

SpA-agarose gel (0.5 ml) was equilibrated with PB-7.5 and 1 mg/ml OVA (PB-7.5). Fifty to one hundred microliters of each ^{125}I-labeled Fc hinge fragment containing 50 μg of protein was loaded onto the column, incubated for 15 min, and then washed with 10 column volumes of the same buffer. Bound Fc hinge fragments were eluted with 100 mM acetic acid. The amounts of radioactivity in the flow-through, washes, and eluates were determined. The ratio of bound/unbound was calculated, and the percentage of binding of each mutant relative to the wt Fc hinge fragment was determined.

Results

Expression and analysis of mouse Fcγ_1 hinge mutants

Plasmids encoding the wt Fc hinge and mutants (Table I) were constructed, and the proteins were expressed and purified using *Escherichia coli* as a host. With the exception of the H285A mutant, the residues that have been mutated are all in close proximity to the CH2-CH3 domain interface (17) and are also highly conserved in the IgG isotypes of both mouse and man (8). As described previously, the radiolabeled Fc hinge derivatives emerged essentially as single peaks with a retention time corresponding to 55 kDa when analyzed on an s-250 column (4) (data not shown). Taken together with HPLC analyses, reducing and nonreducing SDS-PAGE analyses indicate that the Fc hinge derivatives are expressed as a mixture of noncovalently linked and sulfhydryl-linked homodimers (Fig. 1). In addition, CD studies of the Fc hinge derivatives show that the mutations do not result in large scale changes in the structures of the recombinant proteins (Fig. 2).

Pharmacokinetic analysis of the Fc hinge fragments

Radiolabeled Fc hinge fragments were injected into mice, and the serum radioactivity was monitored at various time points following injection. For each Fc hinge derivative, the elimination curves in different mice were similar, and Figure 3 shows representative curves for one mouse from each group.

For each recombinant Fc hinge fragment, the serum samples collected at the 24 h point from mice within one group were pooled

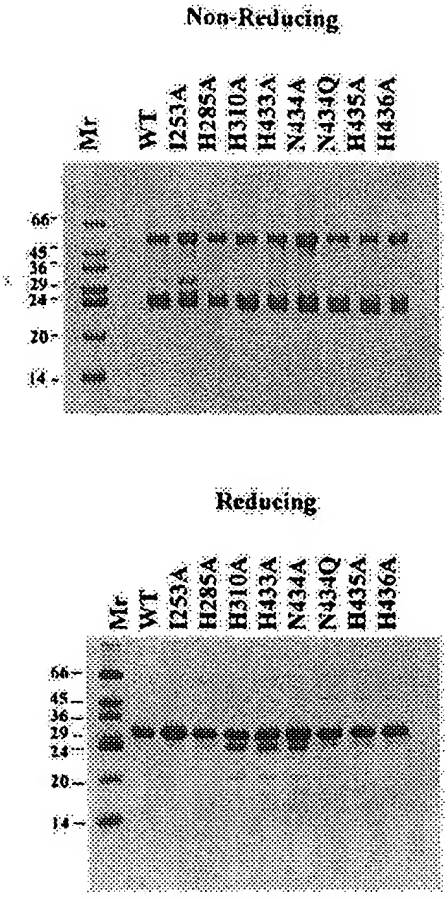

FIGURE 1. SDS-PAGE of wt and mutant Fc hinge fragments using nonreducing and reducing conditions. The molecular mass of size standards (Mr) are indicated on the *left margins*.

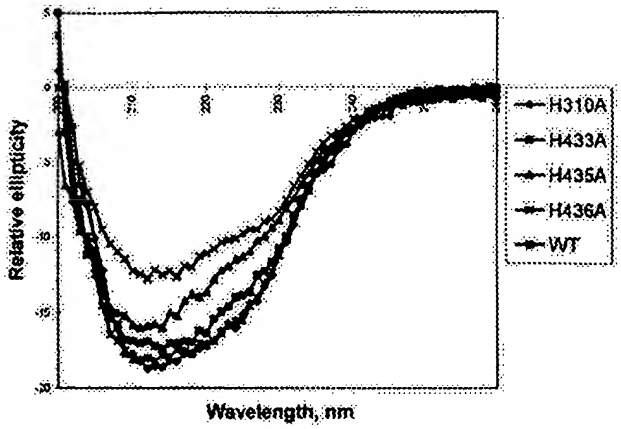

FIGURE 2. CD spectra of recombinant Fc hinge fragments.

and subjected to HPLC on an s-250 column. For all the Fc hinge fragments, the majority of the radioactivity eluted as a single peak with a retention time corresponding to the molecular mass of the injected protein (55 kDa; data not shown). In agreement with our previous results (4), this indicates that the Fc hinge derivatives persist in serum as homodimeric molecules and are not proteolytically digested or associated with other serum proteins. The pharmacokinetic parameters of the Fc hinge derivatives are shown in Table II, and the α-phase represents the equilibration time between the intra- and extravascular space, whereas the β-phase represents the elimination of the equilibrated protein from the intravascular space. Furthermore, during the α-phase, any misfolded protein molecules that might be present in the recombinant protein preparations are eliminated (C. Medesan, unpublished observations), and therefore, the β-phase represents the elimination of correctly folded protein from the intravascular space.

The data clearly demonstrate that some mutations have a significant effect on the β-phase half-life of the corresponding Fc hinge fragment. Thus, mutation of H310 in the CH2 domain has a marked effect on the catabolic rate (Table II). In contrast, mutation of H285, located in a loop on the external surface of the CH2 domain distal to the CH2-CH3 interface (17), has no effect on the catabolic rate, and this is consistent with our previous findings (5). Simultaneous mutation of H433 and N434 decreases the β-phase half-life to 77 h (36% decrease), while single mutation at each of these positions yielded two mutants (H433A and N434A) with the same half-life as the wt Fc hinge. Substitution of N434 with glutamine instead of alanine (N434Q) also yielded an Fc hinge fragment with a half-life similar to that of the wt Fc hinge (Table II). The half-life of the H433A-N434Q mutant (76.9 h) is greater than the value reported previously (50.3 h) (4), and this is also observed for the wt Fc hinge fragment (119 vs 82.9 h), H285A (106 vs 85 h), and I253A (26 vs 20 h). An explanation for these apparent discrepancies is that the BALB/c mice used in the present work (from Harlan Laboratories) have an IgG concentration of 1.0 ± 0.4 mg/ml (average of 25 mice), which is considerably lower than that in BALB/c mice from our own animal colony (4.6 ± 0.8 mg/ml) used in earlier experiments (4, 5). The concentration-catabolism relation (18) predicts that the half-life of IgG will be longer in mice with lower serum IgG concentrations, and this may explain the longer half-lives of the Fc hinge fragments in the cases above where direct comparisons have been made.

Mutation of H435 in the CH3 domain has an effect as marked as that induced by mutation of I253 or H310 in the CH2 domain, clearly indicating that this CH3 domain residue plays an important role in building the catabolic site of mIgG1. Furthermore, the H436A mutant has a half-life of 49 h, demonstrating that H436 plays a more minor role than I253, H310, or H435 in controlling catabolism (Table II).

Maternofetal transfer

The analysis of the pharmacokinetics of the Fc hinge fragments was extended to maternofetal transfer studies. The transfer of radiolabeled Fc hinge derivatives from the circulation of near-term pregnant SCID mice to the fetuses was analyzed by measuring the protein-bound radioactivity taken up by fetuses of one litter relative to the radioactivity present in the maternal blood during the 24-h interval used for the transfer experiment. The results are shown in Figure 4*A*. In an earlier study it was demonstrated that both wt and mutant Fc hinge fragments are transferred to the fetuses as intact molecules (7). Thus, differences in transfer do not appear to be due to differences in susceptibility to proteolysis of wt vs mutant molecules. The transmission of I253A, H310A, and H435A mutants was only approximately 10 to 20% that of the wt Fc hinge or H285A, demonstrating the central role played by these residues in the maternofetal transfer of IgG. Thus, these mutations have similar effects on maternofetal transfer and catabolism. However, the correlation between the β-phase half-life and maternofetal transmission found for I253A, H310A, H433A, and H435A was not observed for the H436A mutant. Relative to wt Fc hinge, this mutant has a similar activity in maternofetal transmission but a shorter half-life (Table II and Fig. 4*A*); possible reasons for this are discussed more fully below.

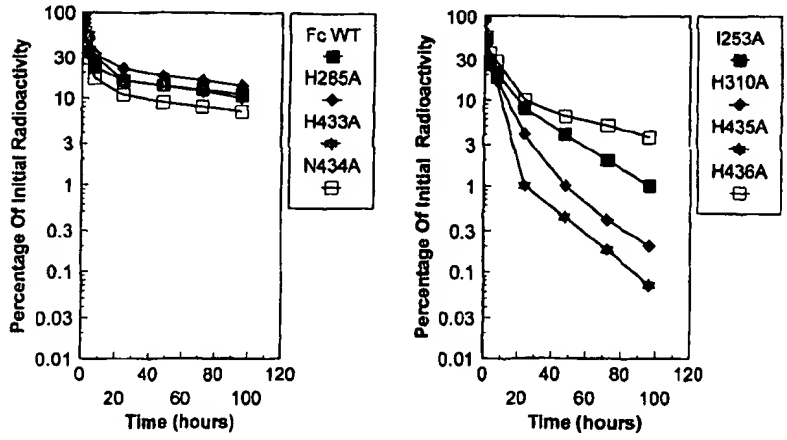

FIGURE 3. Elimination curves of recombinant Fc hinge fragments. The percentage of initial radioactivity (logarithmic scale) is plotted vs time post-initial injection of radiolabeled Fc hinge fragment. Representative curves for one mouse from each group are shown.

Table II. *Catabolism of recombinant Fc-hinge fragments in BALB/c mice*

Fc-hinge Fragment	No. of Mice	α-Phase Half-Life	β-Phase Half-life
WT Fc-hinge	5	11.9 ± 0.2	119.1 ± 11.5
I253A	11	9.0 ± 1.8	26.2 ± 1.9
H285A	6	10.8 ± 3.0	106.4 ± 11.7
H310A	9	5.8 ± 0.2	16.8 ± 1.2
H433A	9	9.6 ± 1.0	114.8 ± 10.8
H433A/N434Q	9	9.4 ± 1.1	76.9 ± 10.3
N434A	4	9.0 ± 0.2	110.0 ± 9.2
N434Q	5	11.7 ± 0.3	115.0 ± 12.6
H435A	6	4.4 ± 0.2	17.4 ± 2.8
H436A	9	8.5 ± 0.3	48.7 ± 2.4

Intestinal transfer

The intestinal transmission of recombinant Fc hinge derivatives was analyzed by measuring their ability to inhibit the transfer of radiolabeled mIgG1 across the intestinal barrier of neonatal mice (Fig. 4*B*). The results are consistent with the data obtained for maternofetal transmission of the I253A, H310A, and H435A mutants, indicating that the same receptor and mechanism of transmission are involved in both transcytotic processes. However, the H436A mutant is transferred across the maternofetal barrier of SCID mice almost as efficiently as the wt Fc hinge (Fig. 4*A*) and yet does not inhibit the transfer of mIgG1 across the neonatal intestine as effectively. Thus, for this mutant, the half-life and inhibition of neonatal transfer are reduced relative to the wt Fc hinge, and yet maternofetal transfer appears to be unaffected.

Affinity for FcRn

The relative affinities of the recombinant Fc hinge fragments for binding to recombinant mFcRn were estimated by measuring their ability to inhibit binding of [^{125}I]FcRn to mIgG1-Sepharose (Fig. 5*A*). The data demonstrate that in all cases, the mutants with short half-life and decreased activity in transcytosis assays (maternofetal and neonatal) also have a lower affinity for binding to FcRn, with the exception of H436A. Despite a lower relative affinity for FcRn, this mutant is transferred across the maternofetal barrier as efficiently as wt Fc hinge, and yet has a reduced serum half-life and activity in intestinal transfer assays.

Binding to SpA

It has been previously shown that the SpA binding site and the catabolic site are located at the CH2-CH3 domain interface of mIgG1 (4), and therefore, the effect of mutations on the binding of the Fc hinge fragments to SpA were analyzed in direct binding studies (Fig. 5*B*). The data indicate that H310A and H435A are greatly impaired in SpA binding (9–12% of wt), whereas mutation of I253 or H433 has a less marked effect (30–35% of wt).

Discussion

This study demonstrates that amino acid residues of the CH2 domain (I253 and H310) and CH3 domain (H435 and, to a lesser extent, H436) are involved in regulating the transcytosis and serum persistence of mIgG1. Although this conclusion is drawn from the analysis of recombinant Fc hinge fragments that are expressed in an aglycosylated form, our earlier studies demonstrated that the wt Fc hinge fragment has the same β-phase half-life (4) and activity in transcytosis assays (6) as complete glycosylated mIgG1. This indicates that for this isotype it is valid to extend studies with aglycosylated Fc hinge fragments to complete IgGs. Thus, residues in both domains play a key role in the two processes that involve FcRn-mIgG1 interactions, and the locations of these amino acids on the three-dimensional structure of the homologous human Fcγ_1 (17) are shown in Figure 6. This conclusion may appear to contradict our earlier statement that mutations in the CH2 domain have a more marked effect than mutations in the CH3 domain (4–7). However, in these earlier studies only the effect of simultaneous mutation of both H433 and N434 on transcytosis/catabolism was analyzed, and this indicated a minor role for these residues. In the current analysis, mutation of each of these two amino acids individually has insignificant effects on both transcytosis and catabolism. The most plausible explanation for the observed effects of mutation of both H433 and N434 is that simultaneous mutation of these two amino acids causes a local perturbation in the orientation of the adjacent histidine (H435), which, in contrast to H433 and N434, plays a critical role in the FcRn-mIgG1 interaction.

Further analysis of the region encompassing H310 and Q311, which had previously been analyzed in the context of simultaneous mutation of H310, Q311 to A310, N311, demonstrates the central role of H310 in the FcRn-mIgG1 interaction. Mutation of H310 to alanine has an effect that is as marked as that seen for the H310A/Q311N mutant analyzed earlier, and for this reason the effect of mutation of Q311 alone was not investigated in the current study. In contrast to I253, H310, and H435, H436 plays a more minor role in maintaining serum IgG levels and transcytosis. Both I253 and H310 are highly conserved in all murine and human IgG isotypes (8), whereas H435 and H436 show a lesser degree of conservation (Y435, Y436 in mIgG2b; L436 in a mIgG2a allotype; Y436 in

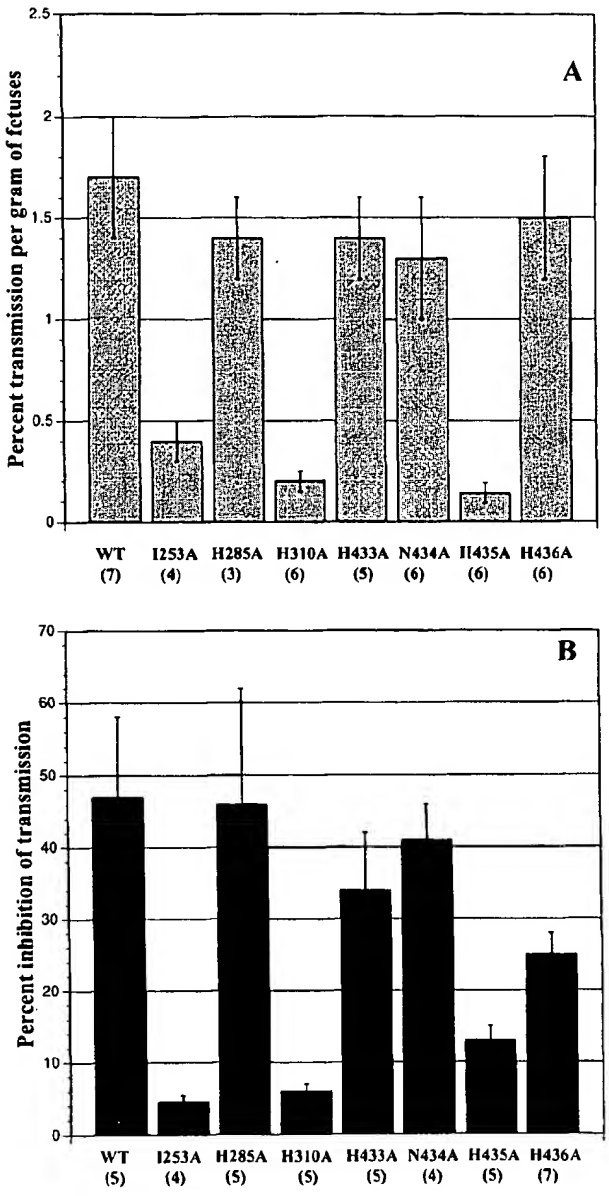

FIGURE 4. Transcytosis of recombinant Fc hinge fragments. The numbers in parentheses represent the number of mice used for each experiment. *A*, Maternofetal transmission of recombinant Fc hinge fragments in SCID mice. *B*, Inhibition of intestinal transmission of radiolabeled mIgG1 by recombinant Fc hinge fragments in BALB/c neonates. The value for H433A is not significantly different from that for wt Fc hinge (by Student's test, $p = 0.127$).

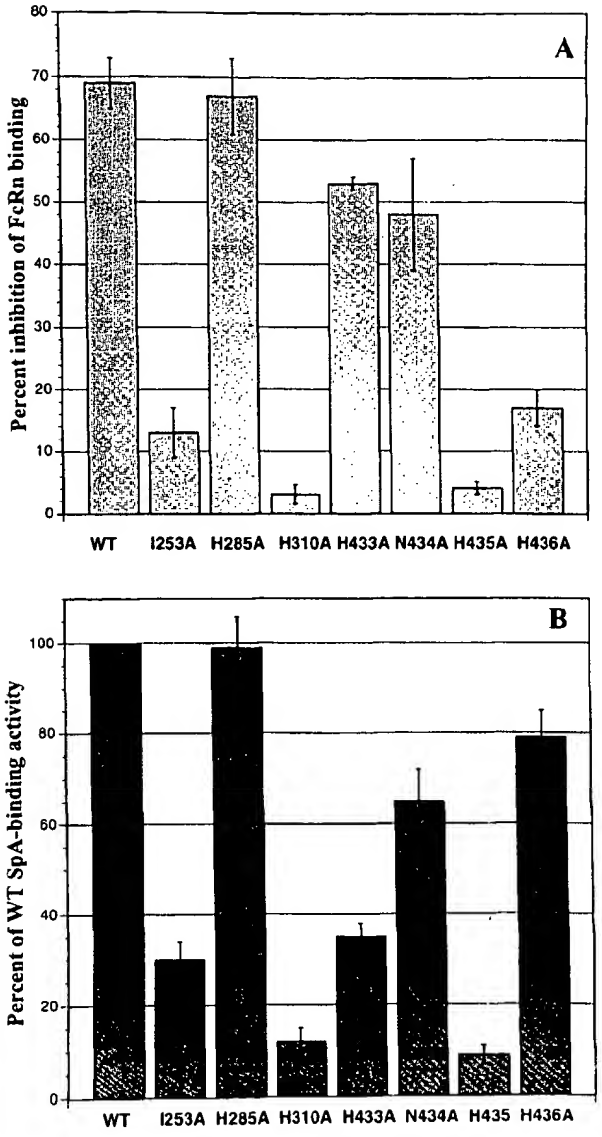

FIGURE 5. Binding of recombinant Fc hinge fragments to FcRn and SpA. *A*, Percent inhibition of FcRn binding to mIgG1-Sepharose relative to binding in absence of inhibitor (average of three separate experiments). *B*, Percentage of Fc hinge fragment binding to SpA-Sepharose relative to the binding of wt Fc hinge (average of three separate experiments).

human IgG1, IgG2, and IgG4; F436 in human IgG3 and R435 in a human IgG3 allotype). These sequence differences might account for the shorter serum half-lives of mIgG2b and human IgG3 (19) relative to other IgG isotypes. To date, there are no consistent data available concerning the relative transcytotic activities of different human (20) and mouse IgG (16) isotypes, and therefore, it is not possible to hypothesize about the effects of amino acid differences at positions 435 and 436 on maternofetal or neonatal transfer. In contrast to IgGs, IgM, IgE, and IgA have short serum half-lives and are not transferred across the placental/yolk sac barrier or neonatal gut (21, 22). Consistent with these observations, none of the residues shown in this study to be important for mediating the Fc-FcRn interaction are present in IgM, IgE, and IgA, although these three Ig classes of both humans and mice share significant homology with IgGs in other regions of the respective molecules (8).

I253 is a highly exposed, hydrophobic residue that is conserved in all IgG molecules belonging to mammals (8). In the present study we have confirmed that mutation of this isoleucine to alanine results in considerable decreases in the serum half-life and transcytosis across the maternofetal barrier or neonatal intestine. This clearly indicates that I253 fulfills a key physiologic role beyond binding to SpA (17). The amino acid residues flanking I253 are involved in the binding of human Fc to SpA (17), and their participation in the binding of FcRn cannot be excluded. Thus, M252 is highly conserved in all IgG isotypes of mouse, rat, guinea pig, rabbit, and human with a few exceptions, such as mIgG1 and rat IgG1/IgG2a, for which threonine replaces methionine (8). Similarly, position 254 is occupied by serine for all isotypes and species

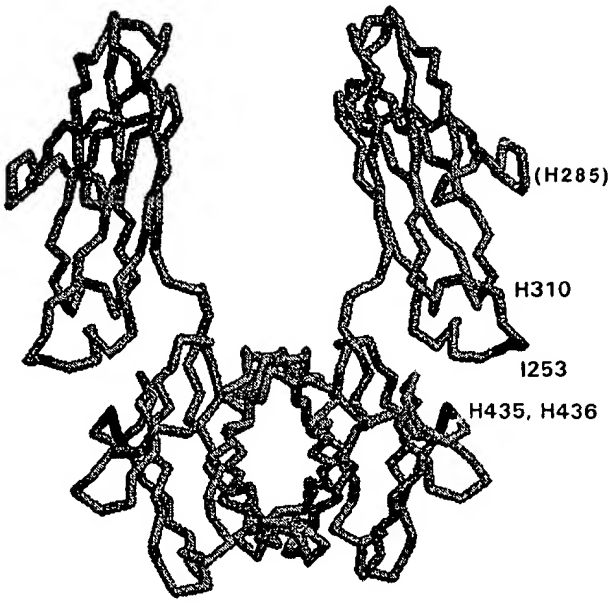

FIGURE 6. The three-dimensional structure of the Fc region of IgG (17), with the amino acids involved in transcytosis and catabolism indicated. The location of H285, which is not involved in interacting with FcRn, is also shown with lettering for H285 in parentheses to indicate that it is not involved in the FcRn-mIgG1 interaction. The program RASMOL (Roger Sayle, Bioinformatics Research Institute, University of Edinburgh, U.K.) was used to display this structure.

except the above-mentioned mouse and rat isotypes that have threonine at this position. These changes in positions 252 and 254 may correlate with longer half-life and more efficient transcytosis of mIgG1 compared with the other isotypes.

For all mutants except H433A and H436A, binding to FcRn and SpA is impaired to a similar degree. H433A has reduced SpA binding relative to wt Fc hinge, but is unaffected when interacting with FcRn. Conversely, the H436A mutation has the opposite effect. Thus, although the SpA and FcRn interaction sites overlap, the overlap is not complete and the "footprints" of SpA and FcRn on mIgG1 are distinct. This is also consistent with the differences in pH dependence that are observed for the FcRn-mIgG1 and SpA-mIgG1 interactions (23–25).

The pH dependence of the interaction between IgG and FcRn (binding at pH 6–6.5 and release at pH 7–7.5) (23, 24) falls in the range of the pK value of the imidazole side chains of histidine. Taken together with the data from this study, this suggests that the marked pH dependence of the IgG-FcRn interaction is determined by the surface accessible histidine residues at positions 310, 435, and 436 located at the interface of the CH2 and CH3 domains. This is in accord with data of Bjorkman and colleagues indicating that for mIgG2a, there are three titratable residues in the pH range of 6.4 to 6.9 (26). Consistent with these studies (26), analysis of the H310A mutant demonstrates that H310A plays a role in mediating the Fc-FcRn interaction both in vitro and in vivo. In contrast, however, analysis of H433A and H435A shows that for mIgG1, mutation of H435 to alanine results in a loss of affinity for FcRn, whereas H433 does not play a role in FcRn binding. Furthermore, mutation of H436 to alanine results in an Fc hinge fragment that has reduced affinity for FcRn. Thus, the histidines that play a role in mediating the high affinity of the mIgG1-FcRn interaction are H310, H435, and, to a lesser extent, H436. The reasons for the apparent differences in H433 and H435 between our data and those of others (26) are not clear, but in the latter study different isotypes (mIgG2a, mIgG2b, and human IgG4) with consequent sequence differences in the residues both at and in proximity to the FcRn interaction site were used. Thus, it is conceivable that in the context of differences in the sequences of surrounding residues, the relative roles of H433 and H435 are distinct in different isotypes.

The close correlation between the effect of mutations of the Fc hinge fragments on pharmacokinetics, transcytosis across neonatal brush border/yolk sac, and affinity for FcRn (Table III) supports the concept that FcRn is involved in all these processes (2, 3). This is also consistent with experiments showing that in mice lacking FcRn due to loss of β_2m expression, IgGs have decreased intestinal transmission (1, 27) and abnormally short serum half-lives (2, 3). For both the control of catabolism and transcytosis, it has been hypothesized that only the IgG molecules bound to FcRn are protected from degradation and reenter the circulation (catabolism) or traverse the yolk sac/neonatal intestine (transcytosis) (28). FcRn was first identified as a functional protein in tissues of different species (placenta, yolk sac, and brush border of neonatal intestine) involved in the transmission of Ab from mother to fetus or neonate (23, 24, 29–32). More recently, mouse FcRn α-chain mRNA has been isolated from organs not involved in maternal transmission of IgGs, such as liver, lung, heart, and spleen (2). Rat and human homologues of FcRn have also been found to be ubiquitously expressed at the mRNA level (33–35). This strongly suggests that FcRn might be synthesized by the endothelial cells within these organs. Consistent with this, FcRn α-chain mRNA (2) and the corresponding protein (J. Borvak et al., unpublished observations) have been isolated from cultivated mouse endothelial cells (SVEC), suggesting that endothelial cells might be the site of IgG catabolism. The isolation of a human homologue of FcRn from human placenta (30–32) that is ubiquitously expressed in adult tissues (33) together with the high degree of conservation of I253, H310, and H435 in human IgGs (8) indicate that the same mechanisms of maternofetal transfer and homeostasis of serum IgGs are operative in humans. Understanding these processes in molecular

Table III. *Pearson's correlation coefficient test*

	Catabolism	Intestinal Transfer	Affinity for FcRn	Protein A Binding
Maternofetal Transmission	$r = 0.8703$ $p = 0.0049$	$r = 0.8928$ $p = 0.0028$	$r = 0.8358^a$ $p = 0.0097$	$r = 0.8838$ $p = 0.0036$
Catabolism		$r = 0.9450$ $p = 0.0004$	$r = 0.9776$ $p = 0.00003$	$r = 0.7107$ $p = 0.0482$
Intestinal Transfer			$r = 0.9531$ $p = 0.00025$	$r = 0.8361$ $p = 0.0097$
Affinity for FcRn				$r = 0.7709$ $p = 0.0251$

[a] Correlation coefficient excluding values obtained for H436A; $r = 0.9917$; $p = 0.00001$.

detail has implications both for the modulation of the pharmacokinetics of therapeutic IgGs and for the enhancement of maternofetal transfer of IgGs that might be of value in passive immunization of fetuses.

The pH dependence of the FcRn-IgG interaction (23, 24) suggests that the subcellular site (cell surface or intracellular compartment) at which binding occurs will differ for neonatal transcytosis and maternofetal transfer/control of catabolism, as discussed previously (2). Other unknown factors, such as the rate of recycling in these different cellular compartments, may also play a role in determining the effective concentration of FcRn. These differences between the processes and the cell types involved, despite the involvement of a common receptor, may explain the behavior of the H436A mutant, for which the half-life, intestinal transfer, and affinity for FcRn do not correlate with the maternofetal transmission as closely as for the other mutants. A further explanation for the anomalous effects of the H436A mutation might be as follows; mutation of H436 to alanine does not have as marked an effect on catabolism, inhibition of intestinal transfer, and binding to FcRn as those observed for I253A, H310A, and H435A, and in contrast to the other three assays, the maternofetal transfer assay is conducted in the absence of competition by endogenous IgGs using SCID mice. Thus, in this situation, the effect of this mutation on maternofetal transfer might only manifest itself if an analysis of the time course of transmission is conducted or if transfer is analyzed in the presence of endogenous competing IgGs in, for example, BALB/c mice. In contrast, for mutants such as I253A, H310A, and H435A that have lower affinity than H436A for binding to FcRn in competition assays, the low activities in all three in vivo assays (catabolism, maternofetal transfer, and inhibition of neonatal transcytosis) correlate closely.

In summary, this study has resulted in the unequivocal identification of a role for three highly conserved histidines of mIgG1 (H310, H435, and, to a lesser degree, H436) in the control of catabolism and maternofetal/neonatal transcytosis. Thus, taken together with earlier data implicating I253 in these processes, these residues are critical for the FcRn-mIgG1 interaction. This study extends further the evidence in support of the involvement of FcRn in both transcytosis and catabolism, and has relevance to understanding the molecular mechanisms that regulate these essential functions of IgGs.

Acknowledgments

We are grateful to Dr. Sergei Popov for carrying out the CD analyses and preparing Figure 2. We also thank Dr. Jozef Borvak and May Fang Tsen for assistance with DNA sequencing and animal work; respectively. The excellent technical assistance of Greg Hubbard and the assistance of Ms. Cindy Self in the preparation of several figures are gratefully acknowledged.

References

1. Israel, E. J., V. K. Patel, S. F. Taylor, A. Marshak-Rothstein, and N. E. Simister. 1995. Requirement for a β_2-microglobulin associated Fc receptor for acquisition of maternal IgG by fetal and neonatal mice. *J. Immunol. 154:6246.*
2. Ghetie, V., J. G. Hubbard, J. K. Kim, M. F. Tsen, Y. Lee, and E. S. Ward. 1996. Abnormally short serum half-lives of IgG in β_2-microglobulin deficient mice. *Eur. J. Immunol. 26:690.*
3. Junghans, R. P., and C. L. Anderson. 1996. The protection receptor for IgG catabolism is the β_2-microglobulin-containing neonatal intestinal transport receptor. *Proc. Natl. Acad. Sci. USA 93:5512.*
4. Kim, J. K., M. F. Tsen, V. Ghetie, and E. S. Ward. 1994. Identifying amino acid residues that influence plasma clearance of mouse IgG1 fragments by site directed mutagenesis. *Eur. J. Immunol. 24:542.*
5. Kim, J. K., M. F. Tsen, V. Ghetie, and E. S. Ward. 1994. Catabolism of the murine IgG1 molecule: evidence that both CH2-CH3 domain interfaces are required for persistence of IgG1 in the circulation of mice. *Scand. J. Immunol. 40:457.*
6. Kim, J. K., M. F. Tsen, V. Ghetie, and E. S. Ward. 1994. Localization of the site of the murine IgG1 molecule that is involved in binding to the murine intestinal Fc receptor. *Eur. J. Immunol. 24:2429.*
7. Medesan, C., C. Radu, J. K. Kim, V. Ghetie, and E. S. Ward. 1996. Localization of the site of the IgG molecule that regulates maternofetal transmission in mice. *Eur. J. Immunol. 26:2533.*
8. Kabat, E. A., T. T. Wu, H. M. Perry, K. S. Gottesman, and C. Foeller. 1991. *Sequences of Proteins of Immunological Interest.* U.S. Department of Health and Human Services, Washington, DC.
9. Popov, S., J. G. Hubbard, J. K. Kim, B. Ober, V. Ghetie, and E. S. Ward. 1996. The stoichiometry and affinity of interaction of murine Fc fragments with the MHC class I-related receptor, FcRn. *Mol. Immunol. 33:521.*
10. Horton, R. M., H. D. Hunt, S. N. Ho, J. K. Pullen, and L. R. Pease. 1989. Engineering hybrid genes without the use of restriction enzymes: gene splicing by overlap extension. *Gene 77:61.*
11. Carter, P., H. Bedouelle, and G. Winter. 1985. Improved oligonucleotide site-directed mutagenesis using M13 vectors. *Nucleic Acids Res. 13:4431.*
12. Kunkel, T. A. 1985. Rapid and efficient site-specific mutagenesis without phenotypic selection. *Proc. Natl. Acad. Sci. USA 82:488.*
13. Sanger, F., S. Nicklen, and A. R. Coulsen. 1977. DNA sequencing with chain terminating inhibitors. *Proc. Natl. Acad. Sci. USA 74:5463.*
14. Laemmli, U. K. 1970. Cleavage of structural proteins during the assembly of the head of bacteriophage T4. *Nature 227:680.*
15. Fraker, P. J., and J. C. Speck. 1978. Protein and cell membrane iodinations with a sparingly soluble chloroamide, 1,3,4,6-tetrachloro-3a,6a-diphenylglycouril. *Biochem. Biophys. Res. Commun. 80:849.*
16. Guyer, R. L., M. E. Koshland, and P. M. Knopf. 1976. Immunoglobulin binding by mouse intestinal epithelial cell receptors. *J. Immunol. 117:587.*
17. Deisenhofer, J. 1981. Crystallographic refinement and atomic models of human Fc fragment and its complex from fragment B of protein A from *Staphylococcus aureus* at 2.9 and 2.8 Å resolution. *Biochemistry 20:2361.*
18. Mariani, G., and W. Strober. 1991. Immunoglobulin metabolism. In *Fc Receptors and the Action of Antibodies.* H. Metzger, ed. American Society for Microbiology, Washington, DC. p. 94.
19. Ward, E. S., and V. Ghetie. 1995. The effector functions of immunoglobulins: implications for therapy. *Ther. Immunol. 2:77.*
20. Mellbye, O. J., and J. B. Natvig. 1973. Presence and origin of human IgG subclass proteins in newborns. *Vox Sang. 24:206.*
21. Zuckier, L. S., L. D. Rodriguez, and M. D. Scharff. 1989. Immunologic and pharmacologic concepts of monoclonal antibodies. *Semin. Nucl. Med. 29:166.*
22. Wild, A. E. 1973. Transport of immunoglobulin and other proteins from mother to young. In *Lysosomes in Biology and Pathology,* Part 3. J. T. Dingle, ed. North Holland, Amsterdam, p. 179.
23. Wallace, K. H., and A. R. Rees. 1980. Studies on the immunoglobulin-G Fc fragment receptor from neonatal rat small intestine. *Biochem. J. 188:9.*
24. Rodewald, R., and J. P. Kraehenbuhl. 1984. Receptor-mediated transport of IgG. *J. Cell Biol. 99:159s.*
25. Ey, P. L., S. J. Prowse, and C. R. Jenkin. 1978. Isolation of pure IgG1, IgG2a and IgG2b immunoglobulins from mouse serum using protein A-Sepharose. *Immunochemistry 15:429.*
26. Raghavan, M., V. R. Bonagura, S. L. Morrison, and P. J. Bjorkman. 1995. Analysis of the pH dependence of the neonatal receptor/immunoglobulin G interaction using antibody and receptor variants. *Biochemistry 34:14649.*
27. Zijlstra, M., M. Bix, N. E. Simister, J. M. Loring, D. H. Raulet, and R. Jaenisch. 1990. β_2-Microglobulin deficient mice lack CD4$^-$8$^+$ cytolytic T cells. *Nature 344:742.*
28. Brambell, F. W. R., W. A. Hemmings, and I. G. Morris. 1964. A theoretical model of gammaglobulin catabolism. *Nature 203:1352.*
29. Roberts, D. M., M. Guenthert, and R. J. Rodewald. 1990. Isolation and characterisation of the Fc receptor from the fetal yolk sac of the rat. *J. Cell Biol. 111:1867.*
30. Simister, N. E., C. M. Story, H.-L. Chen, and J. S. Hunt. 1996. An IgG-transporting Fc receptor expressed in the syncytiotrophoblast of human placenta. *Eur. J. Immunol. 26:1527.*
31. Kristoffersen, E. K., and R. Matre. 1996. Co-localisation of the neonatal Fcγ receptor and IgG in human placental term syncytiotrophoblast. *Eur. J. Immunol. 26:1668.*
32. Leach, J. L., D. D. Sedmark, J. M. Osborne, B. Rahill, M. D. Lairmore, and C. L. Anderson. 1996. Isolation from human placenta of the IgG transporter, FcRn, and localization to the syncytiotrophoblast. *J. Immunol. 157:3317.*
33. Story, C. M., J. E. Mikulska, and N. E. Simister. 1994. A major histocompatibility complex class I-like Fc receptor cloned from human placenta: possible role in transfer of immunoglobulin G from mother to fetus. *J. Exp. Med. 180:2377.*
34. Simister, N. E., and K. E. Mostov. 1989. Cloning and expression of the neonatal rat intestinal Fc receptor, a major histocompatibility complex class I antigen homolog. *Cold Spring Harb. Symp. Quant. Biol. 54:517.*
35. Blumberg, R. S., T. Koss, C. M. Story, D. Barisani, J. Polischuk, A. Lipin, L. Pablo, R. Green, and N. E. Simister. 1995. A major histocompatibility complex class I-related Fc receptor for IgG on rat hepatocytes. *J. Clin. Invest. 95:2379.*

1: J Exp Med 1991 Jun 1;173(6):1483-91 Related Articles, Links

Entrez PubMed

PubMed Services

Related Resources

The binding affinity of human IgG for its high affinity Fc receptor is determined by multiple amino acids in the CH2 domain and is modulated by the hinge region.

Canfield SM, Morrison SL.

Department of Microbiology, Columbia University, College of Physicians and Surgeons, New York, New York 10032.

A family of chimeric immunoglobulins (Igs) bearing the murine variable region directed against the hapten dansyl linked to human IgG1, -2, -3, and -4 has been characterized with respect to binding to the human high affinity Fc gamma receptor, Fc gamma RI. Chimeric IgG1 and -3 have the highest affinity association (Ka = 10(9) M-1), IgG4 is 10-fold reduced from this level, and IgG2 displays no detectable binding. A series of genetic manipulations was undertaken in which domains from the strongly binding subclass IgG3 were exchanged with domains from the nonbinding subclass IgG2. The subclass of the CH2 domain was found to be critical for determining IgG receptor affinity. In addition, the hinge region was found to modulate the affinity of the IgG for Fc gamma RI, possibly by determining accessibility of Fc gamma RI to the binding site on Fc. A series of amino acid substitutions were engineered into the CH2 domain of IgG3 and IgG4 at sites considered potentially important to Fc receptor binding based on homology comparisons of binding and nonbinding IgG subclasses. Characterization of these mutants has revealed the importance for Fc gamma RI association of two regions of the genetic CH2 domain separated in primary structure by nearly 100 residues. The first of these is the hinge-link or lower hinge regions, in which two residues, Leu(234) and Leu(235) in IgG1 and -3, are critical to high affinity binding. Substitution at either of these sites reduces the IgG association constant by 10-100-fold. The second region that appears to contribute to receptor binding is in a hinge-proximal bend between two beta strands within the CH2 domain, specifically, Pro(331) in IgG1 and -3. As a result of beta sheet formation within this domain, this residue lies within 11 A of the hinge-link region. Substitution at this site reduces the Fc receptor association constant by 10-fold.

PMID: 1827828 [PubMed - indexed for MEDLINE]

R combinant human IgG molecules lacking Fcγ receptor I binding and monocyt triggering activities

Kathryn L. Arm ur[1, 2], Mike R. Clark[1], Andrew G. Hadley[3] and Lorna M. Williamson[2, 4]

[1] Division of Immunology, Department of Pathology, University of Cambridge, Cambridge, GB
[2] Division of Transfusion Medicine, Department of Haematology, University of Cambridge, Cambridge, GB
[3] International Blood Group Reference Laboratory, Bristol, GB
[4] National Blood Service East Anglia, Cambridge, GB

Subclasses of human IgG have a range of activity levels with different effector systems but each triggers at least one mechanism of cell destruction. We are aiming to engineer non-destructive human IgG constant regions for therapeutic applications where depletion of cells bearing the target antigen is undesirable. The attributes required are a lack of killing via Fcγ receptors (R) and complement but retention of neonatal FcR binding to maintain placental transport and the prolonged half-life of IgG. Eight variants of human IgG constant regions were made with anti-RhD and CD52 specificities. The mutations, in one or two key regions of the CH2 domain, were restricted to incorporation of motifs from other subclasses to minimize potential immunogenicity. IgG2 residues at positions 233–236, substituted into IgG1 and IgG4, reduced binding to FcγRI by 10^4-fold and eliminated the human monocyte response to antibody-sensitized red blood cells, resulting in antibodies which blocked the functions of active antibodies. If glycine 236, which is deleted in IgG2, was restored to the IgG1 and IgG4 mutants, low levels of activity were observed. Introduction of the IgG4 residues at positions 327, 330 and 331 of IgG1 and IgG2 had no effect on FcγRI binding but caused a small decrease in monocyte triggering.

Received	9/12/98
Revised	19/4/99
Accepted	10/5/99

Key words: IgG effector function / Structural motif / Fcγ receptor / Monocyte chemiluminescence

1 Introduction

The repertoire of human Ig H chain classes and subclasses provides Ab which are active via different combinations of effector mechanisms, through the binding of FcR and C1q. This can be exploited when producing Ab for therapeutic use since the H chain constant region can be chosen to suit the application. Our interest lies in designing an Ab for the treatment of fetomaternal alloimmunization to the human platelet alloantigen-1a (HPA-1a), the leucine-33 form of glycoprotein IIIa in the platelet membrane glycoprotein IIb/IIIa complex. Severe fetal thrombocytopenia due to transplacental passage of maternal anti-HPA-1a Ab is seen in 1 in 1200 normal pregnancies, with intrauterine death or intracerebral hemorrhage being the major complications [1]. Maternal therapy with high-dose, non-specific IgG is of variable efficacy while *in utero* platelet transfusion remains a hazardous procedure. As an alternative therapy, we wish to develop a non-destructive Ab, utilizing the properties of a human single-chain variable region fragment (Fv), specific for HPA-1a-positive platelets, which has been isolated previously using phage display technology [2]. This Ab fragment can inhibit the binding of human polyclonal anti-HPA-1a alloantibody to antigen-positive platelets and thus provides potential for a competitive, whole Ab therapy. Ideally, the Ab would be administered to the mother, cross the placenta and block the interaction of the maternal alloantibodies with HPA-1a on fetal platelets without itself causing platelet destruction by activating effector mechanisms. Transplacental transport requires that the Ab has an IgG heavy chain but no IgG subclass fulfils the criterion of being inactive in all killing mechanisms, although IgG2 and IgG4 are, in general, less active than IgG1 and IgG3 (reviewed in [3]). To circumvent this problem, we have attempted to engineer inactive constant domains by substituting critical residues from IgG subclasses lacking certain functions into their active counterparts.

We have first considered interactions with the human high-affinity Fc receptor, FcγRI, to which human IgG1

[I 19125]

Abbreviations: HPA: Human platelet antigen **CL:** Chemiluminescence or chemiluminescent

0014-2980/99/0808-2613$17.50+.50/0

and IgG3 bind with a K_a of approximately 5×10^8 M^{-1}. The affinity of IgG4 for the receptor is 2.5- to 20-fold lower and that of IgG2 more than 100-fold less [4]. Domain swap experiments involving IgG1 and IgG2 [5] or IgG3 and IgG2 [6] show that the nature of the CH2 domain largely determines the degree of FcγRI binding although it may be modulated by changes in other parts of the constant region. Two regions in the primary sequence of the CH2 domain have been implicated in the interactions with FcγRI as well as with other FcγR and C1q of the complement cascade [3]. The first area comprises residues 233–236 (EU numbering system [7]), which is part of the hinge-link or lower hinge region since, although genetically part of the CH2 domain, it is N-terminal to the first β-strand of the domain and is not resolved in the crystal structure of the Fc [8]. The second area involves residues 327–331 from a bend joining two β-strands at the N-terminal end of the CH2 domain and close in the tertiary structure to the lower hinge region. Together, these regions contain half of the positions in the CH2 domain at which the sequences of the human IgG subclasses differ and have been targets for site-directed mutagenesis studies which sought to explain th functional differences between the subclasses. Point mutations in the region 233–237 which exchanged residues between mouse IgG2a and IgG2b [9], human IgG1 and IgG2 [5, 10] or human IgG3 and IgG4 [6] or which introduced alanine residues [11] showed the importance of this region in determining the strength of the Ab interaction with FcγRI. It has been demonstrated that mutation of P331 in IgG3 to S, as found in IgG4, reduced the affinity for the receptor [6], indicating that residues in this second area might also be important for FcγRI binding. Although interactions with FcγRII and FcγRIII may involve other regions of the IgG molecule [12], the areas discussed here are likely to influence binding to these receptors in addition.

With the aim of creating inactive Ab, we have designed eight variant human IgG constant regions which incorporate IgG2 residues in the region 233–236 and/or IgG4 residues at positions 327, 330 and 331. By restricting the substitutions to residues which occur in other subclasses, an immune response to the therapeutic Ab should be minimized. The templates were limited to IgG1, where the small number of allotypes can be overcome by making null allotypic variants, and IgG2 and IgG4 where only isoallotypes exist. IgG3 was not used as th number of allotypic residues precludes the creation of null allotypic variants and the lower stability and shorter *in vivo* half-life make this subclass undesirable. To facilitate assay of constant region function across the full range of effector mechanisms, the constant regions have been combined with CD52 [13] and anti-RhD [14] variable regions, giving specificity to two natural human antigens with different site densities. Here, we describ the production of the two series of Ab and appraisal of binding to FcγRI in rosetting and flow cytometry assays using FcγRI-b aring cell lines. The triggering of monocytes in respons to anti-RhD-sensitized RBC was assessed by measurement of chemiluminescence (CL). In addition, mutant Ab have been assayed by for their ability to inhibit FcγRI binding and monocyte activation by wild-type recombinant and human polyclonal Ab.

2 Results

2.1 Generation and basic characterization of antibodies

The mutations chosen to eliminate the effector functions of human IgG Ab are shown in Table 1. The Δa mutation, made in IgG1 and IgG2 genes, introduces IgG4 residues at positions 327, 330 and 331. Similarly, residues at positions 233–236 of IgG1 and IgG4 were replaced with the corresponding amino acids of IgG2 but, since IgG2 has a deletion at 236 where the other subclasses have a glycine residue, the mutation was made omitting (Δb) or including (Δc) G236. For IgG1, the Δa, Δb and Δc mutations were made separately and in combination, namely G1Δab and G1Δac.

Two sets of vectors, allowing expression of CAMPATH-1 (CD52) or Fog-1 (anti-RhD) V_H DNA in conjunction with each of the three wild-type and eight mutant constant region genes, were assembled and each of these vectors was cotransfected with the appropriate L chain expression construct into rat myeloma cells. Stable transfectants were isolated for each combination, expanded and Ab purified from culture supernatant on protein A-agarose. For each Fog-1 Ab, a precipitate formed after purification and was removed by filtration with no further precipitation being apparent. Approximate Ab concentrations were obtained from the 280 nm absorbance values and then assessed in an ELISA which measures the relative amounts of human κ-chain present. For four Ab, the absorbance measurements appeared to overestimate the amount of Ab and the concentrations were adjusted to correct for contaminating bovine IgG. The Ab were subjected to reducing SDS-PAGE. Each sample showed two bands with apparent molecular masses of approximately 25 and 55 kDa which represent the expected sizes of the L and H chains (data not shown). There was no discernible difference in H chain size within each Ab series but both chains of the Fog-1 Ab appeared to be slightly smaller than their CAMPATH-1 counterparts. For the Ab with CAMPATH-1 specificity, the yield after purification varied from 0.6 to 9 μg/ml

supernatant, wh reas the yield of soluble Fog-1 Ab was b tween 3 and 20 μg/ml.

The specificities of the two seri s of Ab were tested. All 11 CAMPATH-1 Ab wer shown to compete, in a dose-d pendent manner, with clinical grade CAMPATH-1H in the binding of th anti-CAMPATH-1 idiotype mAb, YID13.9.4 (data not shown). All 11 Fog-1 Ab were able to agglutinate RhD-positive RBC in the presence of goat anti-human IgG Ab as cross-linking molecules. The IgG subclasses of the Fog-1 Ab were checked by coating RhD-positive RBC and assessing the agglutination using anti-G1m(a), anti-IgG2 or anti-IgG4 Ab as the cross-linking reagent. The results confirmed that the Ab were of the correct subclasses. The agglutination of RhD^+ RBC by Fog-1 IgG1 and anti-G1m(a), by Fog-1 IgG2 and anti-IgG2 and by Fog-1 IgG4 and anti-IgG4 was then carried out in the presence of excess Ab from the CAMPATH-1 s ries. The CAMPATH-1 Ab were able to inhibit the hem-agglutination, by competing for the anti-globulin cross-linking reagent, only where they were of the same sub-classes as the Fog-1 Ab, thus verifying their subclasses (data not shown).

2.2 FcγRI binding

RBC with approximately 30 000 RhD sites per cell (R_2R_2) w re coated with each of the 11 Fog-1 Ab over a range of concentrations and added to human FcγRI-expressing transfectants, B2KA, growing in wells. After incubation, excess RBC were washed away and the perc ntage of B2KA cells rosetted by RBC was recorded (Fig. 1). For G1 and G1Δa, where IgG4 residues are included at positions 327, 330 and 331, similar levels of rosetting were achieved, with half-maximal rosetting occurring when the RBC were coated with Ab at about 0.1 μg/ml, a concentration at which Fog-1 Ab would be xpected to occupy approximately one-third of the RhD sites. Slightly higher concentrations of G4 were needed to obtain the same levels of rosetting. No rosettes were formed when using RBC coated with the G1 and G4 Ab containing the Δb and Δc mutations or the G2 Ab. In the experiment shown in Fig. 1, the highest coating concentration tested was 10 μg/ml, predicted to correspond to approximately 90 % occupancy of RhD sites. The experim nt was repeated using coating concentrations of up to 80 μg/ml, essentially saturating the RhD sites, and still no rosettes were seen for G2 and the Ab containing the Δb or Δc mutations and thus incorporating IgG2 residues in the lower hinge region. This indicates that, even when the RBC were coated with these Ab at the maximum density for this antigen, there was insufficient IgG/FcγRI interaction for rosette formation.

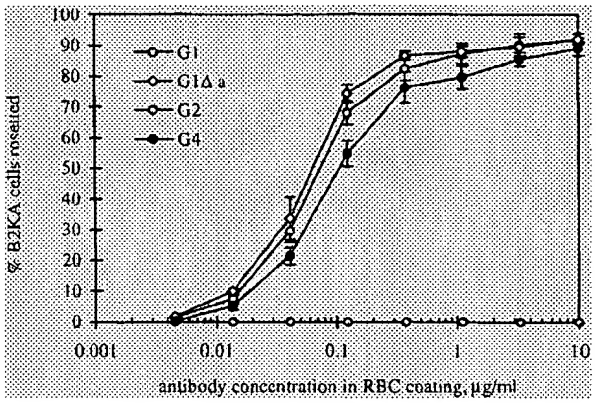

Figure 1. Rosetting of FcγRI-bearing cells by RBC coated with Fog-1 Ab. R_2R_2 RBC were coated with Fog-1 Ab at a range of Ab concentrations, incubated with B2KA cells growing in a 96-well plate and the percentage of B2KA cells with rosettes of RBC determined. Error bars indicate the SD values for triplicate wells. For the mutants Fog-1 G1Δb, G1Δc, G1Δab, G1Δac, G2Δa, G4Δb and G4Δc, as for G2 (shown), there was no rosetting between B2KA cells and RBC at any of the coating concentrations.

Centrifuging the sensitized RBC and B2KA cells together before observing rosettes on a microscope slide was found to give a higher proportion of rosettes than incubating the cells in wells so this method was used to investigate the inhibition of rosette formation. R_2R_2RBC were coated with a mixture of 1 μg/ml Fog-1 G1 and different amounts of Fog-1 G2Δa or Fog-1 G4Δb before mixing with B2KA cells. When 1 μg/ml Fog-1 G1 was used alone, the coated RBC formed rosettes on 95 % of the B2KA cells whereas sensitization in the presence of

Table 1. Amino acid residues present at key positions[a] of the IgG constant regions

	233	234	235	236[b]	327	330	331
G1	E	L	L	G	A	A	P
G1Δa	E	L	L	G	S	S	S
G1Δb	P	V	A	-	A	A	P
G1Δc	P	V	A	G	A	A	P
G1Δab	P	V	A	-	S	S	S
G1Δac	P	V	A	G	S	S	S
G2	P	V	A	-	G	A	P
G2Δa	P	V	A	-	G	S	S
G4	E	F	L	G	G	S	S
G4Δb	P	V	A	-	G	S	S
G4Δc	P	V	A	G	G	S	S

a) Residue positions according to EU numbering sytem [7]. Shaded regions indicate residues mutated from the IgG1, IgG2 or IgG4 wild-type sequences (G1, G2 and G4).

b) A dash indicates that no amino acid residue is present in the sequence alignment.

64 μg/ml G2Δa or G4Δb completely abolish d the rosetting (data not shown).

Flow cytometry was used to measure the binding of Ab from both series to B2KA cells and to cells of a second line which also expr ss human FcγRI on their surfac . Fig. 2 shows representative experiments. The level of surface-expressed FcγRI, as detected using the CD64 Ab, was higher for the 3T3 transfectants than for the B2KA line and this was reflected in the higher signals obtained when measuring binding of the test Ab. For both series, the G1 and G1Δa Ab bound to the cell lines with identical dose-response curves, indicating that the mutations at positions 327, 330 and 331 did not significantly affect the interaction. The binding of G4 was approximately threefold lower than that of the G1 and G1Δa Ab when assessed at the midpoint of the binding curves. As xpected, th G2 Ab did not bind to th cells. Little binding was seen for any of the other mutant Ab, suggesting that the Δb and Δc mutations in IgG1 and IgG4 wer sufficient to reduce binding to FcγRI by at least 10^4-fold. Ab containing the Δc mutation and thus th extra glycin residu , especially G1Δc, showed a small degree of binding to cells from both lines at the highest concentrations tested if the level of fluorescence is compared to the background or to the equivalent Ab with the Δb mutation. If the fluorescence intensity histograms are overlaid, as seen in Fig. 3 for the highest concentrations of CAMPATH-1 Ab and B2KA cells, the plots for G1 and G1Δa coincide. The profiles obtained for G1Δb (shown), G1Δab, G2Δa and G4Δb are indistinguishable from that of G2 which is expected to be negative in this experiment. The histogram obtained with G1Δc shows a significant shift to higher fluorescent

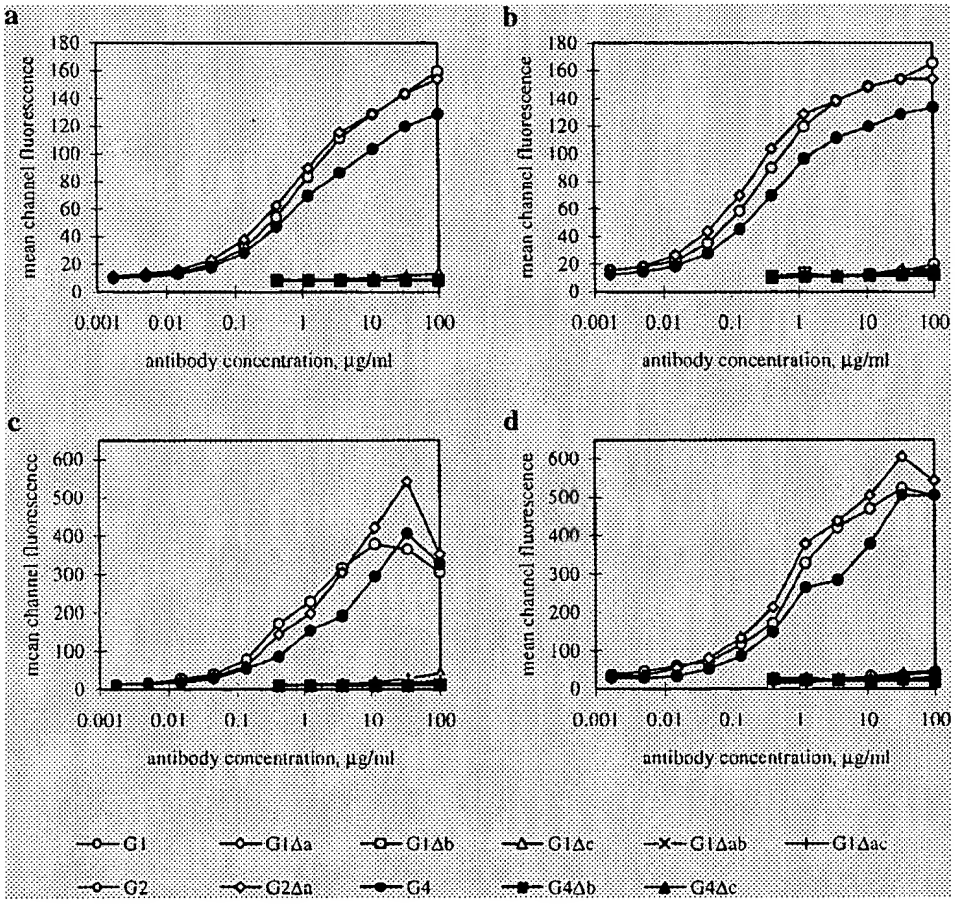

Figure 2. Fluorescent staining of FcγRI-bearing cells. FcγRI transfectant cell lines, B2KA(a and b) and 3T3+FcγRI+γ-chain (c and d) were incubated sequentially with antibodies of the CAMPATH-1 (a and c) or Fog-1 (b and d) series, biotinylated anti-human κ antibodies and ExtrAvidin-FITC. The fluorescence intensities were measured for 10 000 events and the geometric mean channel of fluorescence plotted.

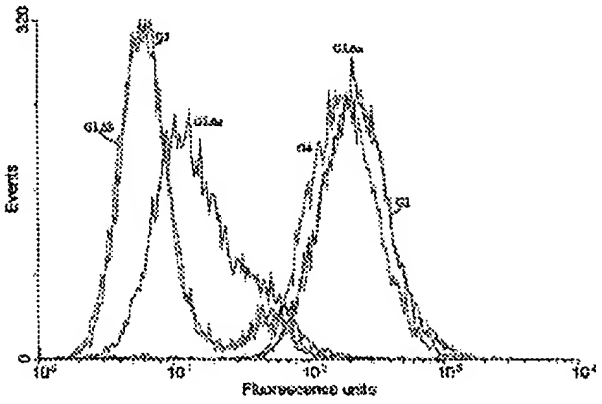

Figure 3. Histrogram representation of fluorescent-stained FcγRI-bearing cells. B2KA cells were stained as in Fig. 2 using 100 μg/ml Ab from the CAMPATH-1 series. The histogram plots showing the number of cells falling in each fluorescence channel were overlaid for representative antibodies.

intensity when compared to the G2 plot (shown) whereas the shift seen with G1Δac and G4Δc is less pronounced (data not shown). None of the Ab bound to a negative control cell line which expressed human β_2-microglobulin rather than FcγRI (data not shown).

2.3 FcγRI triggering measured by CL

To measure functional activity, the CL response of monocyt s, believed to be mediated mainly through FcγRI [15], was measured using R_1R_1 RBC, sensitized with Ab from the Fog-1 series, as the target cells. Fig. 4 shows th CL respons plotted in relation to the number of Ab mol cules bound p r RBC. A differenc betw en the G1 and G1Δa Ab was seen with higher amounts of Ab, although both gave higher responses than the G4 Ab across the range of Ab concentrations. A significant observation is that the use of G1Δc and, to a lesser extent, G1Δac and G4Δc lead to monocyte triggering slightly above background levels whereas neither G1Δb, G1Δab nor G4Δb gave any response. Both G2 and G2Δa were also negative.

Fog-1 Ab, selected for lack of binding to FcγRI-expressing cell lines, were tested for their ability to block monocyte CL triggering due to Fog-1 G1. These Ab were mixed in increasing concentrations with 2 μg/ml Fog-1 G1 and were used to sensitize RBC. The CL response to the Ab-coated RBC, expressed as a percentage of the response to RBC sensitized with 2 μg/ml Fog1 G1 only, is shown in Fig. 5. By comparing these responses to those obtained when different amounts of G1 were used in sensitization, it is apparent that six of the eight Ab inhibit the reaction to an extent which would be predicted if the only activity of the mutants was to displace

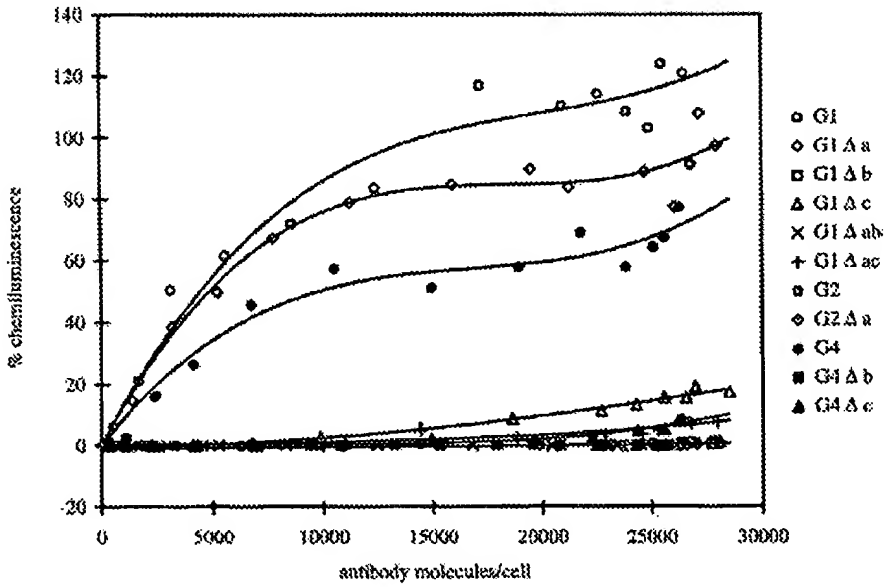

Figure 4. CL response of human monocytes to RBC sensitized with the Fog-1 series of Ab. R_1R_1 RBC were coated with Ab over a range of concentrations. The number of Ab molecules bound per cell and the CL response of monocytes to the RBC was determined for each sample as described.

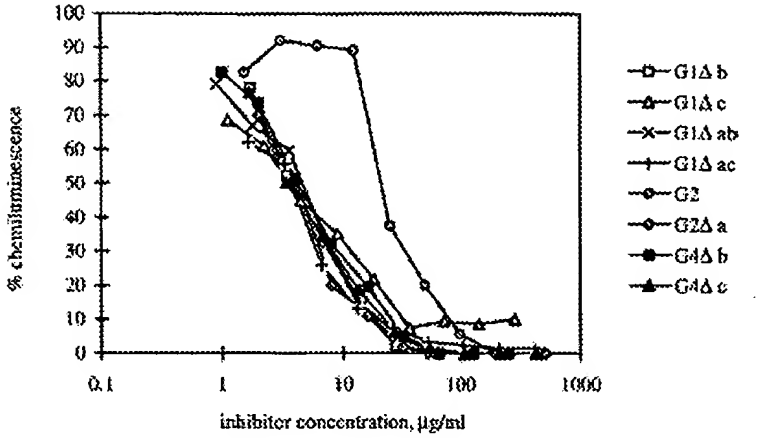

Figure 5. Inhibition of CL due to Fog-1 G1 by other Fog-1 antibodies. RBC were sensitized with 2 μg/ml Fog-1 G1 and different concentrations of the Fog-1 Ab indicated. These Ab gave a low CL response in Fig. 4. The CL response of monocytes was measured and the 100 % response assigned to be that due to 2 μg/ml G1 alone.

G1 from RBC in proportion to their relative concentrations. In these cases, 4 μg/ml of Ab gave 50 % inhibition whereas, although G2 did inhibit, fivefold more Ab was required to give the same degree of inhibition. G1Δc inhibits to approximately the same extent as the other mutants except that the response is not reduced to zero.

One of the inactive mutant Ab, Fog-1 G2Δa, was tested for its ability to inhibit the CL response to RBC sensitized with human sera containing clinically significant Ab. The sera contained anti-RhD, anti-RhC+D or anti-K activities and, in the absence of inhibitor, gave CL responses of greater than 30 %, previously shown to predict severe hemolytic disease of the fetus [16, 17]. The sera were mixed with different concentrations of G2Δa, the mixtures used to sensitize RBC and the responses of monocytes measured (Fig. 6). The addition of G2Δa Ab reduced the CL signals due to all five anti-RhD sera to

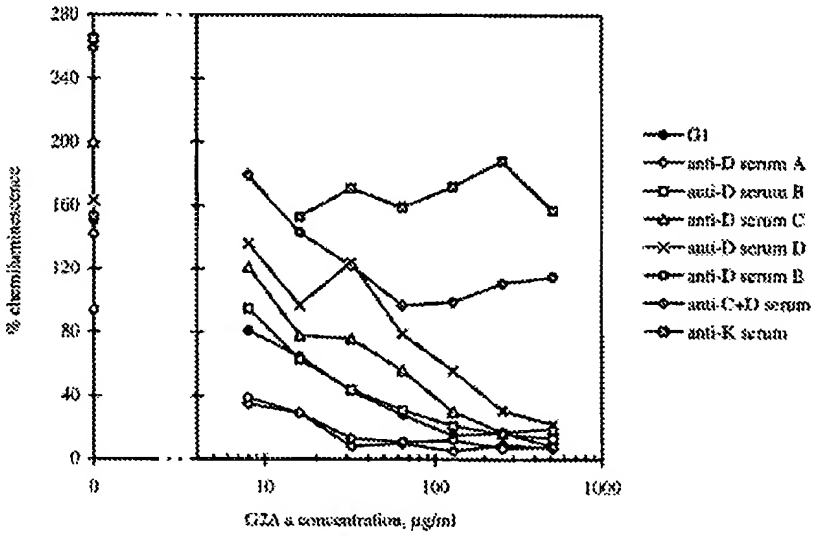

Figure 6. Inhibition of CL response to clinical sera by Fog-1 G2Δa. RBC were sensitized with a constant amount of Fog-1 G1 (20 μg/ml) or clinically relevant serum and different amounts of Fog-1 G2Δa and the CL response of monocytes determined.

below the 30 % cutoff. The amount of Ab required ranged from 16 to 260 μg/ml, probably reflecting th differing conc ntrations, affinities and subclasses of anti-RhD Ab in the sera. Anti-RhD Ab would not be xpected to inhibit the binding of anti-K Ab to RBC and th negative control anti-K serum was not blocked at all by G2Δa. Only part of the activity of the anti-RhC+D serum could be inhibited by G2Δa, presumably indicating non-inhibition of anti-RhC by Fog-1 Ab.

3 Discussion

W have demonstrated that substitution of critical residues in the lower hinge region of human IgG is sufficient to eliminate binding to FcγRI and the mutant Ab are able to block effector activity of wild-type Ab. The Ab investigated comprised eight mutant and three corresponding wild-type constant regions combined with both CD52 and anti-RhD specificities. There was no correlation in the ranking of the purification yields for the two series of Ab, suggesting that none of the mutations affected the production of the Ab or their ability to bind to protein A. For each variable region, the H chains were visualized as bands of the same apparent molecular mass by reducing SDS-PAGE, indicating that there were no extensive differences in the glycosylation of the proteins. The use of two Ab series has allowed confirmation of the reactivity patterns, especially where small differences between constant regions were observed.

Transfer of the IgG2 lower hinge sequence to IgG1 and IgG4 in the form of the G1Δb and G4Δb mutants was sufficient to eliminate FcγRI binding (Figs. 1, 2 and 3); the G1Δb result being in agreement with published data for an anti-MHC class II Ab [10]. The low level of binding shown by Ab with the Δc mutation (including G236) relative to G2 and those carrying the Δb mutation (deleting G236) is of interest. It was found that the deletion of G236 from an IgG1 Ab abolished its ability to inhibit the binding of labeled IgG1 to U937 cells whereas binding remained undetectable upon addition of G236 to IgG2 [5]. This residue presumably alters the alignment of the lower hinge residues relative to receptor interaction sites in the remainder of the CH2 domain. The lower hinge of IgG2 may be able to support a low level of binding to FcγRI when this alignment is changed as in the G1Δc and G4Δc Ab. There appears to be little difference in FcγRI binding between the G1 and G1Δa Ab, which contrasts with the reported finding that the single substitution P331 to S in IgG3 caused a fourfold reduction in affinity [6].

Unlike the assays of FcγRI binding, the CL measurement of monocyte triggering shows a difference between the Fog-1 G1 and G1Δa Ab (Fig. 4). This may indicate a distinction between binding to and triggering via FcγRI or th involvement of oth r receptors. Human monocytes can also express FcγRII and low amounts of FcγRIII [18] and interaction of th Ab with these receptors may possibly cause production of oxygen radicals either directly, or indirectly by strengthening the contact betwe n RBC and monocyte. It is conceivable that, at low Ab concentrations, binding is mainly to the high-affinity FcγRI resulting in similar curves for G1 and G1Δa whereas the stronger interactions of G1 with low-affinity receptors lead to divergence of the activity curves at higher concentrations. Encouragingly, Ab containing the Δb mutation failed to trigger CL even at the highest concentrations tested. It is worth noting that the reactions seen in CL with G1Δac, G4Δc and, to a greater extent, G1Δc were above background and thus mirror the pattern of binding to FcγRI.

When the Fog-1 Ab were assayed for their ability to inhibit monocyte triggering by Fog-1 G1 (Fig. 5), three different patterns of inhibition were seen. Most of the Ab tested (G1Δb, G1Δab, G1Δac, G2Δa, G4Δb and G4Δc) appeared to reduce the level of CL to the extent expected if only G1 was significantly active and the amount of G1 bound to the RBC was in proportion to its relative concentration. With G1Δc, the inhibition curve was similar to that of the other mutants except that the response was not reduced to zero, presumably because high concentrations of the Ab can themselves significantly activate monocytes as seen in Fig. 4. Although G2 did give complete inhibition, higher amounts of Ab were required, suggesting that, although G2 did not activate monocytes in the absence of G1, it may enhance the G1 reaction by interacting with other receptors on the monocyte. This result suggests that some of the mutant Ab may have less affinity than IgG2 for FcγRII or III and the difference between G2 and G2Δa in this regard, as well as the comparison between G1 and G1Δa made above, points to involvement of residues 327–331 in such interactions. Preliminary data, obtained using transfectants bearing FcγRIIa or FcγRIIIb, suggest that the Δa mutation, made in G1 and G2, does reduce binding to these receptors, as do the Δb and Δc mutations in G1.

One of the variant Ab, Fog-1 G2Δa, was shown to inhibit the CL response to clinically significant anti-RhD Ab in human sera. The CL assay has been developed as a means of using maternal serum to predict the severity of hemolytic disease of the fetus [16, 17]. Results above 30 % are associated with hemolysis and suggest that invasive antenatal intervention procedures are appropriate. Inclusion of the G2Δa Ab effected a reduction in the CL response to below this 30 % threshold for each anti-RhD serum.

Our data have reinforced th importance of IgG residues 233–236 and 327–331 in determining interactions with FcγR. These regions seem able to accommodate mutations without distorting th domain structure and pr - sumably act to modulat the strength of th contact made with the effector mol cul by a larger area of th Ab. Our results are likely to be relevant in the fetal setting since fetal leucocytes bear the same classes of FcγR found on equivalent adult cells, albeit at generally reduced densities [18]. *In vitro* experiments with sensitized RBC show that phagocytosis by fetal monocytes can be inhibited by Ab which block FcγRI and may be partially reduced by the use of an anti-FcγRIIa Ab. Phagocytosis by fetal splenic mononuclear phagocytes was decreased by blockage of FcγRI and FcγRIII [19, 20].

These studies have also contributed to knowledge concerning the binding of wild-type IgG subclasses to FcγRI. In Fig. 2b, the curve representing the binding of the Fog-1 G1 Ab to the FcγRI-bearing B2KA cells shows a plateau level so the midpoint can be used to estimate the affinity. The midpoint occurs at a concentration of 0.4 μg/ml, equating to a K_a of 4×10^8 M^{-1}, which is consistent with the previously quoted value of approximately 5×10^8 M^{-1} [4]. The midpoint concentration for IgG4 appears to be threefold higher than that for IgG1. If this represents solely the difference in affinities, it would fall at the low end of the 2.5-fold to 20-fold range observed in published studies. These were complicated by the use of human monocytes or cell lines expressing more than one type of FcR and myeloma protein preparations which may contain small amounts of Ab of other subclasses (reviewed in [4]). However, our binding curves for IgG4 also appeared to plateau at a lower level than the IgG1 curves (Fig. 2). This observation does not seem to be due to a difference in detection of IgG1 and IgG4 Ab since, when the Ab were compared in their ability to inhibit the binding of FITC-labeled human IgG to B2KA cells, approximately threefold more IgG4 than IgG1 was needed to reduce the binding of the labeled Ab by the same degree (data not shown). This is in agreement with the apparent relative affinities seen in Fig. 2 and suggests that use of the anti-κ reagent detects both Ab equally. Another explanation for the different plateau levels is that the curves may represent a situation which is further from equilibrium for IgG4 than for IgG1 and preliminary experiments in our laboratory have indicated that IgG4 binds to the receptor more slowly than IgG1. Alternatively, results obtained using U937 cells [21] question whether IgG molecules bind to FcγRI with identical stoichiometries. Evidence that the interaction involved one receptor molecule for each Ab molecule came from data where hybrid Ab with heavy chains from binding and non-binding subclasses were able to bind to the receptor [22]. However, th affinity of th int raction was low r than that with the wild-typ binding Ab, leading to the suggestion that this supports a model in which dimerization of th receptor occurs and is accompani d by a threefold increas in affinity for Ab [23]. The interaction of FcγRI with IgG1 and IgG4 will be examined furth r.

This set of mutant constant regions contains candidates for further development as an inactive constant region. We are currently assaying the Ab for their ability to function via FcγRII and FcγRIII and in complement-mediated lysis. An assay system for evaluating the binding of the Ab to FcRn, the novel FcR believed to be critical for placental transport of IgG [24], is being developed. Constant regions with the best combination of properties will be expressed with the anti-HPA-1a variable region and assessed as possible therapeutic Ab. The potential applications of an inert constant region are numerous. Ab which do not activate effector functions are ideal in therapies which require blocking of specific B cell epitopes or other sites of protein-protein interaction. Fc domains are often employed in fusion proteins to endow the product with the long *in vivo* half-life of IgG and the use of an inert Fc might be advantageous to reduce side effects.

4 Materials and methods

4.1 Construction of expression vectors

The human IgG1 constant region gene of allotype G1m(1,17) was obtained as a 2.3-kb insert in M13tg131 with a modified polylinker [25], such that there are *Bam*HI and *Hind*III restriction sites at the 5' end and *Sph*I, *Not*I, *Bgl*II and *Bam*HI sites at the 3' end. The human IgG2 constant region gene had previously been obtained as a *Hin*dIII-*Sph*I fragment in M13tg131, the *Hin*dIII site destroyed and the *Sal*I-*Sph*I fragment cloned to replace the equivalent fragment in the IgG1 vector. The human IgG4 constant region gene was obtained as a *Hin*dIII-*Sma*I fragment in M13tg131 and the *Hin*dIII site deleted. The *Sma*I site is located between the 3' end of the CH3 exon and the polyadenylation site so the polyadenylation site was restored by addition of the equivalent *Sma*I fragment from the IgG1 vector.

Site-directed mutagenesis was used to introduce an *Xba*I restriction site between the CH1 and hinge exons, a *Xho*I site between the hinge and CH2 exons and a *Kpn*I site between the CH2 and CH3 exons in order to facilitate exchange of exon sequences. This was similar to the manipulation of IgG1 and IgG4 genes carried out previously [26].

The changes in CH2 were introduced by overlap extension PCR, using Pwo DNA polymerase (Boehringer Mannheim,

Lewes, GB). For the Δa mutation, the oligonucleotides were 5' TCTCCAACAAAGGCCTCCCGTCCTCCATCGAGAAAA 3' (coding strand) and 5' TTTTCTCGATGGAGGACGGGAGGCCTTTGTTGGAGA 3' (complementary strand). The Δb and Δc mutations were encoded by 5' TCCTCAGCACCTCCAGTCGCGGGGGGACCGTCAGTC 3' (coding strand, Δc) and 5' GACTGACGGTCCCGCGACTGGAGGTGCTGAGGA 3' (complementary strand, Δb). The mutant CH2 exons were cloned as *Xho*I-*Kpn*I fragments to replace the existing CH2 of the constant region genes in M13 and correctly mutated constant regions identified by nucleotide sequencing.

The IgG1, 2 and 4 wild-type and mutated constant region genes were each excised from replicative form (RF) DNA as a *Bam*HI-*Not*I fragment and cloned into a modified CAMPATH Hu4VH HuIgG1 pSVgpt vector [25] to replace the existing constant region. The resulting vectors were designated pSVgptCAMPATHHu4VHHuIgG1Δa, etc. The vector allows expression of the constant region DNA with the humanized CAMPATH-1 Hu4VH variable region. The CAMPATH-1 humanized L chain gene was provided in the vector CAMPATH HuVL pSVneo [13].

By sequential overlap extension PCR, the Fog1 variable region DNA [14] were each joined, at their 5' end, to DNA providing promoter and signal peptide sequences and, at their 3' end, to DNA representing the 5' end of the V_H-C_H intron (both taken from M13VHPCR1 [27]). The *Bam*HI restriction site internal to the Fog-1 V_H was deleted by the same method. The complete PCR products were cloned into M13mp19 as *Hin*dIII-*Bam*HI fragments and their DNA sequence confirmed.

The *Hin*dIII-*Bam*HI fragment containing the Fog-1 V_H was used to replace the fragment containing the CAMPATH-1 V_H in the pSVgpt vectors described above, giving expression vectors designated pSVgptFog1VHHuIgG2, etc. For the IgG1 vectors, the extra *Hin*dIII restriction site meant that this was not possible. Instead, the relevant pSVgptCAMPATHHu4VHHuIgG1 vectors were digested with *Hin*dIII and linkers, designed to delete the *Hin*dIII site and add a *Bam*HI site, were ligated onto the cut ends. The constant regions were isolated *Bam*HI and *Not*I fragments and cloned into pSVgptFog1VHHuIgG2 to replace the IgG2 constant region. The *Hin*dIII-*Bam*HI fragment containing the Fog-1 V_κ was transferred to the vector pSV*hyg*-HuCK [27] giving pSVhyg-Fog1VKHuCK.

4.2 Production of Ab

The expression vectors were transfected into the rat myeloma cell line YB2/0 [28] and transfectants selected in 96-well plates essentially as previously described [29]. Eighteen days after transfection, supernatants were assayed for the presence of IgG in an ELISA using goat anti-human IgG Fc-specific Ab (Sigma, Poole, GB) and horseradish peroxidase (HRPO)-conjugated goat anti-human κ Ab (Harlan Sera-lab, Loughborough, GB) as the capture and detection reagents. Transfectants from wells containing the highest amounts of Ab were expanded. Ab was purified from the supernatant of cells grown in Iscove's modified Dulbecco's medium containing 2 % FBS by protein A-agarose affinity chromatography. Fractions containing significant amounts of protein were identified from A_{280nm} readings, dialyzed against PBS, filter-sterilized and the approximate Ab concentration determined by A_{280nm} measurement.

The purity and integrity of the Ab were established by reducing SDS-PAGE, using 12.5 % acrylamide. The concentrations were checked in an ELISA which used goat anti-human κ Ab (Seralab) as the capture reagent and biotinylated goat anti-human κ Ab (Sigma) followed by ExtrAvidin-HRPO (Sigma) for detection. This meant that the nature of the H chain was unlikely to influence the level of binding obtained.

The specificities of the Ab were analyzed in two assays. In the competitive anti-CAMPATH-1 idiotype assay, wells, coated with clinical grade CAMPATH-1H, were incubated with a mixtures of the test Ab and a constant amount of biotinylated YID13.9.4 [30] followed by ExtrAvidin-HRPO. To test for RhD specificity, RhD-positive (R_2R_2) RBC were incubated with dilutions of the Ab at room temperature for 1 h and excess Ab removed by washing. Agglutination was observed by incubating the coated RBC with goat anti-human IgG Fc-specific Ab (Sigma). In the agglutination assays to determine the H chain subclasses, anti-G1m(a) mAb (CLB, Amsterdam, Netherlands), anti-human IgG2 mAb (Sigma) and anti-human IgG4 mAb (Sigma) were used as additional cross-linking reagents, in the absence or presence of test Ab as potential inhibitors.

4.3 Rosetting of FcγRI transfectants

Washed R_2R_2 RBC were incubated with Ab samples in 100 μl PBS in 96-well plates at room temperature for 1 h. The RBC were washed three times, resuspended in PBS and incubated at 37°C for 40 min with transfectants expressing FcγRI cDNA, B2KA (S. Gorman and G. Hale, unpublished), growing in 96-well plates. The supernatant was discarded and the wells washed once to remove excess RBC. For each well, 200 B2KA cells were examined and the number with RBC rosettes noted. The mean percentage and SD for triplicate wells was plotted. Alternatively, the sensitized RBC and B2KA cells were mixed in microcentrifuge tubes, pelleted and gently resuspended before transfer to a microscope slide.

4.4 Fluorescent staining of FcγR transfectants

Transfectants expressing FcγRI cDNA, B2KA and 3T3+ FcγRIa+γ-chain [31] were obtained as single-cell suspen-

sions in PBS containing 0.1 % (w/v) NaN_3, 0.1 % (w/v) BSA (wash buffer) following treatment with cell dissociation buffer (Gibco-BRL). Cells were pelleted at 10^5 cells/well in 96-well plates, resuspended in 100 µl dilutions of the CAMPATH-1 or Fog-1 Ab and incubated on ice for 30 min. Cells were washed three times with 150 µl/well wash buffer and similarly incubated with 20 µg/ml biotin-conjugated goat anti-human κ-chain Ab (Sigma) and then with 20 µg/ml ExtrAvidin-FITC (Sigma). After the final wash, cells were fixed in 100 µl wash buffer containing 1 % (v/v) formaldehyde. Surface expression of FcγRI was confirmed by staining with CD64 mAb (Serotec, Oxford, GB) and FITC-conjugated goat anti-mouse IgG Ab (Sigma). Fluorescence intensities were measured on a FACScan (Becton Dickinson, Oxford, GB).

4.5 CL assay

Group O R_1R_1 RBC were washed in PBS and resuspended in RPMI + 10 % FBS at a final concentration of 5 % v/v. Ten microliters of cells was added to 50 µl Ab, serially diluted in RPMI/FBS, in V-bottom well plates and incubated for 60 min at 37°C to achieve a range of RBC-bound IgG. In competition experiments, the RBC were sensitized in a mixture of 25 µl competing Ab and 25 µl wild-type Ab or 25 µl serum containing alloantibodies. After sensitization, cells were washed four times with 200-µl volumes of PBS and resuspended in 50 µl RPMI/FBS (final concentration = 1 % v/v). An aliquot of cells (E-IgG) was used in the CL assay and an aliquot was assayed by flow cytometry to determine the level of RBC-bound IgG.

PBMC were isolated by density gradient centrifugation from EDTA-anticoagulated blood pooled from six normal donors. PBMC were washed four times with PBS containing 1 % globulin-free BSA and then resuspended at 2×10^6/ml in HBSS containing 25 % RPMI and 2.5 % FBS. Aliquots (100 µl) were dispensed into 96-well flat-bottom white opaque plates and incubated for 2 h at 37 °C in a humidified atmosphere of 5 % CO_2 in air. The plates were then placed in a luminometer (Anthos Lucy 1, Labtech International, Uckfield, GB) and 100 µl HBSS containing 4×10^{-4} M luminol (Sigma) and 20 µl E-IgG were added to each well. The CL response was monitored at 37 °C for 60 min and, except where stated, expressed as a percentage of the response to RBC sensitized in a saturating concentration of IgG1 anti-RhD (clone BRAD-5 [32]) Intra-assay variability was less than 10 %.

To determine RBC-bound IgG, 25-µl aliquots of E-IgG were transferred to a V-bottom well plate, washed once with PBS, centrifuged to a pellet and resuspended in 50 µl FITC-conjugated anti-IgG $F(ab')_2$ (diluted 1/30 in PBS/1 % BSA). After 30 min at room temperature, the cells were washed once with 200 µl PBS/BSA and kept on ice until analyzed by flow cytometry (EPICS XL-MCL, Coulter Electronics, Luton, GB), The mean channel fluorescence was recorded. Mean channel fluorescence was converted to IgG molecules/cell by use of a standard curve which was prepared by adding 100 µl of 5 % v/v R_1R_1 cells to 900 µl of serial twofold dilutions of human monoclonal IgG1 anti-D (BRAD-5). Sensitized RBC were washed three times with PBS/BSA and resuspended to 1 % v/v in PBS/BSA. Aliquots (25 µl) were removed and analyzed by flow cytometry as described above. The remaining RBC were counted, centrifuged to a pellet, lysed in a buffer containing Triton X-100 and IgG in lysates was determined by ELISA as described [33]. The number of IgG molecules bound/RBC was deduced from the IgG concentration and the number of RBC from which each lysate was prepared. A standard curve was then plotted comparing fluorescence intensity with the number of IgG molecules bound/RBC.

Acknowledgements: We are grateful to Drs. S. Gorman and G. Hale for providing the B2KA cell line and to Dr. N. A. C. Westerdaal and Prof. J. G J. van de Winkel for the 3T3+FcγRIa+γ-chain cell line. We wish to thank Prof. J.-P. Allain for constructive criticism of the manuscript, Dr. W. H. Ouwehand for helpful discussions and Dr. M.-L. Laukkanen for assistance. This work was supported by a grant from the National Blood Authority.

5 References

1 **Williamson, L. M., Hackett, G., Rennie, J., Palmer, C. R., Maciver, C., Hadfield, R., Hughes, D., Jobson, S. and Ouwehand, W. H.,** The natural history of fetomaternal alloimmunization to the platelet-specific antigen HPA-1a ($P1^{A1}$, Zw^a) as determined by antenatal screening. *Blood* 1998. **92:** 2280–2287.

2 **Griffin, H. M. and Ouwehand, W. H.,** A human monoclonal antibody specific for the leucine-33 ($P1^{A1}$, HPA-1a) form of platelet glycoprotein IIIa from a V gene phage display library. *Blood* 1995. **86:** 4430–4436.

3 **Clark, M. R.,** IgG effector mechanisms. *Chem. Immunol.* 1997. **65:** 88–110.

4 **Burton, D. R.,** Immunoglobulin G: functional sites. *Mol. Immunol.* 1985. **22:** 161–206.

5 **Chappel, M. S., Isenman, D. E., Everett, M., Xu, Y.-Y., Dorrington, K. J. and Klein, M. H.,** Identification of the Fcγ receptor class I binding site in human IgG through the use of recombinant IgG1/IgG2 hybrid and point-mutated antibodies. *Proc. Natl. Acad. Sci. USA* 1991. **88:** 9036–9040.

6 **Cranfield, S. M. and Morrison, S. L.,** The binding affinity of human IgG for its high affinity Fc receptor is determined by multiple amino acids in the CH2 domain and is modulated by the hinge region. *J. Exp. Med.* 1991. **173:** 1483–1491.

7 **Kabat, E. A., Wu, T. T., Perry, H. M., Gottesman, K. S. and Foeller, C.,** Sequences of proteins of immunological interest. US Department of Health and Human services, NIH, Bethesda 1991.

8 **Deisenhofer, J.,** Crystallographic refinement and atomic models of a human Fc fragment and its complex with fragment B of protein A from *Staphylococcus aureus* at 2.9 and 2.8 Å resolution. *Biochemistry* 1981. **20:** 2361–2367.

9 **Duncan, A. R., Woof, J. M., Partridge, L. J., Burton, D. R. and Winter, G.,** Localization of the binding site for the human high-affinity Fc receptor on IgG. *Nature* 1988. **332:** 563–564.

10 **Morgan, A., Jones, N. D., Nesbitt, A. M., Chaplin, L., Bodmer, M. W. and Emtage, J. S.,** The N-terminal end of the CH2 domain of chimeric human IgG1 anti-HLA-DR is necessary for C1q, FcγRI and FcγRIII binding. *Immunology* 1995. **86:** 319–324.

11 **Lund, J., Winter, G., Jones, P. T., Pound, J. D., Tanaka, T., Walker, M. R., Artymiuk, P. J., Arata, Y., Burton, D. R., Jefferis, R. and Woof, J. M.,** Human FcγRI and FcγRII interact with distinct but overlapping sites on human IgG. *J. Immunol.* 1991. **147:** 2657–2662.

12 **Gergely, J. and Sarmay, G.,** The two binding-site models of human IgG binding Fcγ receptors. *FASEB J.* 1990. **4:** 3275–3283.

13 **Riechmann, L., Clark, M. R., Waldmann, H. and Winter, G.,** Reshaping human antibodies for therapy. *Nature* 1988. **332:** 323–327.

14 **Bye, J. M., Carter, C., Cui, Y., Gorick, B. D., Songsivilai, S., Winter, G., Hughes-Jones, N. C. and Marks, J. D.,** Germline variable region gene segment derivation of human monoclonal anti-Rh(D) antibodies. *J. Clin. Invest.* 1992. **90:** 2481–2490.

15 **Kumpel, B. M. and Hadley, A. G.,** Functional interactions of red cells sensitized by IgG1 and IgG3 human monoclonal anti-D with enzyme-modified human monocytes and FcR-bearing cell lines. *Mol. Immunol.* 1990. **27:** 247–256.

16 **Hadley, A. G.,** In vitro assays to predict the severity of hemolytic disease of the newborn. *Transfus. Med. Rev.* 1995. **9:** 302–313.

17 **Hadley, A. G., Wilkes, A., Goodrick, J., Penman, D., Soothill, P. and Lucas, G.,** The ability of the chemiluminescense test to predict clinical outcome and the necessity for amniocenteses in pregnancies at risk of haemolytic disease of the newborn. *Br. J. Obstet. Gynaecol.* 1998. **105:** 231–234.

18 **Mawas, F., Wiener, E., Ryan, G., Soothill, P. W. and Rodeck, C. H.,** The expression of IgG Fc receptors on circulating leucocytes in the fetus and the new-born. *Transfus. Med.* 1994. **4:** 25–33.

19 **Wiener, E., Mawas, F., Dellow, R. A., Singh, I. and Rodeck, C. H.,** A major role of class I Fcγ receptors in immunoglobulin G anti-D-mediated red blood cell destruction by fetal mononuclear phagocytes. *Obstet, Gynecol.* 1995. **2:** 157–162.

20 **Wiener, E., Dellow, R. A., Mawas, F. and Rodeck, C. H.,** Role of FcγRIIa (CD32) in IgG anti-RhD-mediated red cell phagocytosis *in vitro*. *Transfus. Med.* 1996. **6:** 235–241.

21 **Pound, J. D., Lund, J. and Jefferis, R.,** Human FcγRI triggering of the mononuclear phagocyte respiratory burst. *Mol. Immunol.* 1993. **30:** 469–478.

22 **Koolwijk, P., Spierenburg, G. T., Frasa, H., Boot, J. H. A., van de Winkel, J. G. J. and Bast, B. J. E. G.,** Interaction between hybrid mouse monoclonal antibodies and the human high-affinity IgG FcR, huFcγRI, on U937. *J. Immunol.* 1989. **143:** 1656–1662.

23 **Harrison, P. T. and Allen, J. M.,** High affinity IgG binding by FcγRI (CD64) is modulated by two distinct IgSF domains and the transmembrane domain of the receptor. *Protein Eng.* 1998. **11:** 225–232.

24 **Story, C. M., Mikulska, J. E. and Simister, N. E.,** A major histocompatibility complex class I-like Fc receptor cloned from human placenta: possible role in transfer of immunoglobulin G from mother to fetus. *J. Exp. Med.* 1994. **180:** 2377–2381.

25 **Clark, M. R.,** Humanised antibodies having modified allotypic determinants (Immunoglobulin allotypes). Patent application WO 92/16562, 1992.

26 **Greenwood, J., Clark, M. and Waldmann, H.,** Structural motifs involved in human IgG antibody effector functions. *Eur. J. Immunol.* 1993. **23:** 1098–1104.

27 **Orlandi, R., Gussow, D. H., Jones, P. T. and Winter, G.,** Cloning immunoglobulin variable domains for expression by the polymerase chain reaction. *Proc. Natl. Acad. Sci. USA* 1989. **86:** 3833–3837.

28 **Kilmartin, J. V., Wright, B. and Milstein, C.,** Rat monoclonal antitubulin antibodies derived by using a new nonsecreting rat cell line. *J. Cell. Biol.* 1982. **93:** 576–582.

29 **Tempest, P. R., Bremner, P., Lambert, M., Taylor, G., Furze, J. M., Carr, F. J. and Harris, W. J.,** Reshaping a human monoclonal antibody to inhibit human respiratory syncytial virus infection *in vivo*. *Biotechnology* 1991. **9:** 266–271.

30 **Cobbold, S. P., Rebello, P. R. U. B., Davies, H. Ff. S., Friend, P. J. and Clark, M. R.,** A simple method for measuring patient anti-globulin responses against isotypic or idiotypic determinants. *J. Immunol. Methods* 1990. **127:** 19–24.

31 **van Urgt, M. J., Heijnen, I. A. F. M., Capel, P. J. A., Park, S. Y., Ra, C., Saito, T., Verbeek, J. S. and van de Winkel, J. G. J.,** FcR γ-chain is essential for both surface expression and function of human FcγRI (CD64) *in vivo*. *Blood* 1996. **87:** 3593–3599.

32 **Kumpel, B. M., Poole, G. D. and Bradley, B. A.,** Human monoclonal anti-D antibodies: their production, serology, quantitation and potential use as blood grouping reagents. *Br. J. Haematol.* 1989. **71:** 125–129.

33 **Kumpel, B. M.,** A simple non-isotopic method for the quantitation of red cell-bound immunoglobulin. *Vox Sang.* 1990. **59:** 34–39.

Correspondence: Kathryn Armour, Division of Immunology, Department of Pathology, University of Cambridge, Tennis Court Road, Cambridge, CB2 1QP, GB
Fax: +44-1223 333875
e-mail: kla22@mole.bio.cam.ac.uk

ELSEVIER

Journal of Biotechnology 53 (1997) 3–12

JOURNAL OF Biotechnology

Genetic engineering of a recombinant fusion possessing anti-tumor $F(ab')_2$ and tumor necrosis factor

Jim Xiang [a,*], Terence Moyana [b], Yumin Qi [a]

[a] *Saskatoon Cancer Center, Department of Microbiology, University of Saskatchewan, 20 Campus Drive, Saskatoon, Saskatchewan S7N 4H4, Canada*

[b] *Department of Pathology, University of Saskatchewan, 20 Campus Drive Saskatoon, Saskatchewan S7N 4H4, Canada*

Received 23 May 1996; received in revised form 16 November 1996; accepted 18 November 1996

Abstract

The construction, synthesis and expression of a genetically engineered bifunctional antibody/cytokine fusion protein is described. In order to target alpha-tumor necrosis factor (TNF) to tumor cells, recombinant antibody techniques were used to construct an RM4/TNF fusion protein containing the chimeric anti-tumor $F(ab')_2$ (RM4) as well as the TNF moiety. The recombinant cDNA of human TNF was linked to the 3′ end of the chimeric heavy-chain gene fragment (M4) containing the V_H, the C_{H1} and the hinge region to form the fused heavy-chain gene fragment M4-TNF. Transfection of the M4-TNF gene fragment into a V_KC_K cell line producing the chimeric light-chain of the same antibody allowed the transfectant secreting the bifunctional fusion protein RM4/TNF. The RM4/TNF was purified by affinity chromatography. Our data showed that RM4/TNF retained the TAG72 antigen-binding reactivity as well as TNF activity as measured by ELISA, Western blotting, flow cytometry analysis, immunohistochemistry and cytotoxicity assays using the human colon cancer cell line LS174T. Therefore, the bifunctional fusion protein RM4/TNF may prove useful in targeting the biological effects of TNF to tumor cells, and in this way stimulate the immune destruction of tumor cells. © 1997 Elsevier Science B.V.

Keywords: Fusion protein: Chimeric Anti-TAG72 antibody; Tumor necrosis factor

1. Introduction

Since the systemic administration of alpha-tumor necrosis factor (TNF) can mediate tumor regression in animal models (Asher et al., 1987), this cytokine has attracted interests as a potential anti-tumor reagent (Moritz et al., 1989). However, cancer clinical trials utilizing systemic TNF have produced disappointing results. This is mainly because patients were found to have significantly lower maximum tolerated dose as compared to

* Corresponding author. Tel.: +1 306 6552917; fax: +1 306 6552910.

PII S0168-1656(96)01639-2

mice (Sherman et al., 1988; Spriggs et al., 1988). Thus, severe side-effects were often seen in cancer patients receiving TNF treatment (Creaven et al., 1987).

Anti-tumor antibodies have been extensively used as vehicles to target therapeutic reagents such as toxins and drugs to tumor cells (Fitzgerald et al., 1987; Harven et al., 1992). In this fashion, these therapeutic reagents can be efficiently targeted to tumors in vivo while at the same time limiting high dosages and the attendant severe side-effects. The human tumor-associated TAG72 antigen originally recognized by the B72.3 antibody is present in the majority of colorectal, gastric and ovarian adenocarcinomas (Thor et al., 1986). We recently constructed an high-affinity anti-TAG72 chimeric antibody ccM4 by genetic engineering (Xiang et al., 1992). More recently, we cloned chimeric heavy- and light-chain genes from a cDNA library of the ccM4 transfectoma (Boyd and Xiang, 1994); this provided us with cDNA gene fragments that are more amenable to gene manipulation and genetic construction of fused genes than their genomic counterparts. In this study, we present the construction of a bifunctional fusion protein RM4/TNF by recombinant DNA technology. We provide an account of its bifunctional activities including the anti-TAG72 immunoreactivity of chimeric $F(ab')_2$ as well as human TNF activity.

2. Materials and methods

2.1. Antibodies, antigens and cell lines

The mouse/human chimeric anti-TAG72 antibody ccM4 (IgG_1) was genetically engineered in our laboratory (Xiang et al., 1992). The plasmid DNA M13mp19-TNF containing the human TNF cDNA gene fragment was purchased from R and D Systems (Minneapolis, MN). The recombinant human TNF and the goat anti-TNF antibody were obtained from Gibco (Burlington, ON). The goat anti-TNF antibody was further biotinylated according to a method described previously (Harlow and Lane, 1988). Mucin type I-S from bovine submaxillary glands containing a large amount of the TAG72 epitope (Kjeldsen et al., 1988) was purchased from Sigma. The V_KC_K cell line expressing the cytoplasmic chimeric light-chain of ccM4 antibody (Xiang et al., 1992) was derived from the myeloma cell line SP2/0Ag14 by transfection of the chimeric light-chain expression vector mpSV2gpt-EP1-V_KC_K. LS174T is a human colon cancer cell line and KLE is a human endometrial adenocarcinoma cell line expressing the cell-surface TAG72 antigen (Hand et al., 1992). Both cell lines were purchased from the American Type Culture Collection (ATCC, Rockville, MD) and maintained in Dulbecco's modified Eagle's medium (DMEM) containing 10% fetal calf serum (FCS), penicillin and streptomycin (100 $\mu g\ ml^{-1}$).

2.2. Construction of the expression vector mpSV2neo-EP1-M4-TNF-PA

For construction of the fused heavy-chain gene fragment M4-TNF, four oligonucleotide primers were designed for amplification of the M4 and the TNF gene fragments in polymerase chain reaction (PCR). The M4 gene fragment includes the variable (V_H), the constant (C_{H1}) and the hinge regions of the chimeric heavy-chain gene M4H2 (Boyd and Xiang, 1994). Primer 1 (5′ GAATTCAACATGGAATGGAG 3′) and primer 2 (5′ GGATCCGGTGGGCATGTGTGAGTTT-TGTCA CAAGAT 3′) were complementary to the 5′ end of V_H region and the 3′ end of M4H2 hinge region in the plasmid DNA pBM4H2 (17) for introduction of an *Eco*RI and a *Bam*HI site to its 5′ and 3′ ends, respectively. Primer 3 (5′ ATG-GATCCTAGCTCCTCTCGCACTCCGTCC 3′) and primer 4 (5′ GGGTCGACATTATTACAGT-GCGATAATACC 3′) were complementary to 5′ and 3′ ends of the TNF region in the plasmid DNA M13mp18-TNF for introduction of a *Bam*HI and a *Sal*I site to its 5′ and 3′ ends, respectively. PCR reactions were carried out as previously described (Xiang et al., 1990). All oligonucleotides were synthesized by DNA Synthesis Lab, University of Calgary, Canada.

Strategies in construction of the fused heavy-chain gene fragment M4-TNF as well as the ex-

pression vector mpSV2neo-EP1-M4-TNF-PA were similar to the one previously described (Xiang et al., 1996). The M4 (*Eco*RI/*Bam*HI) gene fragment that was purified from PCR by using primers 1 and 2 was ligated to the *Eco*RI/*Bam*HI site of PUC18 to form the PUC18-M4. The TNF (*Bam*HI/*Sal*I) fragment that was purified from PCR by using primers 3 and 4 was cloned into the *Bam*HI/*Sal*I site of PUC18-M4 to form the PUC18-M4-TNF. The entire sequence of the fused gene fragment M4-TNF was verified by the dideoxy nucleotide sequencing method (Xiang et al., 1990). The M4-TNF (*Eco*RI/*Sal*I) fragment that was purified from the PUC18-M4-TNF was then ligated into the *Eco*RI/*Xho*I site of mpSV2neo-EP1-PA (Xiang et al., 1996) to form the expression vector mpSV2neo-EP1-M4-TNF-PA.

2.3. Expression and purification of RM4/TNF

The ligated expression vector mpSV2neo-EP1-M4-TNF-PA was transfected into V_KC_K cells by electroporation using a BioRad Gene Pulser (Xiang et al., 1990). Transfected cells were selected in DMEM containing 10% FCS and G418 (2 mg ml^{-1}) (Sigma). One clone V_KC_K/RM4-TNF secreting a maximal amount of the bifunctional fusion protein RM4/TNF was detected by enzyme-linked immunosorbent assay (ELISA). It was further subcloned in DMEM containing 10% FCS without G418 and then expanded in 2000 ml of culture medium for large-scale purification. The bifunctional fusion protein RM4/TNF was purified from the V_KC_K/RM4-TNF transfectant supernatants by using a kappa-lock affinity column with binding-specificity for the immunoglobulin kappa light-chain (Upstate Biotech., Lake Placid, NY). The bound RM4/TNF was eluted from the column with an elution buffer (50 mM glycine, pH 2.7) as described in the manual. Its protein concentration was then determined by using a BioRad protein assay kit (Bio-Rad, Richmond, CA) according to the method described in the manual. Its purity was visualized via SDS-PAGE under reducing and nonreducing conditions. Gels were then stained with Coomassie blue (Xiang et al., 1990).

2.4. Western blotting

In order to check the presence of TNF moiety in the fusion protein, RM4/TNF samples were run on polyacrylamide gels under reducing and nonreducing conditions and then transferred onto the nitrocellulose paper (Xiang et al., 1996). The paper strips were blocked with 5% BSA in PBS, incubated with the biotinylated goat anti-TNF antibody (10 $\mu g\ ml^{-1}$) at 37°C for 1 h and then incubated with avidin conjugated with alkaline phosphatase (1:3000). After three washes, 10 ml of substrate containing 66 μl of nitroblue tetrazolium and 33 μl of 5-bromo-4-chloro-3-indolyl phosphate in reaction buffer (100 mM Tris-HCl, pH 9.5, 100 mM NaCl, 5 mM $MgCl_2$) were added for generation of the color reaction. After a 10 min incubation, the color reaction was terminated by adding stop solution (20 mM Tris–HCl, pH 8.0, 5 mM EDTA).

2.5. Enzyme-linked immunosorbent assay (ELISA)

Two ELISAs were carried out in this study, the TAG72- and the TNF-binding ELISA. The TAG72-binding ELISA was performed to measure the binding-reactivity of RM4/TNF for the TAG72 antigen, whereas the TNF-binding ELISA was performed to examine the presence of TNF moiety in the fusion protein. In the TAG72-binding ELISA, 50 ng of bovine mucin containing a large amount of the TAG72 epitope were coated to each well of a disposable ELISA plate (Corning, NY). The plate was blocked with 5% bovine serum albumin (BSA) in phosphate buffered saline (PBS). Then, 50 μl of the RM4/TNF, the ccM4 antibody and the human IgG at 12 nmol l^{-1}, and their 2-fold dilutions were added to each well and incubated at 37°C for 1 h. After three washes, plates were incubated with the rabbit anti-human IgG antibody (10 $\mu g\ ml^{-1}$) and then with donkey anti-rabbit IgG conjugated with the horseradish peroxidase. After another three washes, plates were subjected to the generation of a color reaction as previously described (Xiang et al., 1990). In the TNF-binding ELISA, 50 μl of RM4/TNF, the recombinant TNF and the human

IgG at 12 nmol l^{-1} and their 2-fold dilutions were coated to microtiter plates. The plates were blocked with 5% BSA in PBS. After this, 50 μl of the biotinylated goat anti-TNF antibody at 10 μg ml^{-1} were added to each well and incubated at 37°C for 1 h. The plates were washed and then incubated with the avidin conjugated with horseradish peroxidase for generation of the color reaction. The optical densities were determined at 405 nm in a Bio-Rad Model 3550 microplate reader.

2.6. The functional TNF assay

The cytotoxic activity of TNF was determined based upon cytotoxicity to the human colon cancer cell line LS174T by using the CellTiter 96 Cytoxicity Assay kit purchased from Promega (Madison, WI) (Yang et al., 1995). Briefly, 90 μl of 2.22×10^5 cells ml^{-1} in culture medium (containing 2×10^4 cells) were added to each well of the 96-well tissue culture plate and incubated overnight at 37°C in a humidified 5% CO_2 atmosphere. To one set of wells containing LS174T cells, 10 μl of the RM4/TNF at 2.4 pmol l^{-1} and its 5-fold dilutions were added. To another set of wells containing LS174T cells, the recombinant human TNF at 2.4 pmol l^{-1} and its 5-fold dilutions were added. At 3 days after incubation at 37°C, 15 μl of dye solution were added to each well. After another 4-h incubation at 37°C, 100 μl of solubilization/stop solution were added to each well. The plates were then read at 595 nm in a Bio-Rad Model 3550 microplate reader.

2.7. Immunohistochemical study

Reactivity of the fusion protein RM4/TNF on formalin-fixed tissue sections was determined using a modification of the avidin- biotin-peroxidase complex (ABC) method (Xiang et al., 1996). Human colonic adenocarcinomas were fixed in 10% neutral-buffered formalin and routinely embedded in paraffin. Tissue sections were deparaffinized in xylene and rehydrated in graded alcohols. Endogenous peroxidase activity was quenched by incubating the slides with 0.3% hydrogen peroxide in methanol for 15 min followed by three PBS rinses. The slides were incubated with normal rabbit serum to reduce any non-specific staining and then incubated with RM4/TNF at 10 μg ml^{-1} overnight at 4°C. The slides were washed and then incubated with the biotinylated goat anti-TNF antibody at 10 μg ml^{-1}. The slides were washed three times with PBS and then incubated with ABC reagents for 30 min. The peroxidase activity was developed with freshly prepared 0.06% 3',3'-diaminobenzidine containing 0.1% hydrogen peroxide. Haematoxylin was used as the counterstain. Each section was evaluated for the presence of cell surface and epithelial intracellular brown diaminobenzidine precipitates indicative of RM4/TNF binding.

3. Results

3.1. Construction of the expression vector mpSV2neo-EP1-M4-TNF-PA

Strategies in construction of the fused gene fragment M4-TNF were described in Section 2. Its entire nucleotide sequence was verified by dideoxy nuleotide sequencing method. Its respective amino-acid sequence was shown in Fig. 1, which includes the immunoglobulin leader sequence, V_H, C_{H1} and hinge regions as well as the TNF moiety. The reading frames of these gene fragments were all maintained. The fused gene fragment M4-TNF (*Eco*RI/*Sal*I) was ligated into the *Eco*RI/*Xho*I site of mpSV2neo-EP1-PA which contains the neo gene as a selection marker, the immunoglobulin enhancer and promoter (EP1) as well as the polyadenylation signal (PA) region to form the expression vector mpSV2neo-EP1-M4-TNF-PA (Fig. 1). This expression vector was then transfected into the V_KC_K cell line for expression of the bifunctional fusion protein RM4/TNF.

3.2. Expression and purification of the RM4/TNF

The transfected cells were selected in culture medium containing G418. The clone V_KC_K/RM4-TNF secreting a maximal amount of the RM4/TNF was subcloned and expanded for large scale purification of the RM4/TNF. The RM4/TNF is

a fusion protein containing the immunoglobulin $F(ab')_2$ (RM4) and the TNF moiety. It was purified from 2 l of the V_KC_K/RM4-TNF culture supernatant by using a kappa-lock affinity column. The final concentration of fusion protein in culture supernatants was estimated to be 40 ng ml^{-1}. To check its purifity, the purified RM4/TNF was subjected to SDS-PAGE analysis. After electrophoresis, gels were stained with Coomassie blue. As shown in Fig. 2A, the fusion protein RM4/TNF showed a single band of approximately 134 kDa under nonreducing conditions (lane a) and showed bands of 42 kDa, as well as 25 kDa, under reducing conditions (lane b), representing the fusion protein molecule under non-reducing conditions and its chimeric heavy- and light-chain under reducing conditions, respectively. In order to confirm the presence of the TNF moiety, Western blotting analysis was performed. As shown in Fig. 2B, the goat anti-TNF antibody recognized the band of approximately 134 kDa under nonreducing conditions (lane a) and the band of 42 kDa under reducing conditions (lane b), indicating that the chimeric heavy-chain of this fusion protein contains the TNF moiety.

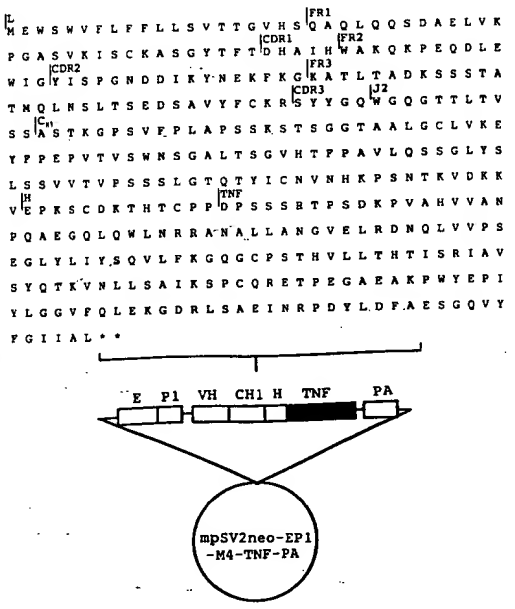

Fig. 1. Expression vector mpSV2neo-EP1-M4-TNF-PA and the amino acid sequence of fused gene fragment M4/TNF. Demarcated are the leader peptide region (L), the framework regions (FR), the complementarity-determining regions (CDR), the joining segment (J), the constant region 1 (C_{H1}), the hinge region (H), and the human tumor necrosis factor (TNF). The asterisk represents the stop codon. In the expression vector mpSV2neo-EP1-M4-TNF-PA, gene fragments are abbreviated as follows: heavy chain variable region, V_H; constant region 1, C_{H1}; hinge region, H; human tumor necrosis factor, TNF; immunoglobulin enhancer and promoter, EP1; polyadenylation signal region, PA.

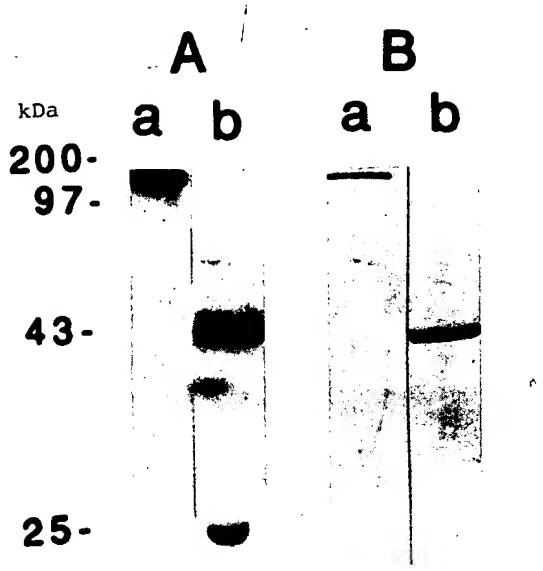

Fig. 2. SDS-PAGE and Western blotting analysis of the purified RM4/TNF. (A) SDS-PAGE analysis of the RM4/TNF. Lane a, RM4/TNF under nonreducing conditions; Lane b, RM4/TNF under reducing conditions. (B) Western blotting analysis of the RM4/TNF. Detection of the presence of TNF moiety in the fusion protein RM4/TNF. Fusion protein (10 μl)RM4/TNF were loaded to each well of polyacrylamide gel and run under nonreducing (lane a) and reducing conditions (lane b). Proteins in the gel were transferred onto the nitrocellulose paper. The paper strips were then incubated with the biotinylated goat anti-TNF antibody and followed by the alkaline phosphatase conjugated avidin.

3.3. Bifunctional activities of the RM4/TNF

In order to check whether RM4/TNF contains functional anti-TAG72 $F(ab')_2$ (RM4) and the functional TNF moiety, TAG72-and TNF-binding ELISAs were performed. As shown in Fig. 3A, RM4/TNF displayed a similar binding-reactivity for the TAG72 antigen as did the ccM4

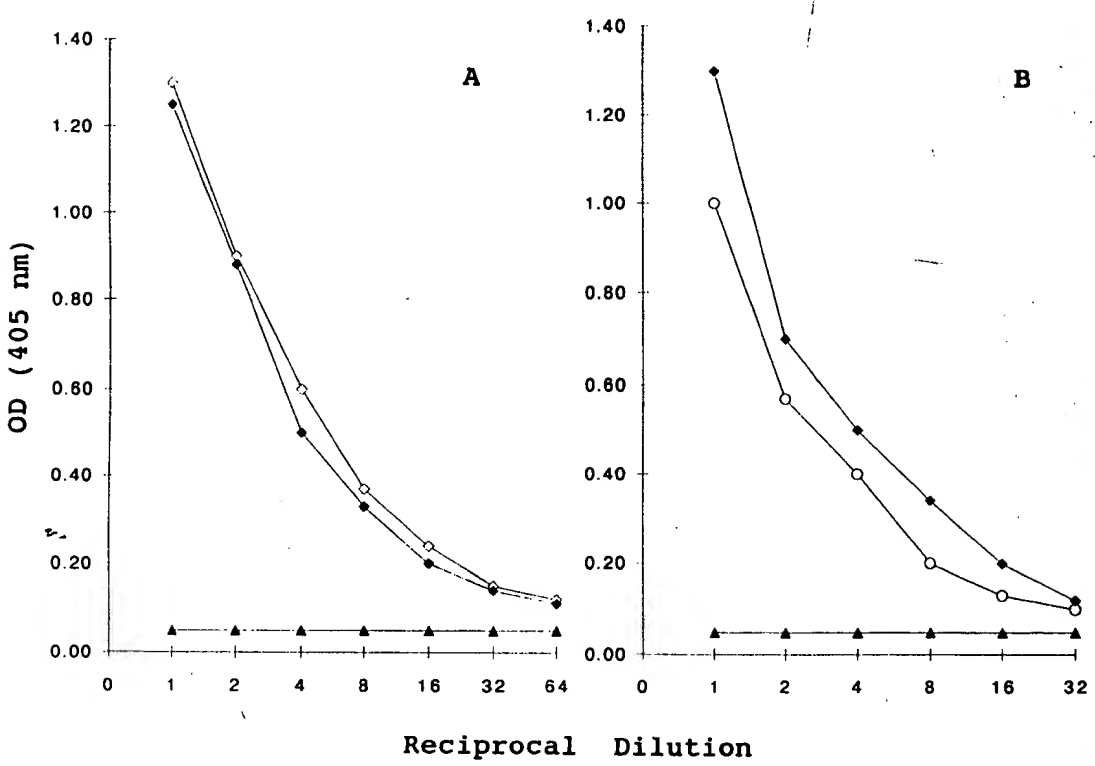

Fig. 3. ELISA analysis of the RM4/TNF. (A) In the TAG72-binding ELISA, 50 μl of the RM4/TNF (◆), the ccM4 (◇) and human IgG (▲) at 12 nmol l^{-1} and their 2-fold dilutions were added to the 50 ng mucin-coated plates. (B) In the TNF-binding ELISA, 50μl of RM4/TNF (◆), the recombinant TNF (○) and the human IgG (▲) at 12 nmol l^{-1}, and their 2-fold dilutions were coated to the plates. The biotinylated goat anti-TNF antibody at 10 $\mu g\,ml^{-1}$ were added to the plates. The S.D. of each determination is less than 5%.

antibody in the TAG72-binding ELISA, indicating that the immunoreactivity of RM4/TNF for the TAG72 antigen was retained very well. As shown in Fig. 3B, the goat anti-TNF antibody showed binding reactivities for both the RM4/TNF and the recombinant TNF protein, indicating that the native form of TNF seems to be maintained well in this fusion protein RM4/TNF.

In order to confirm the TAG72-binding reactivity of RM4/TNF, the human endometrial adenocarcinoma cell line KLE expressing the cell-surface TAG72 antigen was analysed using RM4/TNF by flow cytometry. As shown in Fig. 4, the TAG72 expression of KLE cells was detected by both the ccM4 antibody and the fusion protein RM4/TNF. This indicates that RM4/TNF retained the binding reactivity for tumor cells expressing the TAG72 antigen as did the ccM4 antibody. In order to further measure the TNF activity of RM4/TNF, TNF cytoxicity assay was performed by using human LS174T colon cancer cells. As shown in Fig. 5, both RM4/TNF and the recombinat TNF showed approximately the same cytotoxicity to LS174T tumor cells at low concentration of 2.4 pmol l^{-1} in the culture medium.

In order to demonstrate the targeting of TNF to tumor cells by the anti-TAG72 RM4 portion of the fusion protein, we conducted an immunohistochemical study by using human colonic adenocarcinoma tissue sections. The binding of RM4/TNF to tumor cells was proved by using the biotinylated goat anti-TNF antibody. As shown in Fig. 6B, RM4/TNF showed binding specificity for the colonic adenocarcinomatous cells. This positivity predominantly involved the suprabasal aspects of the tumor cells. In contrast, normal

B

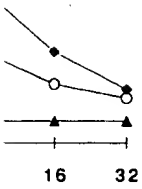

cM4 (◇) and human
'NF-binding ELISA.
dilutions were coated
f each determination

easure the TNF
)xicity assay was
'4T colon cancer
M4/TNF and the
imately the same
ls at low concen-
ılture medium.
argeting of TNF
RM4 portion of
l an immunohis-
n colonic adeno-
he binding of
)ved by using the
body. As shown
inding specificity
ıtous cells. This
d the suprabasal
contrast, normal

colonic mucosa showed no positivity at all (Fig. 6A). This indicates that the RM4 of the fusion protein was able to bind to tumor cells expressing the TAG72 antigen, and that the functional TNF was able to be targeted by the RM4 portion of the fusion protein to tumor cells on tissue sections in vitro.

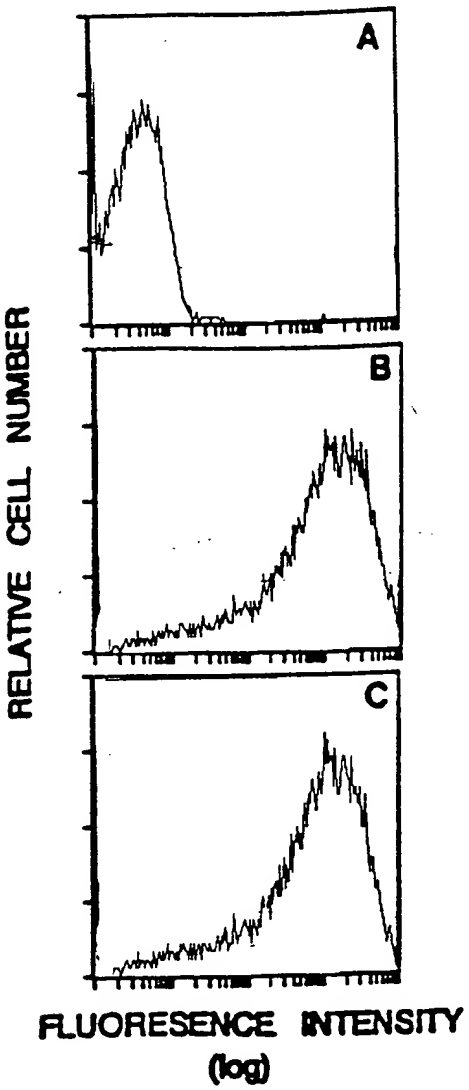

Fig. 4. TAG72 expression of KLE cells determined by RM4/TNF.KLE cells were incubated with the RM4/TNF (B) or the ccM4 antibody (C) (2μg ml^{-1}) followed by the incubation with the FITC-goat anti-human K antibody. (A) The control represents KLE stained with FITC- goat anti-human K antibody alone. A total of 10 000 cells were analysed for each sample by flow cytometry.

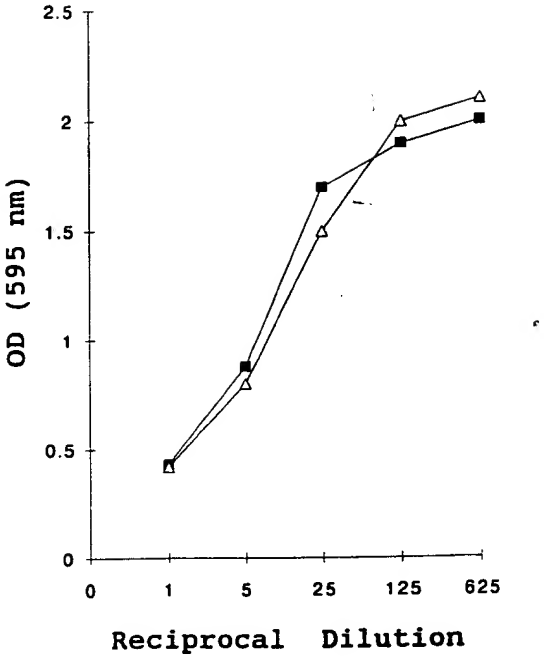

Fig. 5. Cytotoxic activity assay. LS174T tumor cells were incubated in culture medium containing the recombinant TNF (■) and the TNF moiety of purified fusion protein RM4/TNF (△) both at 2.4 pmol l^{-1}, and their 5-fold dilutions. The S.D. of each determinant is less than 5%.

4. Discussion

The data presented here describe the construction and expression of a fused gene M4-TNF in a transfectant cell line (V_KC_K) expressing the chimeric light-chain of the ccM4 antibody. In this fusion protein, the TNF moiety was linked to the C-terminus of the ccM4 heavy-chain hinge region, yielding potential F(ab')$_2$-like molecules. Linkage to this 'classical' site in the hinge region resulted in the expression and secretion of a fusion protein with the expected size and composition. The hinge region encodes part of the structural C_{H1} domain, including cysteine residues necessary for connecting the heavy-chain to the light-chain. Furthermore, it has been shown that some amino acids in upper part of the hinge region interact with residues in the C_{H1} domain (Schneider et al.,

Fig. 6. Immunohistochemical study of formalin-fixed paraffin-embedded human colonic adenocarcinoma using RM4/TNF and biotinylated goat anti-TNF antibody. (A) normal colonic mucosa; (B) colonic adenocarcinoma.

1988). The lower part of the hinge region is a rigid part containing proline and cysteine amino acids necessary for heavy-chain dimerization which confers each fusion protein molecule with two antigen binding-sites. The fusion protein was expressed by transfecting the fused chimeric heavy-chain gene M4-TNF into the V_KC_K cell line expressing the chimeric light-chain of the same antibody ccM4. Our data showed that this fusion protein RM4/IFN-τ retained both the anti-TAG72 reactivity of $F(ab')_2$ and the TNF activity as measured in ELISA, Western blotting, flow cytometry analysis of TAG72 expression, and cytotoxicity assay by using the human mammalian cancer cell line. It may indicate that both the $F(ab')_2$ (RM4) and the TNF moiety in this fusion protein assume their native configurations.

To date, the dose-limiting toxicity of TNF has been particularly apparent in humans (Creaven et al., 1987). Therefore, the ability to combine the targeting of a tumor-specific antibody together with a potent cytokine such as TNF should be useful because the tumor-specific antibody would direct and localize the effect of TNF at tumor sites. Consequently, the dose of TNF necessary for killing tumor cells could be decreased, thus, reducing its dose-related toxicity. A recent report by Sabzevari further showed evidence that a recombinant antibody-interleukin 2 fusion protein was able to significantly suppress the growth of hepatic human neuroblastoma metastases in severe combined immunodeficiency mice (Sabzevari et al., 1994). Therefore, the bifunctional protein RM4/TNF with tumor-specific immunoreactivity may prove useful in vivo by targeting biological effects of the TNF to tumor cells and inducing anti-tumor immune responses, and in this way limit the otherwise severe side-effects of high dose of TNF.

using RM4/TNF and

Acknowledgements

This study was supported by a research grant of the National Cancer Institute of Canada with funds from the Canadian Cancer Society.

References

Asher, A., Mule, J., Reichert, C., Shiloni, E. and Rosenberg, S. (1987) Studies on the anti-tumor efficacy of systemically administered recombinant tumor necrosis factor against several murine tumors in vivo. J. Immunol. 138, 963–974.

Boyd, M. and Xiang, J. (1994) Molecular cloning and expression of functional cDNA genes of a mouse/human chimeric antibody rcM4. Tumori. 80, 473–480.

Creaven, P., Plager, J., Dupere, S., Huben, R., Takita, H., Mittelman, A. and Proefrock, A. (1987) Phase-I clinical trial of recombinant human necrosis factor. Cancer Chemother. Pharmac. 20, 137–144.

Fitzgerald, D., Willingham, M., Cardarelli, C., Hamada, H., Tsuruo, T., Gottesman, M. and Pastan, I. (1987) A monoclonal antibody-pseudomanas toxin conjugate that specifically kills multidrug-resistant cells. Proc. Natl. Acad. Sci. U.S.A. 84, 4288–4292.

Hand, P., Calvo, B., Milenic, D., Yokota, T., Finch, M., Snoy, P., Garmestani, K., Gansow, O., Schlom, J. and Kashmiri, S. (1992) Comparative biological properties of a recombinant chimeric anti-carcinoma mAb and a recombinant aglycosylated variant. Cancer Immunol. Immunother. 35, 165–174.

Harlow, E. and Lane, D. (1988) Antibodies: A Laboratory Manual. Cold Spring Harbor Laboratory Press, Cold Spring Harbor, NY.

Harven, E., Fradet, Y., Connolly, J., Hana, W., He, S., Wang, Y., Choi, B., McGroarty, R., Bootsma, G., Tilup, A. and Christensen, H. (1992) Antibody drug carrier for immunotherapy of superficial bladder cancer. Ultrastructural studies. Cancer Res. 52, 3131–3137.

Kjeldsen, T., Clausen, H., Hirohashi, S., Ogawa, T., Iijima, H. and Hakomori, S. (1988) Preparation and characterization of monoclonal antibodies to the tumor-associated *O*-linked sialosy 2.6α-*N*-acetyl-galactosaminyl (Sialosyl-Tn) epitope. Cancer Res. 48, 2214–2220.

Moritz, T., Niederle, N., Baumann, J., May, D., Kurschel, E., Osieka, R., Kempeni, J., Schick, E. and Schmidt, C. (1989) Phase I study of recombinant human tumor necrosis factor α in advanced malignant disease. Cancer Immunol. Immunother. 29, 144–149.

Sabzevari, H., Gillies, S., Muller, B., Pancookk, J. and Reisfeld, R. (1994) A recombinant antibody-interleukin 2 fusion protein suppresses growth of hepatic human neuroblastoma metastases in severe combined immunodeficiency mice. Proc. Natl. Acad. Sci. U.S.A. 91, 9626–9632.

Schneider, W., Wensel, T., Stryer, L. and Oi, V. (1988) Genetically engineered immunoglobulins reveal structural features controlling segment flexibility. Proc. Natl. Acad. Sci. U.S.A. 85, 2509–2513.

Sherman, M., Spriggs, D., Arthur, K., Immamura, K., Frei, E. and Kufe, D. (1988) Recombinant human tumor necrosis factor administered as a 5-day continuous infusion in cancer patients: phase toxicity and effects on lipid metabolism. J. Clin. Oncol. 6, 344–359.

Spriggs, D., Sherman, M., Michie, H., Arthur, K., Imamura, K., Wilmore, D., Frei, E. and Kufe, D. (1988) Recombinant human tumor necrosis factor administerred as a 24-h intravenous infusion, a phase I and pharmacologic study. J. Nat. Cancer. Inst. 80, 1039–1044.

Thor, A., Ohuchi, N., Szpak, C., Johnston, W. and Schlom, J. (1986) Distribution of the oncofetal antigen, tumor-associated glycoprotein-72 defined by the monoclonal antibody B72.3. Cancer Res. 46, 3118–3124.

Xiang, J., Roder, J. and Hozumi, N. (1990) Production of murine V/human Cr1 chimeric anti-TAG72 antibody using V region cDNA amplified by PCR. Mol. Immunol. 27, 809–817.

Xiang, J., Moyana, T., Kalra, J., Hamilton, T. and Qi, Y. (1992) Construction and characterization of a high affinity chimeric anti-colorectal carcinoma antibody ccM4. Mol. Biother. 4, 174–183.

Xiang, J., Moyana, T. and Qi, Y. (1996) Targeting of gamma interferon to tumor cells by a recombinant fusion protein secreted by myeloma cells. Hum. Antibodies Hybridomas 7, 1–10.

Yang, J., Moyana, T. and Xiang, J. (1995) A genetically engineered single-chain FV/TNF molecule possesses the anti-tumor immunoreactivity of FV as well as the cytotoxic activity of tumor necrosis factor. Mol. Immunol. 32, 873–881.